# DUST-
# DUSTSTORM GENERATION AND PREVENTION

**Third International Symposium**
**on**
**AIR QUALITY MANAGEMENT**
**at Urban, Regional and Global Scales**
**&**
**14 th IUAPPA Regional Conference**
**26-30 September 2005**
**Istanbul, Turkey**

## DUSTSTORM GENERATION AND PREVENTION

# CHANGES IN DUST STORM OCCURRENCE OVER CENTRAL EASTERN AUSTRALIA: 1950 TO 2004

**Lance M. Leslie[1] and Milton S. Speer[2]**

[1]School of Meteorology, University of Oklahoma, Norman, Oklahoma, USA
email: lmleslie@ou.edu
[2]Bureau of Meteorology, Sydney, Australia,
email:mss@lighthill.maths.unsw.edu.au

**ABSTRACT**

A sudden decrease in dust storm frequency began in the mid-1970s over central eastern Australia. This decrease is linked to changes in the synoptic circulation during that period. NCEP/NCAR reanalysis data shows a change from anomalous low level south to southeast winds, to anomalous northwesterly winds over central eastern Australia during 1950-1974 and 1975-2004, respectively. Consequently, postfrontal south to southeast winds have decreased and fewer dust storms have occurred. Results from climate model simulations exhibit similar changes in wind anomalies. There appears to be a strong link between these circulation changes and the phases of the Pacific Decadal Oscillation (PDO).

**Key Words**: Dust Storms; Central Eastern Australia; Anomalies; Circulation; Climate; SST

## 1. INTRODUCTION

The major dust source regions over inland Australia lie mostly between 25 deg. and 35 deg. S, particularly over the 1.3 million km $^2$ Lake Eyre drainage basin in central eastern Australia (Washington et al. 2003). This is an area devoid of vegetation especially during prolonged dry periods that often halt or restrict the flow in the rivers and tributaries that drain into the basin. When the dry crusty surface comprising mainly of fine drainage basin sediment becomes broken through erosion processes, strong winds can cause the underlying fine dust particles to become airborne. At those Australian Bureau of Meteorology (BoM) synoptic stations where dust is reported, new World Meteorological Organization (WMO) guidelines were introduced from 1957. They consisted of several visibility categories, including: a dust storm/sand storm; well-developed dust devils; raised dust/sand; widespread dust in suspension; or a thunderstorm with dust or sand storm. Prior to 1957, reports of dust in Australia were recorded under just one dust storm category (Bureau of Meteorology 1925).

According to Sprigg (1982) and Ekström et al. (2004), dust storms and raised dust in central, northeastern and eastern Australia occur mainly in spring and summer as a result of strong low level south or southeasterly winds, following mid-latitude frontal systems. The southeasterly winds can extend north as far as 15-20 deg. S. For frontal related dust reports between 1995 and February 2005, Speer and Leslie (2005) found that there were two distinct synoptic types. One type occurs with frontal systems embedded in the zonal westerlies or low pressure systems that sweep across southeast

Australia and the east coast. The other synoptic type occurs with high pressure systems in the Great Australian Bight (GAB), following frontal systems that weaken or at least slow down over southeast Australia, particularly through central Queensland (QLD).

The aims of this study are to analyze the trends in duststorm frequency over the period 1950 to 2004 by investigating their relation first to synoptic scale circulation features over eastern Australia and, second, to large scale circulation features affecting the same region. Finally, the implications for possible changes in dust storm frequency under enhanced greenhouse warming conditions will be discussed for east central Australia.

## 2. DATA

The dust source region that affects central eastern Australia is the Lake Eyre drainage basin (Speer and Leslie 2005). Dust has been reported along with reductions in visibility for various categories defined by the Australian Bureau of Meteorology synoptic stations since 1957, using WMO standard criteria. Prior to 1957, dust was reported in Australia simply as a single category consisting of a dust storm. Clearly, with the change in reporting practice in 1957 the number of days on which dust was reported will have increased due to that change alone. Concentrating on central eastern Australia, 24 representative synoptic stations were selected and all days on which dust storm criteria were reported from at least at one of the 24 stations were calculated. This calculation produced a total of 2,669 dust storm days (see Fig.1). The key feature in Fig. 1 is the sudden and significant decrease in reported dust days in the early to mid-1970s, a result found earlier by Ekström et al. (2004). Twenty-one of the 24 stations have been operational throughout the entire period and reporting practices have not changed since 1957.

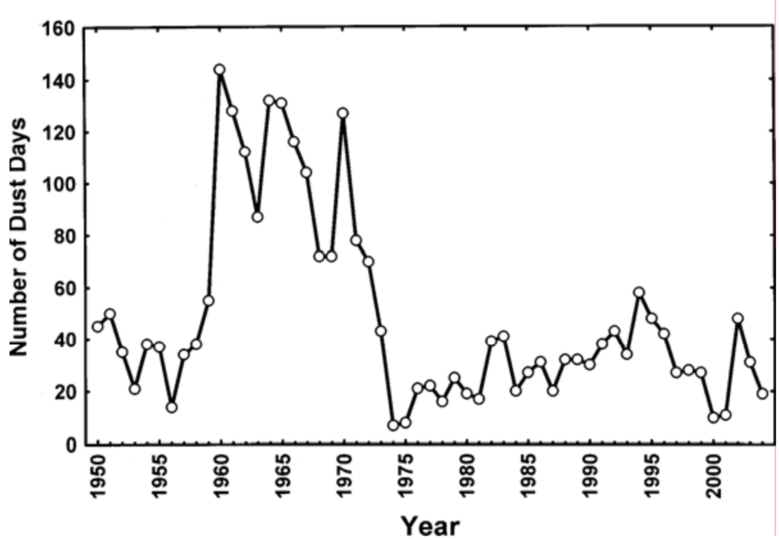


Figure 1. The number of dust days recorded in central eastern Australia during the period 1950 to 2004 from 24 synoptic stations.

A rise or fall in the number of dust reports is expected to coincide with a rise or fall in the number of synoptic scale frontal wind events. Several studies have indicated that the major synoptic influence responsible for dust storms are postfrontal south to southeast winds over eastern Australia resulting from high pressure systems in the GAB following the passage of cold frontal systems (see, e.g., Sprigg 1982; Ekström et al. 2004). However, during the most recent ten-year period, namely 1995 to 2004, Speer and Leslie (2005) have noted that frontal-related dust events accounted for just 18 out of a total of 43 (i.e. 42%), while the remaining 24 out of 43 (i.e. 58%) resulted from the influence of zonal westerlies or low pressure systems in the GAB. Figures 2a and 2b show examples of each of these two synoptic types, Figure 2a being an example of a dust storm produced by a high pressure system in the GAB, and Figure 2b, a dust storm event resulting from a low pressure system in the GAB.

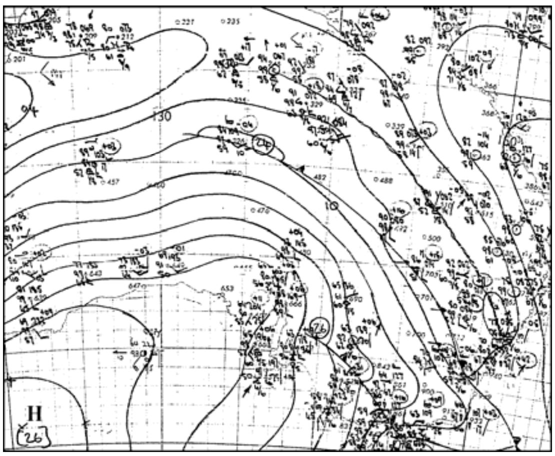

(a)

Figure 2(a). MSLP chart valid at 11 UTC 8 Feb. 1962. Dust was reported over central eastern Australia, from a high pressure system in the GAB and associated postfrontal S/SE winds

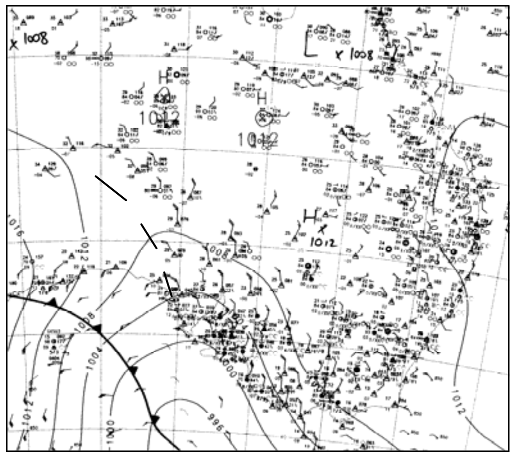

(b)

Figure 2(b). MSLP chart valid at 00 UTC 19 Oct. 2002. In this case dust was reported over central eastern Australia, generated by a cold front located in the GAB

The following question immediately arises from the above analysis: "Is the reduction in the number of dust reporting days since the early to mid-1970s due to a corresponding decrease in the influence from high pressure in the GAB, because of fewer postfrontal south to southeast wind events?" In attempting to answer this question the approach adopted in the next Section focuses on a comparison of climate anomalies computed from the NCEP/NCAR re-analysis data. First, the climate reference anomalies for the tropospheric wind vector circulation over the period from 1950 to 2004 are analysed. The climate anomalies are calculated for the time intervals 1950-1974 and 1975-2004, measured relative to the climate mean over the entire time period 1950-2004. Next, a comparison is made of these reanalysis based synoptic circulation anomalies with those of a fully coupled climate model for the same period, based on the recently developed OU-CGCM climate model located at The University of Oklahoma (Karoly and Leslie, 2005). Finally, the possible role of the Pacific Interdecadal Oscillation (PDO) over central east Australia and the adjacent Tasman Sea will be discussed and changes in the tropospheric circulation over eastern Australia during the period 1950-2004 are related to the changes in observed duststorm frequencies.

## 3. TROPOSPHERIC CIRCULATION AND SST ANOMALIES 1950 TO 2004

### Reference climatology

From the analyses of spring and summer 925 hPa vector wind anomalies derived from the NCEP/NCAR reanalyses for the period 1950 to 1974, anomalous south to southeasterly winds were found to be present in Spring (SON) and Summer (DJF) over the dust reporting locations (Figs. 3(a), 4(a)). This is consistent with the strong ridging that occurred south of the continent in that period, following cold frontal system passages. The results are confirmed by the 850 hPa geopotential height anomalies which show anomalous high pressures in the GAB for the same period (not shown). Conversely, the observed anomalous north to northwesterly winds in both spring and summer for the period 1975 to 2004 (Figs. 3(b), 4(b)) are consistent with reduced postfrontal south to southeasterly winds and anomalous negative pressure anomalies in the GAB for the same period (not shown). As a result, the 24 synoptic stations and particularly those nearest to the strongest anomalies have been much less affected by dust from the Lake Eyre basin source region for the period 1975 to 2004 than for 1950-1974.

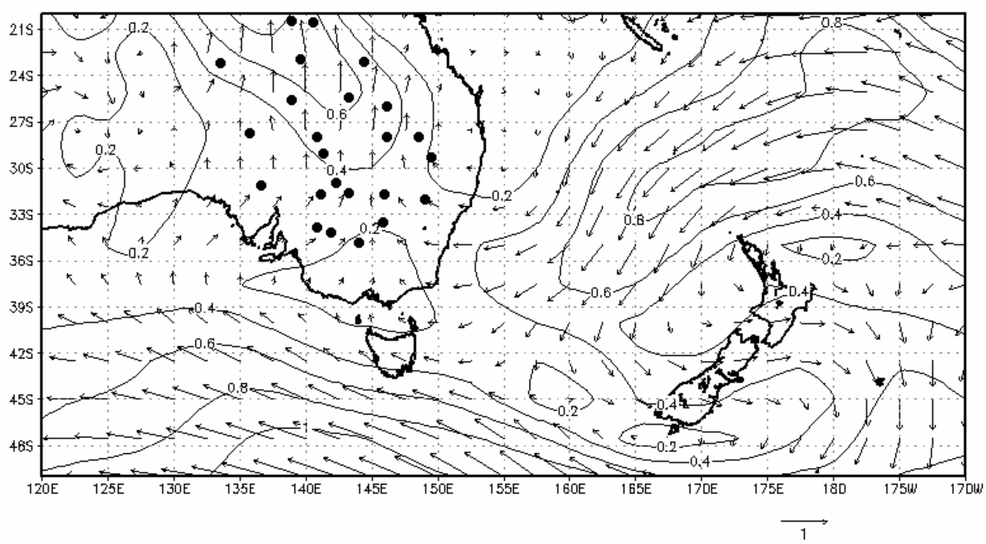


Figure 3(a). The September-November 1950-1974 NCEP 925 hPa vector wind anomaly field (m/s). Dust reporting stations indicated by bullet point symbols (•).

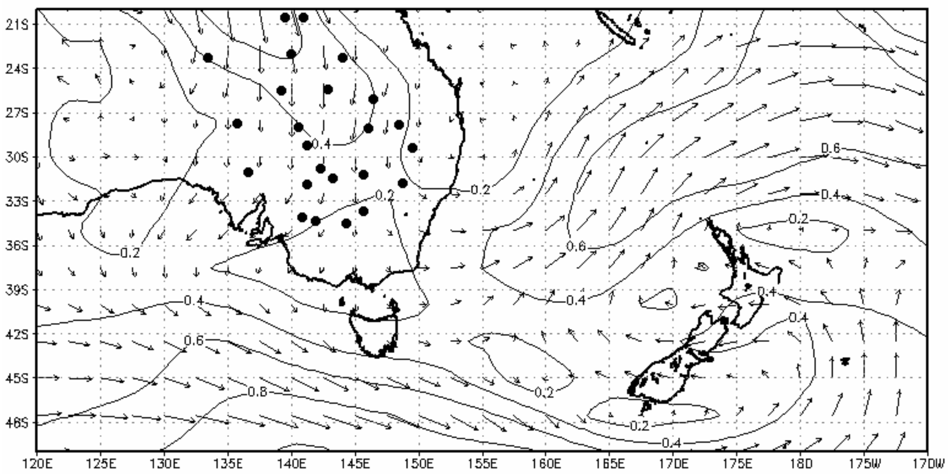


Figure 3(b). Same as in Fig. 3(a), except for 1975-2004

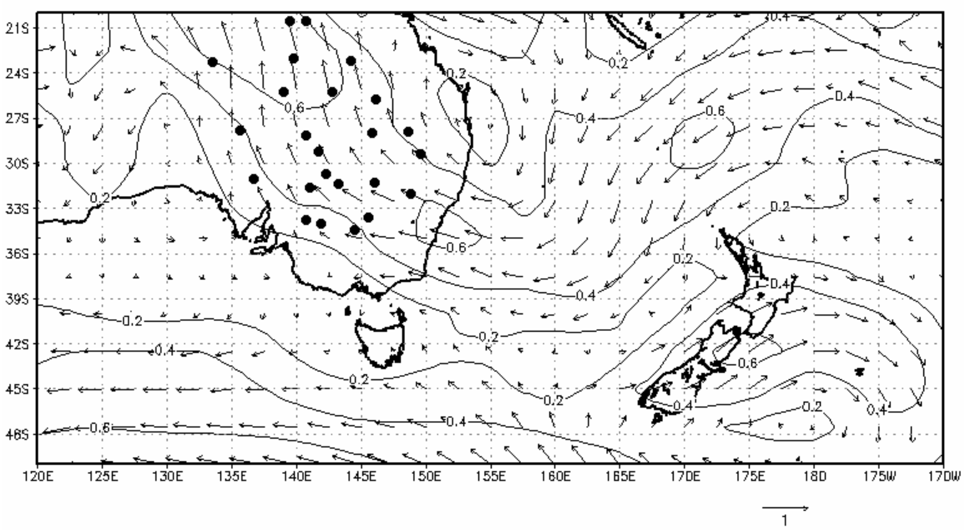


Figure 4(a). The December–February 1950 – 1974 NCEP 925-hPa vector wind anomaly (m/s). Dust reporting stations again are indicated by the bullet point symbol (•).

## Climate model anomalies

In this section and thereafter we concentrate on the Southern Hemisphere (SH) summer season (DJF) only. Figures 5(a) and 5(b) show the model 925 hPa December to February wind anomalies over eastern Australia for the two periods 1950 to 1974 and 1975 to 2004, respectively. They should be compared directly with Figs. 4(a) and 4(b), respectively, because the anomalies in both periods are calculated with reference to the same climatological period 1950-2004. There is a striking similarity in the anomaly patterns from the NCEP/NCAR reanalysis data and the OU-CGCM climate model for both periods. In Figure 5(a) the key features are the moderate to strong anomalous south to southeast winds that affect the same area as in Figure 4(a).

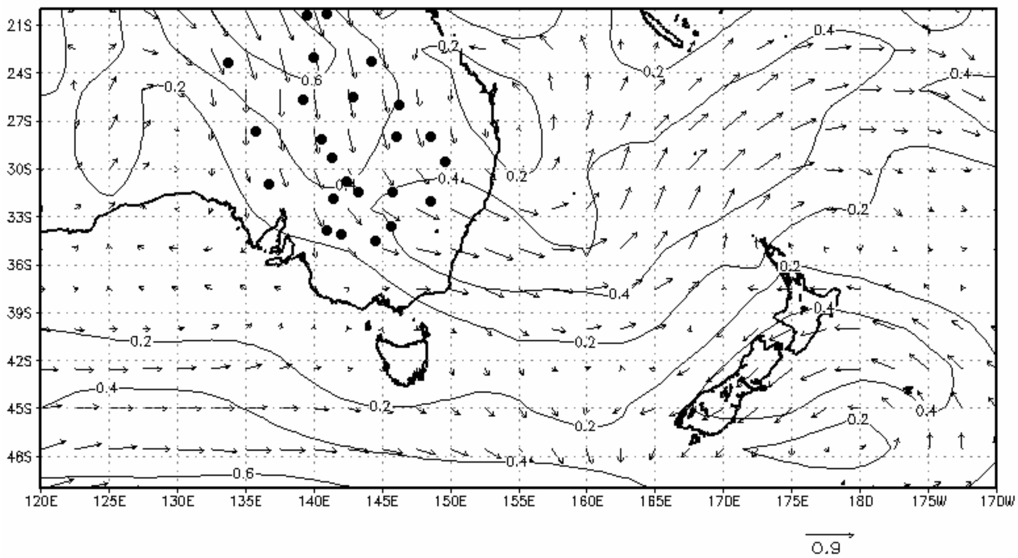


Figure 4(b). Same as in Figure 4(a) except for 1975–2004

Moreover, anomalously weak northerly winds over central eastern Australia in Figure 5(b) closely match the patterns shown by the NCEP/NCAR reanalysis data (Figure 4(b)).

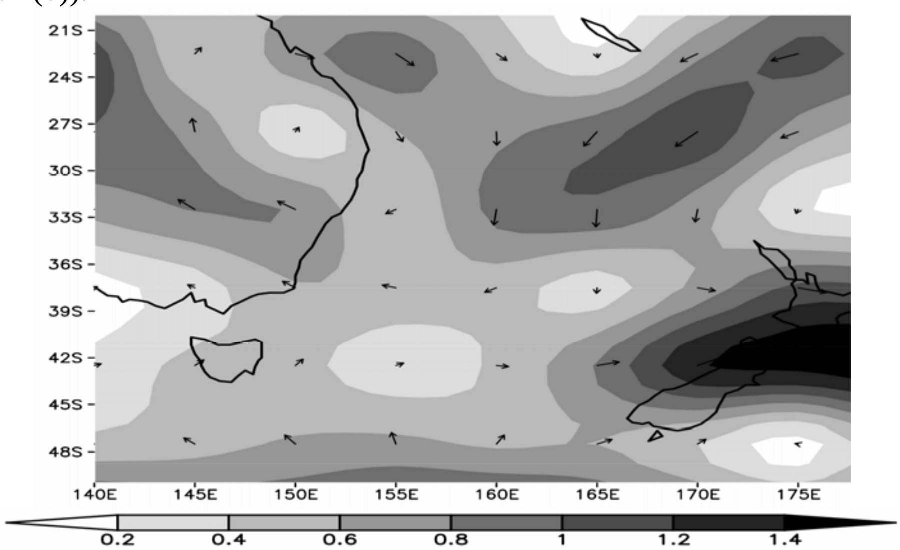


Figure 5(a). Model derived Dec. to Feb. wind anomalies (m/s) at 925hPa for the period 1950-1974 (the model climate reference period is 1950-2004)

## Links to the Pacific Decadal Oscillation (PDO)

The PDO is a long-lived, El Niño-like, ocean-atmosphere pattern of Pacific climate variability (Zhang et al. 1997; Mantua et al. 1997). As far as the authors are aware there have been no climate impacts in the SH that have been linked to the PDO thus far. In its last cool phase (includes the period 1950 to mid-1970s) NH SST and

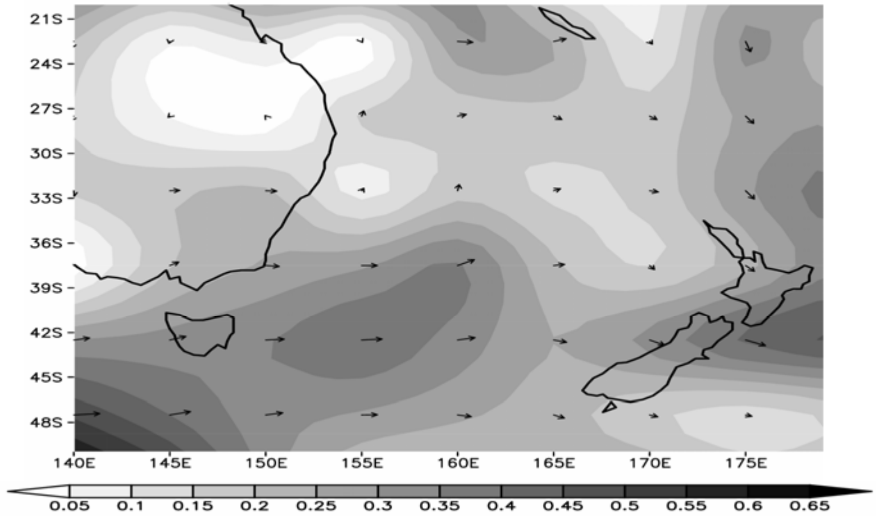


Figure 5(b). As in 5(a), except for 1975 to 2004.

atmospheric anomalies contrast with its warm phase (after 1976) when the PDO exhibits El Nino like characteristics in the NH (Zhang et al. 1997). This contrast in anomalies for the two phases is also the case for the SH to the extent that NCEP DJF climate wind anomalies in Figs. 4(a) and 4(b) show anomalous south to southeasterly winds and north to northwesterly winds, respectively, over southeastern Australia which are consistent with NCEP anomalous positive and negative precipitable water anomalies, respectively, over southeastern Australia for the same periods (see Figs. 6(a) and (b), respectively).

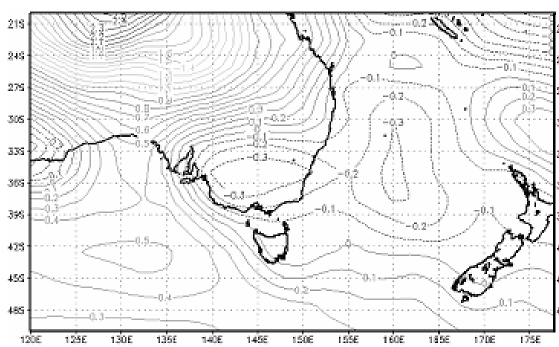

Figure 6(a). NCEP derived DJF precipitable water anomalies for the period 1950-1974

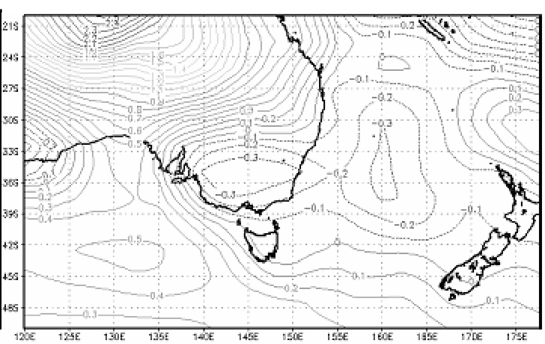

Figure 6(b). NCEP derived DJF precipitable water anomalies for the period 1975-2004

In terms of the SST distribution both the summertime (SH) warm phase and cool phase patterns are consistent with those of Mantua et al. (1997) covering the period 1900 to 1993. The cool phase DJF OU-CGCM pattern in Figure 7(a), that is from 1950 to 1974, closely matches the local NCEP reanalysis SST anomaly pattern for the same period shown in Figure 8(a). Similarly, the current warm phase DJF OU-CGCM pattern in Figure 7(b) matches the local NCEP reanalysis SST anomaly pattern from 1975 to 2004 in Figure 8(b). A key point to note in the figures is the change from anomalously strong positive SST values between New Zealand and Australia in the cool phase of the PDO (1950-1974) to the weak negative SST values between New Zealand and Australia in the warm phase of the PDO which began from about 1975.

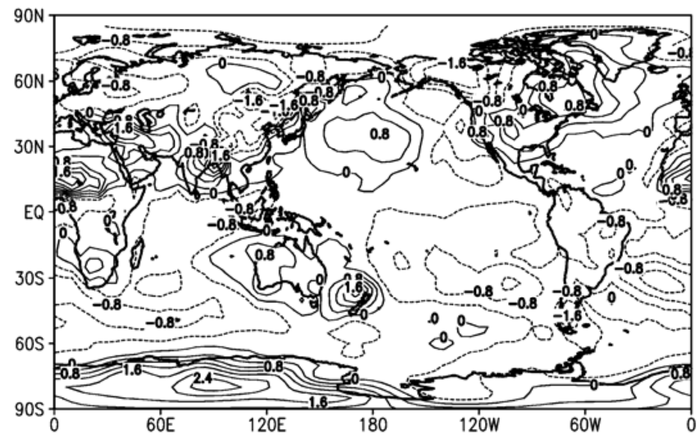


Figure 7(a). DJF model calculated SST (C $^{0}$) anomaly for the period 1950 – 1974.

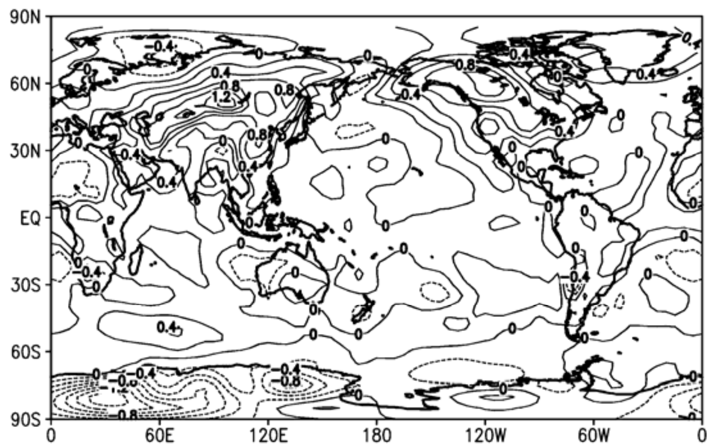


Figure 7(b). As in 7(a) except for the period 1975 – 2004.

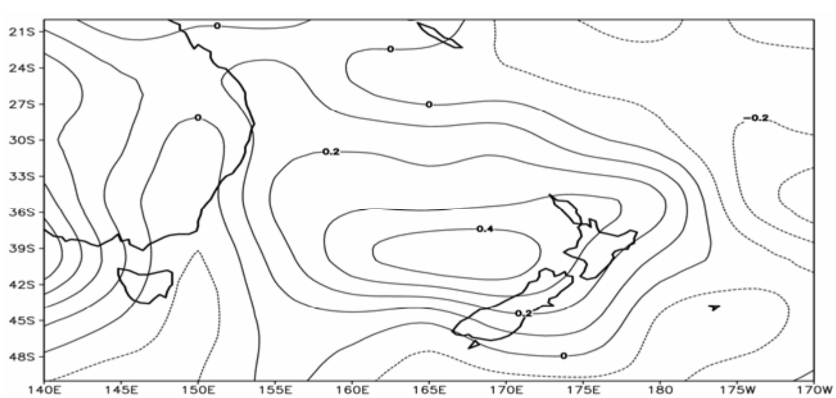


Figure 8(a). NCEP reanalysis SST anomaly (C $^{0}$) DJF 1950 – 1974

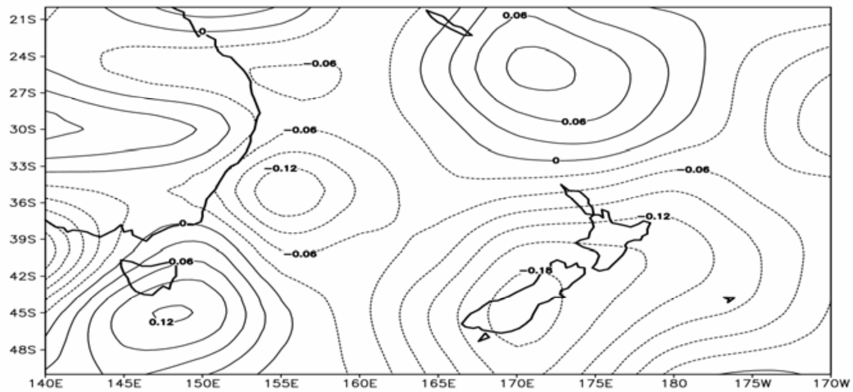


Figure 8(b). as in (a) except for 1975 - 2004

## 4. FUTURE PLANS TO STUDY THE IMPACTS OF FUTURE CLIMATE CHANGE UNDER ENHANCED CO2 CONDITIONS

The next stage of this study is to assess the impact on future climate of enhanced CO2 concentrations on the multi-decadal oscillation that we have identified here. Before this can be attempted, we must examine how well the OU-CGCM climate model performs under current climate conditions. In particular, can the climate model reproduce the main features observed in the period 1950-2004. We carried out this experiment by spinning up the climate model over 30 years from 1920 and then integrating it for a further 55 years, from Jan 1 1950 to the end of 2004. We then compared the wind vector anomalies and the SST distributions over the region of interest with the NCEP reanalyses, for the two periods 1950-1974 and 1975-2004. The results of this comparison are shown in the previous section. They are sufficiently encouraging that we have decided to analyse the OU_CGCM model run out to 2100 in a future study that will be reported on when it is completed.

## 5. CONCLUSIONS

In this study we identified a multi-decadal oscillation in the large scale circulation of the east central Australian region and the Tasman Sea that covered the periods 1950-1974 and 1975-2004 approximately. The impacts of this oscillation, which almost certainly is part of the larger Pacific Decadal Oscillation, are numerous and include the following. In the earlier period there are anomalous low level easterly winds over the near coastal region and east Australian coast accompanied by anomalously high precipitable water values. Further inland over central eastern Australia the anomalous southeast winds are linked to increased dust storm activity over the same area. In contrast, for the latter period there are anomalous low level northwest to westerly winds over the near coastal region and east Australian coast accompanied by anomalously low precipitable water values. This means that fronts with postfrontal south to southeasterly winds and dust storms sourced from the Lake Eyre region have affected the area much less in this period than the first period.

**ACKNOWLEDGEMENTS**

The authors wish to thank the Australian Bureau of Meteorology and Matt Bastin (Sydney), in particular, for providing much of the data and the NOAA-CIRES Climate Diagnostics Center for providing the NCEP reanalysis data.

**References**

Bureau of Meteorology, 1925: Australian Meteorological Observer's Handbook. Available from the Australian Bureau of Meteorology, GPO Box 1289, Melbourne, Victoria, Australia.

Ekström, M., G.H. Mctainsh and A. Chappell, 2004: Australian dust storms: Temporal trends and relationships with synoptic pressure distributions (1960-99), *Int.J.Climatol.,* **24,** 1581-1599.

Karoly, D.J. and L.M. Leslie, 2005: The impact of convective parameterization schemes on climate sensitivity. *Proc. Amer. Meteor. Soc*., Seattle, January 2005

Mantua, N.J., S.R. Hare, Y. Zhang, J.M. Wallace and R.C Francis, 1997: A Pacific Interdecadal Climate Oscillation with impacts on Salmon production, *Bull. Amer. Met. Soc.,***78,** 1069-1079.

Speer, M.S. and L.M. Leslie: Local to long-range dust transport over the Australian region, *Proc. Asia-Oceania Geosciences Society 2nd Annual Meeting,* June 2005, Singapore.

Sprigg, R.C. 1982: Alternating wind cycles of the Quaternary era and their influence on Aeolian sedimentation in and around the dune deserts of southeastern Australia. In *Quarternary dust mantles of China, New Zealand, and Australia,* ed. R.J. Wasson, 211-40. Proceedings of workshop at the Australian National University, Canberra, 3-5 December, 1980. Canberra, Australia: Australian National University Press.

Washington, R., M. Todd, N.J. Middleton and A.S. Goudie, 2003: Dust-Storm Source Areas Determined by the Total Ozone Monitoring Spectrometer and Surface Observations, *Annals of the Association of American Geographers,* **93(2),** pp. 297-313.

Zhang, Y., J.M. Wallace and D.S Battisti, 1997: ENSO-like Interdecadal Variability: 1900-93, *J. Climate*, **10,** 1004-1020.

*Proceedings of the Third International Symposium on Air Quality Management at Urban, Regional and Global Scales. 26-30 September 2005, Istanbul – Turkey*

# EXTREMELY HIGH CONCENTRATION OF TSP AFFECTED BY ATMOSPHERIC BOUNDARY LAYER IN SEOUL METROPOLITAN AREA DURING DUSTSTORM PERIOD

**H. Choi and C. H. Jang***

Kangnung National University, Department of Atmospheric Environmental Sciences, Kangnung, Kangwondo 210-702, Korea, du8392@hanmail.net
* Hanbat National University, Department of Civil & Urban Engineering, Daejeon 305-719, Korea, jangch@hanbat.ac.kr

## ABSTRACT

Hourly concentrations of TSP, PM10, PM2.5 near the griund surface at Seoul city were examined from March 20 to March 25, 2001 (duststorm event) in order to investigate the effect of duststorm on the local aerosol concentration, The ratios of between fine and coarse particles such as TSP to PM10, TSP to PM2.5 and PM10-PM2.5 to PM2.5showed that a great amount of dust transported from the origin of duststorm generation were remarkable with a maximum ratio of 9.77 between TSP and PM2.5. Back trajectories of air masses at ever 6 hour showed the movement of dust partilcles in the lower atmosphere near 500m ~ 1500m (atmospheric boundary layer), which implied to transport from Baotou in the inner Mongolia to the direction of Seoul city and then the back trajectories passed near southern border of Mongolia and Baotou through Zengzhou on the middle (3000 m height) and lower levels (500 m height) and finally reached Seoul city. So, the TSP concentration at Seoul city was partially influenced upon the duststorm, under the prevailing westerly wind and the transported aerosol could influence upon high concentrations of pollutants of TSP, PM10 and PM2.5 of the city. The sudden high concentrations of TSP and PM10 were found for few hours, especially at 15 to 18, March 22. At 1200 LST, before the passage of cold front through Korean peninsula, the convective boundary layer (CBL) near Seoul was not shallow, but at 1500 LST, under the frontal passage, the CBL was remarkably shallower less than 300 m, due to the compression of boundary layer under the intrusion of cold air and resulted in the increase of the TSP concentration, even though mixed layer above maintained almost the same depth. At 1800 LST shortly after the front passage, that is, near sunset, the nocturnal cooling of the ground surface could cool down air parcels, enhanceing the shallower nocturnal surface inversion layer and casuing the maximum concentration of TSP of 1388 $\mu g/m^3$ near Seoul city.

**Key Words :** TSP, PM10, PM2.5, Dust storm, Convective Boundary Layer

## 1. INTRODUCTION

In the past ten years, dust storms called Asian Dust, Yellow Sand and KOSA have frequently and periodically occurred under strong wind blowing soil in the dried area of the northern China included five provinces of Xinjiang, Inner-Mongolia, Ningxi, Shanxi, Gansu and Gobi desert in Mongolia, and the storms have transported a great amount of dusts to eastern China, Korea, Japan, even north America. Duststorm can remove several hundred thousand tons of sand and dust from dried area such as western and northern dried area of China or desert area (Chon, 1994; Chung et al., 2001; Chung and Yoon, 1996; Jigjidsuren and Oyuntsetseg, 1998; Middleton, 1986; Natsagdorj, and Jugder, 1992a).

Particulate matters during Asian Dust event in 2001 and 2002 could be transported along with westerly wind of about 20 m/s wind speed (Kim and Kim, 2003; Kim, et al., 2003). Zhang and Zhong (1985) estimated that about the half of the total quantity of particulate matter are deposited near the source area (30%) and re-distributed on a local scale (20%) and the other half of them are expected to be subject to long-range transport. The transported amount of dust can serve as one of the major particulate matter sources all across the Asia and Pacific.

In order to investigate aerosol cycle, Aerosol Characterization Experiment in Asia (ACE-ASIA) was performed by many scientific groups in many locations of east Asia of Korea, China and Japan in 2001 (Carmichael et al., 1997; Chung et al., 2003). During the period of ACE-Asia, major measurement and researches in Korea had been done at the Gosan Supersite of Jeju island in the southern Korea. In other sites, except for Gosan, some of scientists personally carried out the measurement of aerosol and among the sites, aerosol data used in this study were acquired at Seoul city, Korea (Kim et al., 2002). Most of previous researches on ACE-Asia experiment have been focused on chemical analysis and synoptic scale meteorological influence for the duststorm with usually Gosan site data, without detail explanation on the effect of frontal passage or the depth of atmospheric boundary layer on the local pollutant concentration.

Thus, the objective of this study is to precisely investigate the evolution of atmospheric boundary layer influencing upon the horizontal transportation of the dust and its vertical distribution on the local pollutant concentration and to explain the effect of frontal passage, considering synoptic and meso-scale motions of atmosphere.

## 2. NUMERICAL METHOD AND AEROSOL DATA

### 2-1. Numerical model and input data

A three dimensional of non-hydrostatic meteorological called MM5, V3.5 with an isentropic coordinate vertically was used for investigating meteorological phenomena during dust storm period from March 18 through 25, 2001. For the numerical simulation using the model, three-dimensional NCEP date of a horizontal resolution of $2.5^0$ x $2.5^0$ including topography, vegetation, snow cover or water, meteorological element-wind temperature, moist content, heat budget, sea surface temperature in the surface layer and sounding data on meteorological elements from the surface to 100 mb upper level were used as initial data for the coarse domain.

Then through the interpolation process of those information, modified input data were set for next triple nesting processes with grid numbers of 125 x 105 with horizontal 27 km interval and vertical grid number of 23 in the coarse domain and in the second domain, grid number of 82 x 82 with 9 km interval and in the third domain, grid number 61 x 61 with 3 km interval. $2.5^0$ degree interval terrain date was used for the largest domain and then the 0.9km interval data was used for fine mesh domain. MRF method was adopted as boundary layer process in the planetary boundary layer, simple ice method for the prediction was also considered. After the nesting process from a large domain to a small domain, author made a straight cutting line from the west toward east, that is, on the dust transportation root from the dust storm generation area, China toward Seoul district, Korea, in order to investigate vertical structure of meteorological distribution of wind, temperature, relative humidity, total cloud mixing ratio for moisture contents of the atmosphere and vertical velocity. In the first large domain, a straight cutting line lay in the line of Mogolia-near Beijing-Seoul-Kyoto-Pacific Ocean like; (10, 90), (130, 40), in the 2nd domain (60, 70) (100, 55) including Seoul city for cutting both upper trough line of cold low at 500 mb level and cold front of low-pressure near surface and in the 3rd domain including Seoul city, (10, 41) (55, 41), respectively

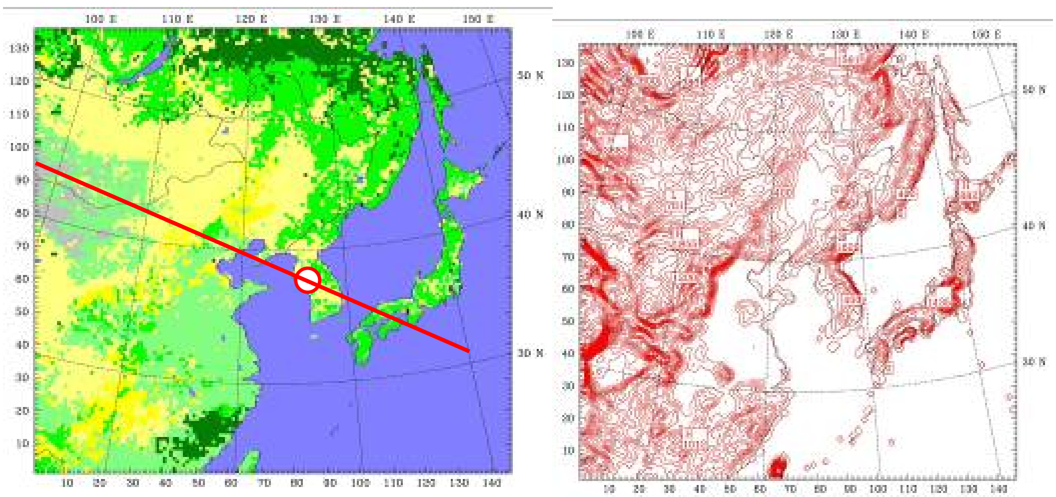


Figure 1. Land-use data and topography for a coarse domain of a horizontal grid size 27 km for MM5 model. Circle denotes Seoul city district, Korea.

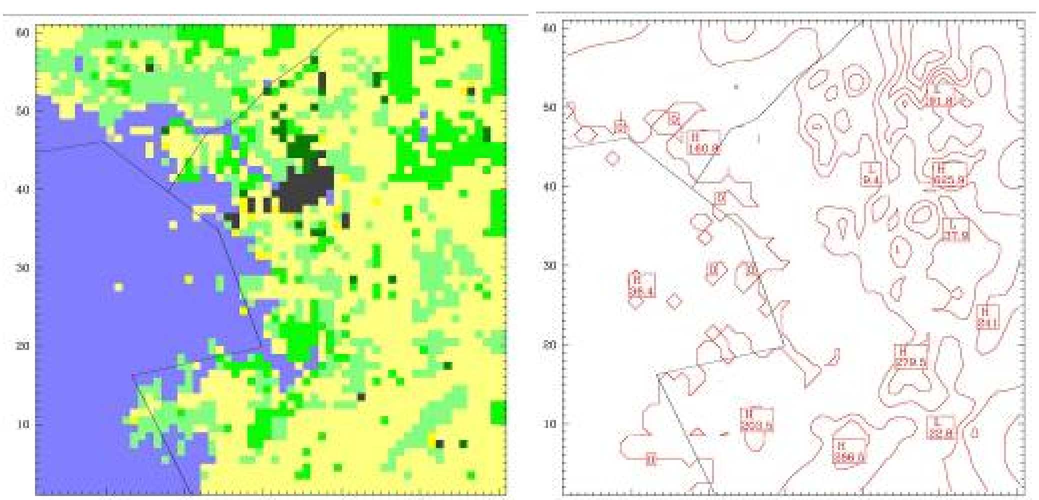

Figure 2. Land-use data and topography for a fine-mesh domain of a horizontal grid size 3 kmfor MM5 model including Seoul city. Major black part of the figure denotes Seoul metropolitan area.

## 2.2 TSP, PM10 and PM2.5 data in Seoul

In general, when the hourly TSP concentration is over 200 μg/m$^3$, one may refer to the effect of the duststorm to the local pollutant state in Korea. Before March 19, the concentration of TSP at Seoul was less than 200 μg/m$^3$ and from March 20, the TSP concentration started to increase over than 200 μg/m$^3$ and visibility became very bad less than 1 km. Thus, Korean Meteorological Administration announced that the effect of duststorm prevailed in the Seoul district.

During ACE-ASIA period from March through May, 2001, Prof. Kim (Kim et al., 2003), Sejong University with a measurement point (37$^0$32'N, 127$^0$04'E) performed the measurement of aerosol for his research from March through May, 2001 (Kim et al., 2002, 2003). The site of collection of particulate matter (PM) samples on the top of the 5$^{th}$ floor, Natural Science Building of the university in the eastern part of Seoul city consists of a moderately developed urban area, surrounded by a large-scale public park in the east, residential area in the north and west and commercial area in the south. After the measurement of the aerosol, some of hourly-data of aerosol from March 19 through 25, 2001 were permitted for author to use this study. Thus, much detail explanation on how to treat the measured data is given by Professor Kim's previous papers (Kim et al., 2003).

# 3. RESULT AND DISCUSSION

## 3.1 Local concentration of aerosol in Seoul: duststorm period

In the past 10 years, previous Asian Dust events were detected for few days or less per year, but the Asian Dust event days in 2001 were found with unexpectedly high frequency with 27 days from January to May. The measurements on duststorm and non-duststorm days were made on only weekday period, such as 11 days from March 19 to 31. Hourly concentrations of TSP, PM10, PM2.5 near the ground surface gave us an important information on how much different concentrations of coarse and fine particles between duststorm period and non-duststorm period. According to the report of Korean Meteorological Administration, duststorm event was detected from March 20 through March 25 in the Seoul district of Korea (Figure 3 and 4).

In general, the concentrations of TSP and PM2.5 during duststorm period were twice as high as the concentrations non-dustorm period. Maximum concentrations of TSP and PM2.5 were also found with values of 1388 μg/m$^3$ and 142 μg/m$^3$ at 1600 LST (LST= 9hours + UTC), March 22, 2001 with a ratio of 9.77 and at 1800 LST, with a ratio of 10.04. For this period, the measurement of PM10 was not successful due to some mechanical problems of the instrument, until 12o'clock on March 23. Then the measurement of PM10 continued to be to 0000 LST on April 1. The ratios of TSP to PM10, TSP to PM2.5 and PM10 - PM2.5 to PM2.5 were about 2, 6 and 2.

During the period of duststorm event, relative humidity was low around 50% with a minimum of 41%, but those vales measured by Korean meteorological Administration. The ratios of TSP to PM10, TSP to PM2.5 and PM10-PM2.5 to PM2.5 were examined in order to investigate the effect of duststorm on the local aerosol concentration, which accompanied a great amount of dust from the origin of duststorm generation. The ratios between fine and coarse particles were remarkable.

In general, the for non-duststorm period, since small size particles are observed in Korea, the Ministry of Environment, of Korean Government measure PM10 concentration instead of TSP in the recent years.

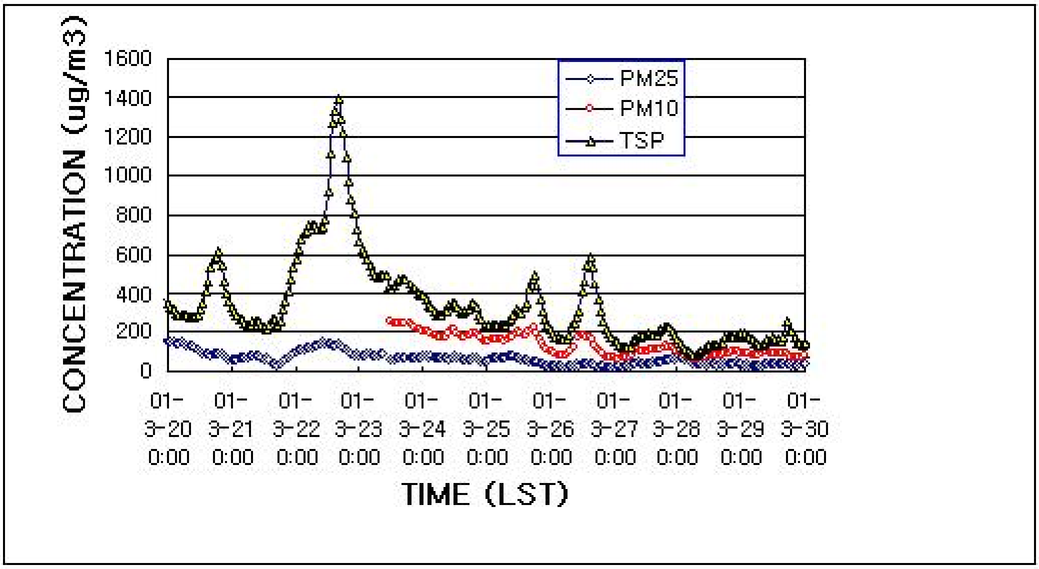


Figure 3. Hourly based concentration of PM2.5, PM10 and TSP from March 20 through 30, 2001, including duststorm and non-duststorm periods.

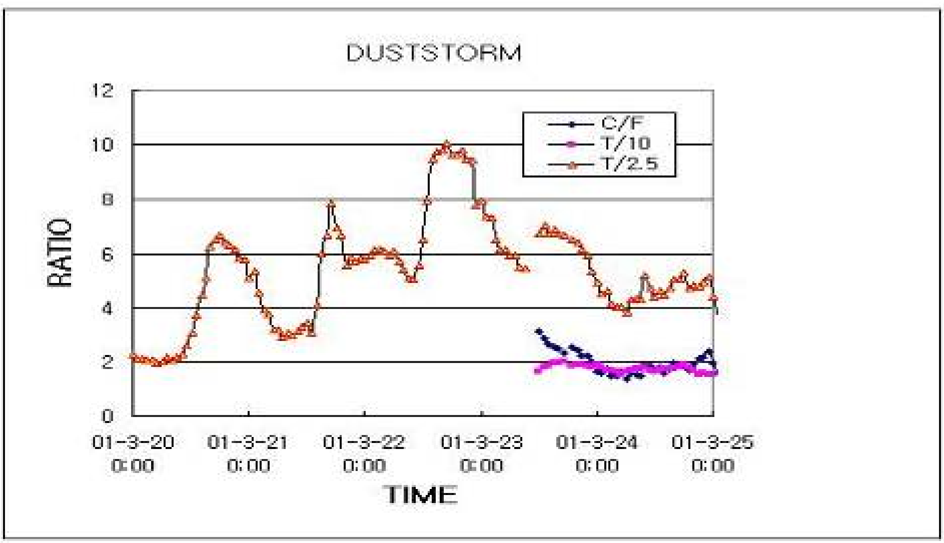


Figure 4. Ratio of TSP to PM10, PM2.5 and PM10-PM2.5 to PM2.5 during duststorm period from March 20 through March 25, 2001 at Seoul city, Korea.

**3.2 Local concentration of aerosol in Seoul: non-duststorm period**

During the non-duststorm period, the ratios of TSP to PM10, TSP to PM2.5 and PM10-PM2.5 to PM2.5 were found with values of about 2, 4 and 0.5, but on March

26, the ratios reached 16.37, 3.4 and 3.81 (Figure 5). On March 26, the aerosol concentration was still under the influence of duststorm, even though visibility was remarkably much improved than the previous days and Korean Meteorological Administration reported that the effect of the duststorm disappeared at Seoul city. Thus, we classified March 26 was to be duststorm day. Through the comparison of TSP, PM10 and PM2.5 between non-duststorm period and duststorm period, coarse particles made a great contribution to the increase of total suspended particulate concentration for the period of duststorm period.at Seoul city, and the ratio of coarse particle to fine particle such as (PM10 - PM2.5)/PM2.5 during the duststorm period was approximately twice as much as that during the non-duststorm period. It means that although a great amount of dust during duststorm period were transported into the Seoul district three times as much as that during non-duststorm period, the amount of coarse particle only twice increased.

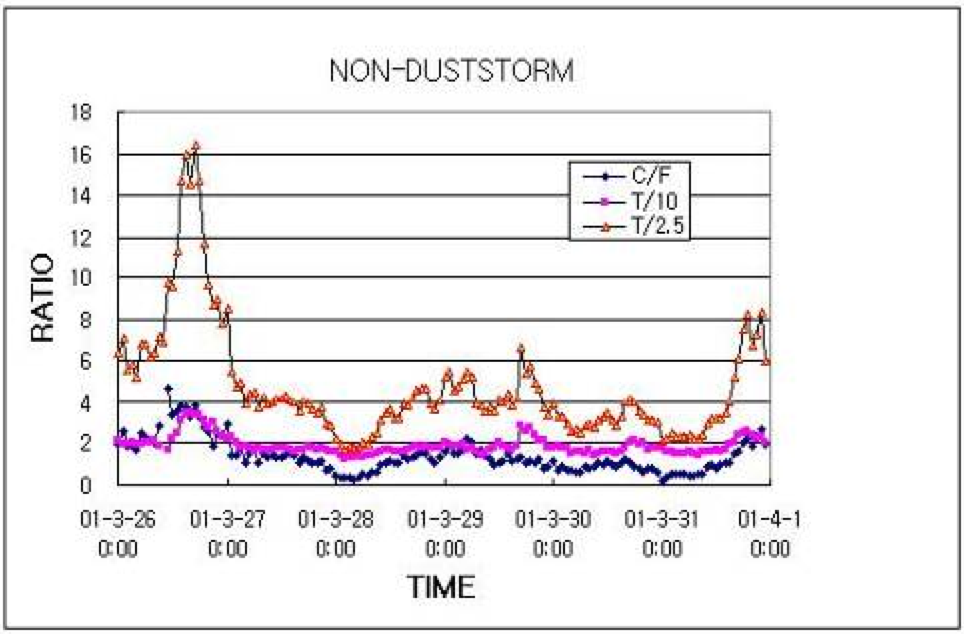


Figure 5. Ratio of TSP to PM10, PM2.5 and PM10-PM2.5 to PM2.5 from March 26 through March 31, 2001. March 26 was treated in non-duststsorm period, as KMA declared non-duststorm day.

### 3.3 Origin of air masses during duststorm and non-duststorm periods

In order to investigate the effect of the dust transported from China on the concentrations of TSP and PM10 at Seoul city, back trajectories of air masses at ever 6 hour were given for duststorm period from March 20 to 25, 2001, including its beginning stage. Backward trajectory of air masses are seen separately in figures. Three levels through the surface to 10km height such as 500m ~ 1500m (showing roughly atmospheric boundary layer), 3km ~ 4500m (middle atmosphere) and 5000m ~ 6000m (high atmosphere including the effect of stratosphere) were considered.

In the inside maps of backward trajectory, trajectories in the upper part indicate the movements of air masses on each levels and ones in the below part indicate the movements of air masses from upper level toward lower level or not. Air trajectories beginning stage of DS on from March 19 before the detection of DS effects at Seoul city gave us that air masses in the upper and middle atmospheres of 5 km and 3km heights passed through in the middle or north-eastern part of Mongolia.

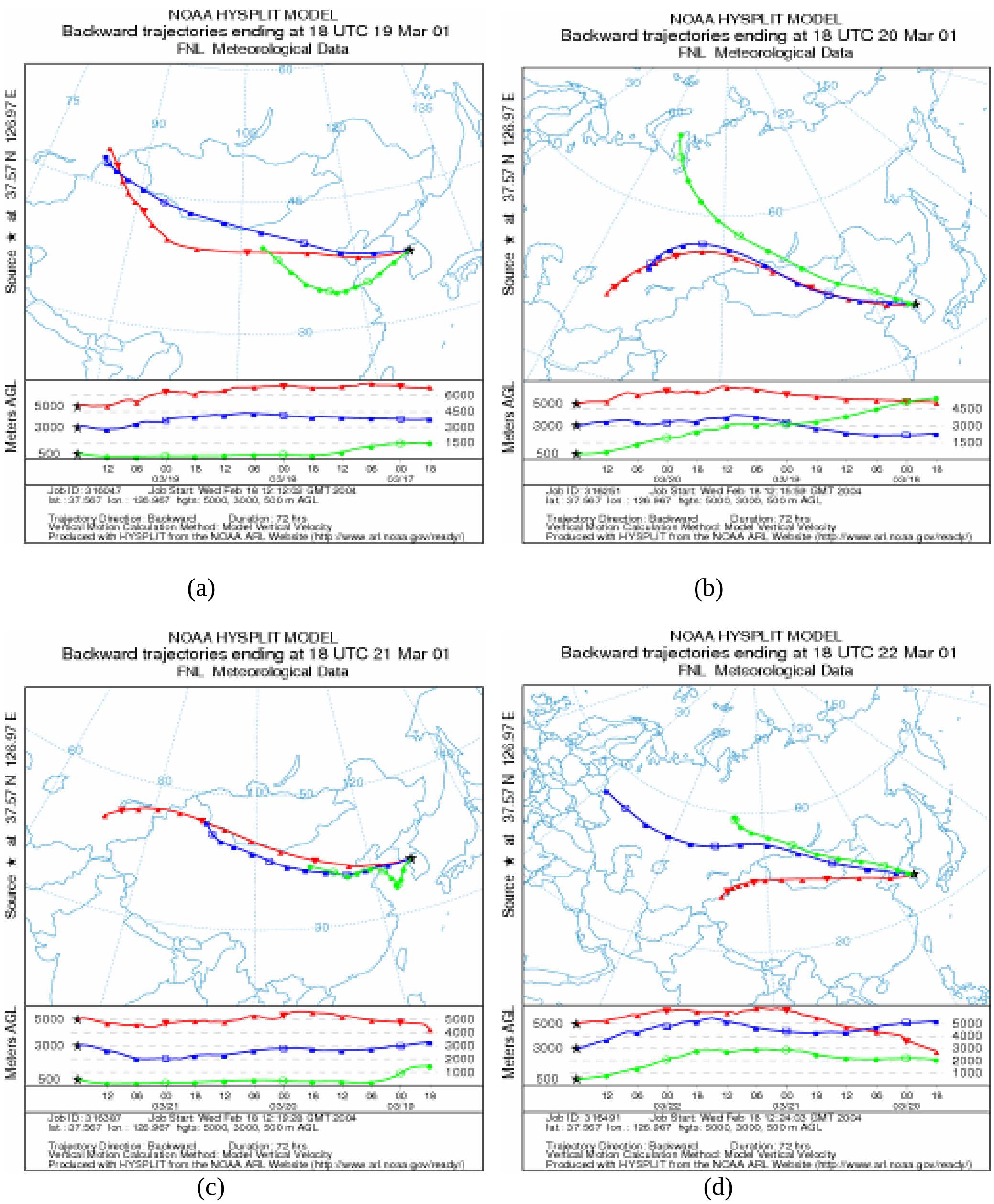


Figure 6. Back trajectory at every 6 hour on 3 levels-5000m (high level; red), 3000m (middle level; blue) and 500m (low level; green) over the ground at Seoul on March 19, 20, 21 and 22, 2001.

It means that air parcels reflecting the environmental aspects in the Siberia and steppes in Mongolia may be assumed to be clean and these air masses are transported into Seoul district. Air masses in the lower atmosphere near 500m ~ 1500m (atmospheric boundary layer) are also transported from Baotou in the Nei Mongo (in the border of northern China) toward Seoul city, showing different pattern to the upper and lower levels. After back trajectories in the middle and lower levels passed near southern border of Mongolia and Baotou through Zengzhou and Xuzhou and finally reached Seoul city, the TSP concentration at Seoul city was partially influenced upon the duststorm.

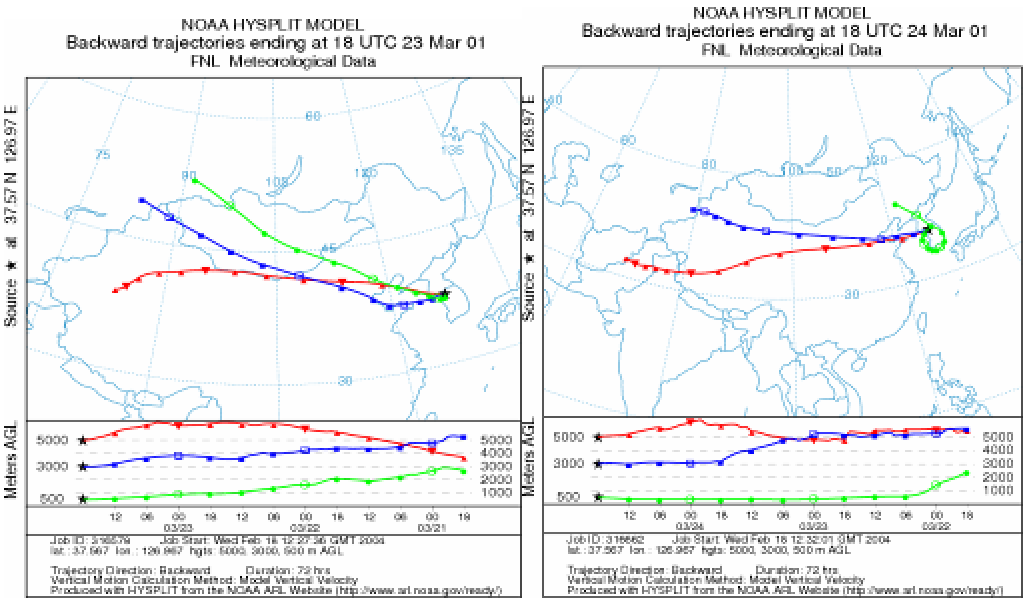

(a) (b)

Figure 7. As shown in Figure 6, except for at Seoul on March 23 and 24, 2001.

Through March 20 to 25 in the main stage of DS event in Korean side, air masses in the 3km and 5km height levels, which blew off from Ximiao, Ningxia and Lang Shan near Nei Mongo below the southern part of Mongolia passed through the northern part of China, reaching the Seoul district. The dust blew off from the ground surface in the source region horizontally under the strong surface wind was uplifted into the atmosphere above at least 3km height over the ground surface and should be transported through Beijing area into Seoul district under the prevailing westerly wind. The transported aerosol could influence upon high concentrations of pollutants of TSP, PM10 and PM2.5 of the city. From back trajectories of air masses, we can partially understand the path of air parcel and from which level the air parcel moved down to the ground surface, vice versa. Since back trajectory does not directly reflect all directions of moving parcels and only their major direction, it is also indirect and qualitative method for the transport of dust to the interested area.
In this research, the sudden high concentrations of TSP and PM10 were found for few hours, especially at 15 to 18, March 22, 2001. One of important goal is to find out why such a sharp concentration of the TSP took a place, even though transported amount of dust was assumed to be in the same for several hours. From the back trajectory, it is difficult to explain the reason why sudden high concentration of TSP occurred at 1800 LT, March 22. The driving mechanism is given in detail in the next section.

From March 26 through, differently from no detection of duststorm effect at Seoul, back trajectory still showed that air masses in the upper atmosphere near 5000 m and 3000 m passed through the southern Monoglia and Nei Mongo, and one in the lower atmosphere had a similar path, even their paths were slightly deviated. Sometimes their trajectories lay on the eastern Mongolia, but these kinds of trajectories maintained until March 26 and TSP concentration at Seoul was still high, but visibility was not bad, except for good visibility until March 31.

### 3.4 Atmospheric boundary layer effect

In the general, during the day, thermal convection on the ground surface of plain area like Seoul city (basin) occurs due to solar heating process to the ground surface, and then heated air parcel from the soil has bouncy force and is uplifted to the convective boundary layer. The emitted pollutant from the source of the ground is also accompanied to the top of the CBL and it should be merged, resulting in a low concentration of pollutant near the ground surface. Oppositely, nighttime cooling of the ground surface produces nocturnal surface inversion layer (NSIL). Shallow surface inversion layer slowly moves down toward the ground surface and air parcels inside the NSIL moves also down to the surface, resulting in calm wind or very weak wind, call a stabilization of air. The uplifted pollutant during the day also moves down and the emitted pollutant for nighttime hours can not move upward by the constraint of the NISL. The pollutant should be merged near the surface, showing the increase of the pollutant concentration at night.

In the coastal region in the left side of Seoul city , during the day, easterly sea breeze due to higher air temperature on the left side of Figure 2 than air temperature over inland basin, Seoul city surrounded by mountains and sea in its west outlet is associated with valley wind due to higher air temperature than that over the mountain surface on the right side, resulting in sea-valley wind from sea toward top of the mountain, which drives onshore wind. The emitted pollutant or particulate matters from the ground surface and transported pollutant from the sea side should all together go toward the top of the convective boundary layer of the city and sequentially go toward the top of the mountain, resulting the high concentration of the TSP in the mountain top, while the TSP concentration is low near the ground surface of the city. Since Seoul city is surrounded by mountains and sea in the west outlet, it has a characterists of coastal and urban topographical effects, its TSP concentration is generally low (Choi, 2004).

However, at night, land breeze occurred from inland toward sea due to cooler air temperature over the land surface than the sea surface. Simultaneously, cooler air temperature over the mountain than that over the inland basin at the same altitude produces mountain wind to blow from the mountain top toward the basin. Then mountain wind associated with land breeze produces land-mountain breeze in the city and results in offshore wind toward the sea in the left of Seoul city.

In addition, we have to consider the effects of atmospheric boundary layer. For instance, between 0900 LST and 1200 LST, March 22, there was a passage of cold front through Korean peninsula. Before the passage of cold front, the convective boundary layer (here white color area in the vertical distribution of potential vorticity) near Seoul was not shallow, but during the passage of the front, convective boundary layer was remarkably shallow, resulting in the compression of boundary layer and the increase of the TSP concentration (Figure 8). Normally, small size particle easily floats up to the convective boundary layer, because its settling velocity is too small, but in the case of duststorm, a great amount of the coarse dusts of large size were observed in the study area (Figure 3 and 4). Thus, the dusts also move down to the ground surface, even inside the convective boundary layer.

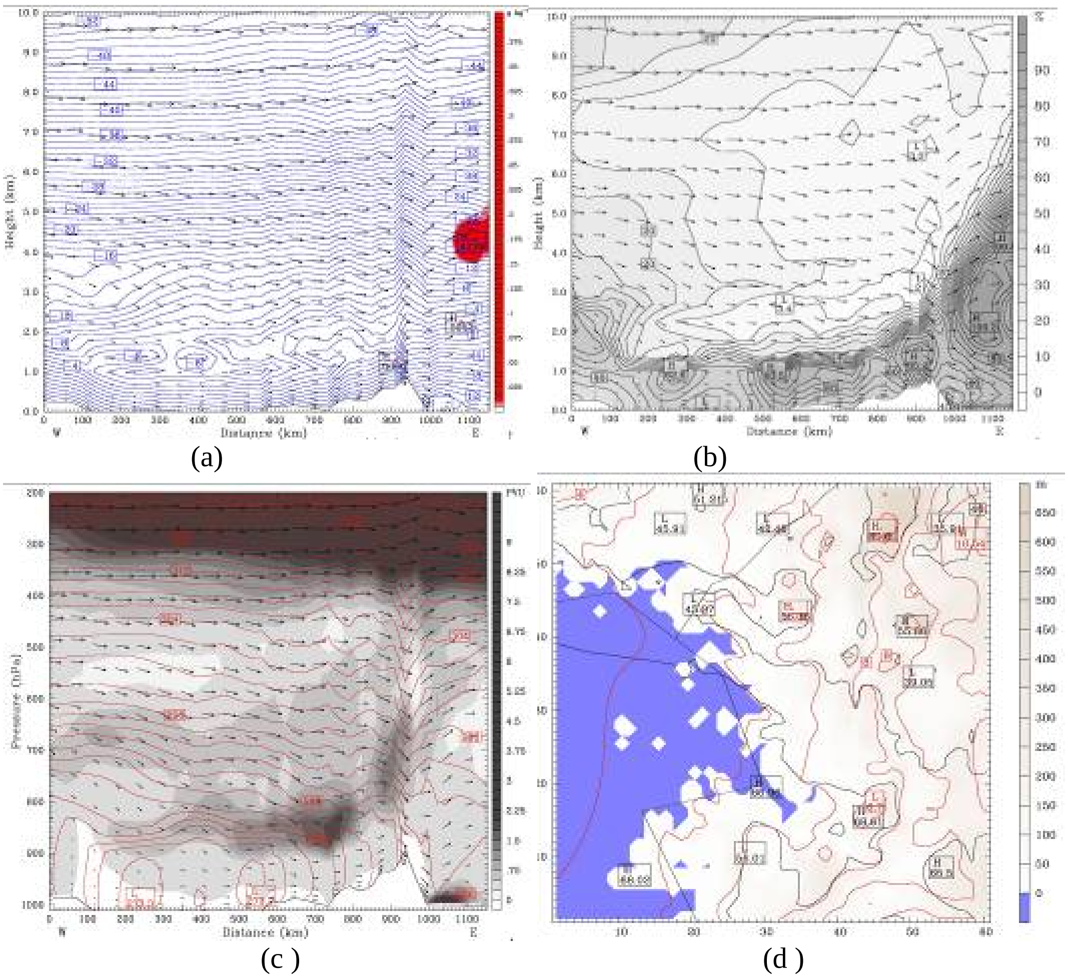


Figure 8. (a) Vertical distribution of air temperature ($^{0}$C)-cloud mixing ratio (g/kg)-wind vector (m/s) on the root of duststorm from China to Seoul city, (b) relative humidity (RH; %)-wind vector (m/s), (c) Ertel potential vorticity (PVU-a function of diabatic and frictional terms. bottom white-unstable layer, gray-mixed layer, dark black-stable layer) and (d) horizontal air temperature ($^{0}$C)-RH in Seoul city at 1200 LST, March 22. In Figure (c), unstable layer (white color near the surface of 50 ~ 1000 on x-axis; Seoul city (700 ~ 750)) is shallow.

On the figures of vertical distribution of air temperature at 1200 LST and 1500 LST, March 22, 2001, air temperature was different front of Seoul city and rear, especially relative humidity was much lower in the left hand side than right hand side, due to the temperature contrast. The intrusion of cold air could more cool down the ground surface, resulting in the shallower nocturnal surface inversion layer near Seoul city and the maximum concentration of TSP (Figure 9). Under the frontal passage, the depth of CBL less than 300 m, even though mixed layer above maintained almost the same depth. Thus, the shrunken CBL may make a great contribution to the increase of the TSP concentration.

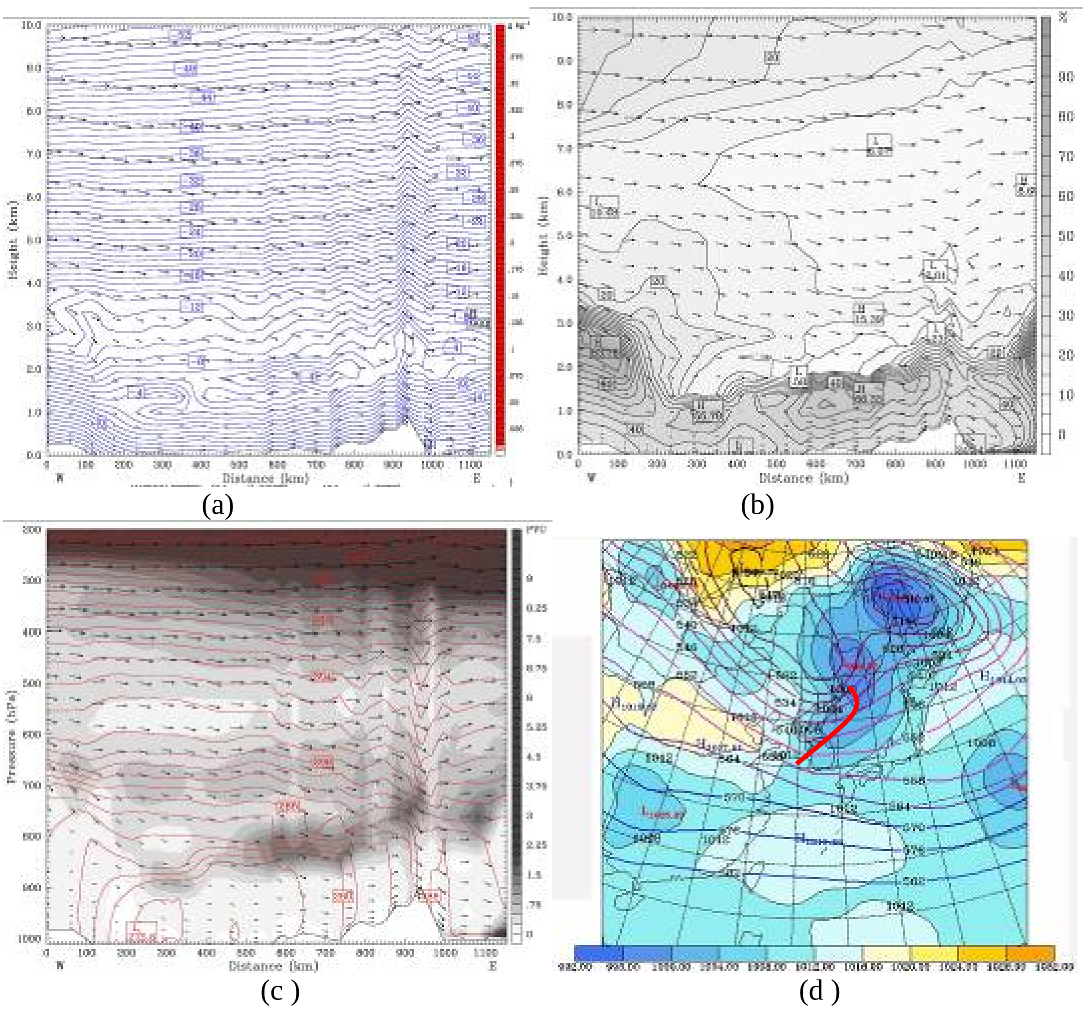

Figure 9. As shown in Figure 8, except for 1500 LST, March 22 and (d) geopotential height at 500 mb level and mean sea surface pressure (red line-surface cold front). In (c), unstable layer (white color near the ground surface of 400 ~ 750 on x-axis; Seoul city (700 ~ 750)) is much shallower than that at 1200 LST (before frontal passage). In (d), Seoul is located in above part of cold front tail.

At this time, the transported amount of dust from the duststorm area was almost the same at Seoul, including the whole Korean peninsula by the numerical simulation by Uno et al. (2001), but the TSP concentration by the measurement of high volume sampler was much higher after the frontal passage than before it (Figure 9).

**4. CONCLUSION**

Shortly after the cold frontal passage over Seoul city, even there was in the reduction state of the long-range transported amount of the dust from the southern part of

Mongolia toward Seoul city, Korea, the extremely high concentration of TSP in Seoul city occurred at 1600 LST. When and after the cold front passes the Seoul area, the atmospheric boundary layer, especially convective boundary layer was much shrunken than before its passage, with the depth of CBL less than 300 m, even though mixed layer above maintained almost the same depth. Thus, the shrunken CBL may make a great contribution to the increase of the TSP concentration. Simultaneously, the positive association of large scale meteorological motion with boundary layer forcing can make a great contribution to the high concentration of TSP in the local area, even in the large area.

## 5. ACKNOWLEDGEMENTS

Authors much thanks the College of Environmental Sciences, Peking University, China for using computer system and anaysis and Prof. K. H. Kim, Sejong University, Korea for using aerosol data of March in 2001 for Asian Dust event.

## REFERENCES

Carmichael, G. R., Hong, M. S., Ueda, H., Chen, L. L., Murano, K., Park, J. K., Lee,H., Kim, Y., Kang, C., Shim, S., 1997. Aerosol composition at Cheju Island, Korea. J. Geophy. Res., 102(5), 6047-6061.

Choi, H., Zhang, Y. H. Takahashi, S., 2004. Recycling of suspended particulates by the interaction of sea-land breeze circulation and complex coastal terrain. Meteor. & Atmos. Phys., 87, 109-120.

Chon, H., 1994. Historical records of yellow sand observations in China. Res. Environ. Sci., 7-6, 1-11.

Chung, Y. S., Yoon, M. B., 1996. On the occurrence of yellow sand and atmospheric loadings. Atmos. Environ., 30, 2387-2397.

Chung, Y. .S., Kim, H. S., Jugder, D., Natsagdorj, L., Chen, S. J., 2003. On sand and duststorms and associated significant dustfall observed in Chongju-Chongwon, Korea. Water, Air, and Soil Pollut: Focuss 3: 5-19.

Jigjidsuren, S., Oyuntsetseg, S., 1998. Pastureland utilization problems and ecosystem. Ecological sustainable development. Ulaanbaatar, No.2, 206-212.

Kim, H. K., Kim, M. Y., 2003. The effects of Asian dust on particulate matter fractionation in Seoul, Korea during spring 2001. Atmos. Environ., 51, 707-721.

Middleton, N. J., 1986. A geography of dust storms in southwest Asia. J. Climate., 6, 183-196.

Natsagdorj, L., Jugder, D., 1992a. Statistics method for prediction of dust storms over the Gobi and steppe area in Mongolia in spring. Scientific report, Ulaanbaaatar, pp83.

Zhang, Y., Zhong, Y., 1985. The simulation and diagnosis for a strong wind associated with northeast low. Acta Meteor. Sinica, 43, 97-105.

Uno, I., Carmichael, G. R., Streets, D. G., Tang, Y., Yienger, J. J., Satake, S., Wang, Z., Woo, J. H., Guttikunda, G., Uematsu, M., Matsumoto, K., Tanimoto, H., Yoshioka, K., Iida, T., 2003. Regional chemical weather forecasting using CFORS: Analysis of surface observations at Japanese island stations during the ACE-Asia experiment. J. Geophy. Res., in press.

*Proceedings of the Third International Symposium on Air Quality Management at Urban, Regional and Global Scales. 26-30 September 2005, Istanbul – Turkey*

# METHODOLOGY FOR QUANTITATIVE ESTIMATION OF ATMOSPHERIC LOADINGS DURING ASIAN DUST EVENTS OBSERVED OVER KOREA IN 2002

**Sang-Keun Song, Yoo-Keun Kim, and Hwa Woon Lee**
Department of Atmospheric Sciences, Pusan National University, Busan, South Korea, songsk@pusan.ac.kr

**ABSTRACT**
Dust transport and its impacts, which are frequently observed in East Asia, have attracted public attention increasingly in recent years. In this study, in order to quantitatively estimate the impacts of Asian dust transport on the air quality in South Korea, we analyzed the relationship between Asian dust frequency and meteorological variables (e.g., wind speed, air temperature, relative humidity, and aridity) in the source regions and estimated the dust emissions from a transport model, well showing the distribution of dust particles concentration. The event periods chosen in this study are 21-23 March 2002 (or March 2002 event) showing the biggest dust phenomenon over Korea and 11-12 November 2002 (or November 2002 event) contrasting with the dust event in the springtime. We here found that there was a close correlation between Asian dust frequency and three variables (wind speed, aridity, and relative humidity). In particular, the dust frequency with high-value aridity in Gobi Desert and its surrounding regions was higher than that in the other regions. From the modeling results based on the selected input variables, we found that a total dust emission amount in the source regions was estimated to be approximately $3.01 \times 10^6$ ton and $0.57 \times 10^6$ ton in March and November event, respectively. In addition, the mass contributions of the total emission amount to atmospheric loadings categorized into inflow, transit, and deposition amounts of Asian dust were evaluated. As the results, the ratio of the total emission amount to dust inflow (approximately 1.03 (0.17) $\times 10^6$ ton in March (November) event) was found to be 0.34 and 0.30, respectively. The ratio of the dust inflow amount to transit and deposition amount to Asian dust were found to be 0.69 (0.72) and 0.31 (0.28) for two dust events, respectively.

**Keywords:** Dust impacts; Dust loadings; Quantitative estimation; Inflow amount; Transit amount; Deposition amount

*Proceedings of the Third International Symposium on Air Quality Management at Urban, Regional and Global Scales. 26-30 September 2005, Istanbul – Turkey*

# PREDICTION OF DUSTSTORM EVOLUTION BY VORTICITY THEORY

**H. Choi and Doo Sun Choi**

Kangnung National University, Department of Atmospheric Environmental Sciences, Kangnung, Kangwondo 210-702, Korea, du8392@hanmail.net

## ABSTRACT

The relation of duststrom in Mongolia and in northern China with vorticity was investigated from March 19 through 31, 2001, using three-dimensional nonhydrostatic model-MM5. Outside area of the maximum negative geopotential height tendency ($\partial\Phi/\partial t$) at the 500 mb level, the area of maximum negative vorticity which induces the strong upward motion of air coincides the area of the duststorm generation in the inner Mongolia of the northern China under relative humidity less than 30 % and wind speed over 8 m/s. The transportation of dust arisen after the source region always follows the negative vorticty area in the downwind side. The region of duststorm generation is the area of maximum negative vorticity and it is the same region of the unstable atmospheric layer (negative potential vorticity layer (PV)) near the ground surface in the vertical distribution of baroclinic PV, which is a function of diabatic heating and frictional terms with respect to time.

Dust parcels during the day are uplifted to about 700 mb level (about 3 km), where potential temperature gradient with pressure ($\partial\theta/\partial p$) is zero, but its uplift motion is confined to 700 mb level, where stable upper atmosphere influenced by the stratosphere exists. Convective boundary layer (CBL; negative PV value) exists in less or more than 1 km and initially dust particle floats from the ground surface to the mixed layer (ML) of about 1.5 km above the CBL and it remains inside the ML. Westerly wind drives the particles to the downwind side. At night, a shallow stable boundary layer near the surface (inversion layer; big positive PV) is developed and the particles inside the stable layer merge to the ground surface and move downwind side. The dust particles in the ML still move downwind side and their dry deposition from the top of stable layer into the surface occurred.

**Key Words :** Duststorm, Vorticity, Potential vorticity, Convective boundary layer, Stable Layer

## 1. INTRODUCTION

Duststorm, called another name of sandstorm or Yellow Sand, KOSA is one of severe meteorological phenomena, where strong winds blow a great amount of sand and dust (even small rock) from desert or dried area into the lower atmosphere and the dusts to travel for long distances out to several thousand kilometers, resulting in the reduction of the visibility less than 1km. As the air turbidity increases with the occurrence of duststorm, the amount of solar radiation reaching to the ground surface reduces and the reduction of solar radiation can cause a great influence upon climate in the Asian continent, partially other continent like northern America.

Asian dust mainly originated from elevated ground at 1500 m or above sea level in Taklamakan, Gobi and Ordos deserts and Loess plateau and have seasonal cycles as generally observed in the dry season, spring. The threshold value of wind velocity for the dust mobilization of dustorm in the Loess Plateau and Gobi desert is in a range of 10 m/s ~12 m/s from field observation and wind tunnel experiments (Qian and Hu, 1997). Xuan and Sokolik (2002) suggested that the threshold valve of friction velocity were in a range of 25 cm/s to 70 cm/s, depending upon particle size and soil type. Tegen and Fung (1994) and Zhang and Zhong (1985) investigated that regions of duststorm occur more than 30 days per year coincide with those regions with relative humidity of air less than 40%, which is the representation of the surface water content of the soil layer.

As previous mentioned, statistic method and numerical simulation for the estimation of the dust amount from the origin of duststorm have been done, but unfortunately, most of previous research papers have not given us detail explanation on the generation of duststorm from meteorological concern, even though synoptic scale meteorological explanation using mainly weather map on the strong wind field near the surface, including few kinds of additional maps has existed. Meteorological approach was usually focused on the beginning stage of the generation of duststorm and how weather was for the formation of the duststorm, considering synoptic weather situation (Austin and Midgley, 1994; Bates et al, 2003; Carmichael, 1997; Chung et al., 2003; Fuelberg et al., 2003; Reed, 1979; Reed and Albright, 1986) . For quantitatively estimation of the duststorm, most of papers have been focused on the evaluation of dust amount from the soil surface into the atmosphere, but unfortunately there have been not much explanation on the generation of duststorm from meteorological point of views such as what kinds of meteorological motion could influence on the generation of the duststorm, rather than simply calculation of generated amount of the dust.

Thus, the objective of this study is to suggest a prediction technique for the duststorm generation and authors would like to explain the generation mechanism on the formation of duststorm and the propagation area of the duststorm by vorticity theory, regarding the contribution of baroclinic potential vorticity to the development of atmospheric boundary layer and the vertical and horizontal dispersion of the dust in the vicinity of the source region.

## 2. NUMERICAL METHOD AND VORTICITY THEORY

### 2-1. Numerical model and input data

A three dimensional of non-hydrostatic meteorological called MM5, V3.5 with an isentropic coordinate vertically was used for investigating meteorological conditions for the generation of dust storm during the period of March 18 through 25, 2001. Three-dimensional NCEP date of a horizontal resolution of $2.5^0$ x $2.5^0$ including topography, vegetation, snow cover or water, meteorological element-wind temperature, moist content, heat budget, sea surface temperature in the surface layer and sounding data on meteorological elements from the surface to 100 mb upper level were used as initial data for the coarse domain. Then interpolated input data were set for next triple nesting processes with grid numbers of 125 x 105 with horizontal 27 km interval and vertical grid number of 23 in the first coarse domain and in the second domain, grid number of 82 x 82 with 9 km interval and in the third domain, grid number 61 x 61 with 3 km interval. $2.5^0$ degree interval terrain date was used for the largest domain and then the 0.9km interval data was used for fine mesh domain. MRF method was adopted as boundary layer process in the planetary boundary layer, simple ice method for the prediction was also considered. After the nesting process from a large domain to a small domain, authors made a straight cutting line from the west toward east, which was major transportation root of dust from the dust storm generation area, China toward Japan, in order to investigate vertical structure of meteorological distribution of wind, temperature, relative humidity, total cloud mixing ratio for moisture contents of the atmosphere and vertical velocity. In the first large domain, a straight cutting line lay in the line of Mogolia-Beijing-Seoul-Kyoto-Pacific Ocean like; (10, 90), (130, 40), respectively

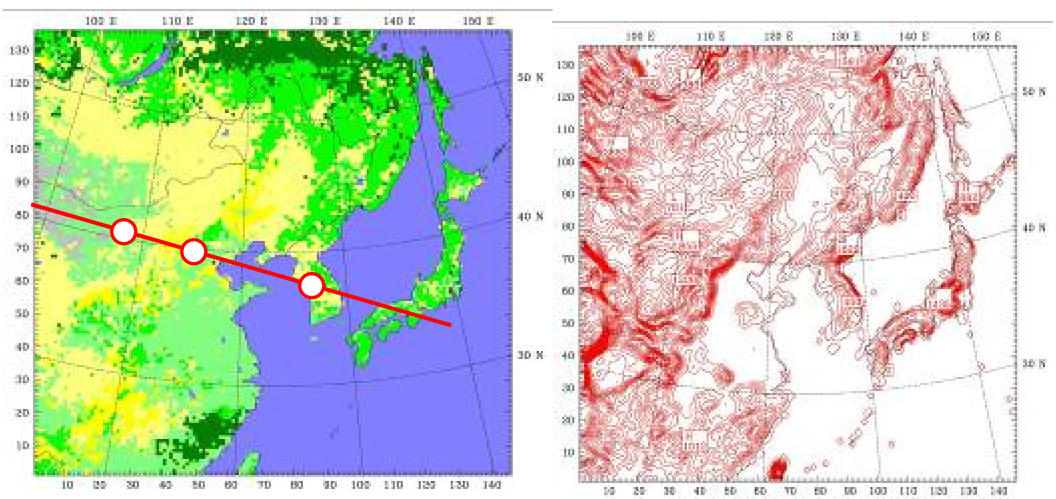

Figure 1. Land-use data and topography for a coarse domain of a horizontal grid size 27 km for
MM5 model. Circles denote Neimongo, Beijing (China) and Seoul (Korea).

**2-2. Vorticity theory**

Rossy (1937, 1940) insisted that potential vorticity on the isentropic surfaces was conserved for frictionless and adiabatic flow. Reed and Sanders (1953) used potential vorticity as a tracer and explained that air in middle and upper tropospheric fronts originated in the stratosphere. Chen et al (1991), Reed (1979), Reed and Albright (1986) and Sanders and Gyakum (1980) explained cyclogenesis and the development of frontal zone using vorticity theory in detail. Later, on the figures produced from the results of numerical simulation on potential vorticity using MM5 model in this research, a large value of potential vorticity is shown in the upper tropospheric atmosphere and sometimes is folded into the lower atmosphere. Haynes and McIntrye (1987) showed that potential vorticity could be diluted or concentrated

only by flow across isentropes: it cannot be created or destroyed within a layer bounded by isentropic surfaces.
However, if diabatic heating or frictional torques are present, potential vorticity is no longer conserved. It means that potential vorticity can be create or destroy and be away from the isentropes. So, if we consider frictional term with the diabatic vertical and horizontal advection terms on the horizontal momentum equation in isentropic coordinates, total derivative isentropic potential vorticity equation can be given by

$$\frac{\tilde{D}P}{Dt} = \frac{\partial P}{\partial t} + \mathbf{V} \cdot \nabla_\theta P = \frac{P}{\sigma}\frac{\partial}{\partial \theta}(\sigma\dot{\theta}) + \sigma^{-1}\mathbf{k} \cdot \nabla_\theta \times \left(\dot{\mathbf{F}}_r - \dot{\theta}\frac{\partial \mathbf{V}}{\partial \theta}\right)$$

Here the density in (x, y, θ) space is defined as $\sigma \equiv -g^{-1}\partial P/\partial\theta$ and $P \equiv (\zeta_\theta. + f) / \sigma$ is Ertel potential vorticity, considering diabatic term in the first of right hand side and frictional term in the second. If the diabatic and frictional terms can be evaluated, it is possible to determine the evolution of the P following the horizontal motion on an isentropic surface. When the diabatic and frictional terms are small, potential vorticity approximately conserved following the motion on isentropic surfaces. However weather disturbances that have sharp gradients in dynamical fields, such as jets and fronts, even the generation of duststorm are associated with large anomalies in the Ertel potential vorticity (baroclinic potential vorticity) in the nonhydrostatic atmosphere.
At 500 mb contours and 1000 mb contours, there is strong vertical motion in the right hand side of trough of geopotential height at 500 mb above the warm sector in the right hand side of cold front at the surface, owing to differential relative vorticity advection and temperature advection. Ertel's potential vorticity theory have usually been focused on the relatively large scale motion of air regarding its small scale disturbance less than few thousand kilometers, but this theory is adopted to the atmospheric boundary layer with comparatively much smaller scale than general meteorological phenomena. In this case, the value of PVU is not necessary to be positive, but it can be negative or positive in the atmospheric boundary layer.

## 3. RESULT AND DISCUSSION

### 3.1 Vorticity effect on the duststorm generation

At 0000 UTC (0800 in China; 0900 LST in Korea), March 19, 2001, at the beginning stage of duststorm in Nei-Mongo, if relative humidity (RH) presenting the moisture content of air attached soil layer on the surface layer is over than 40%, under strong surface wind more than 6 m/s, wind can not generate dust from the surface, but it can blow the dust off soil layer under RH less than 30% (Yamamoto et al., 2003). As Zhong' research (1985) indicates that the regions of duststorm occurred more than 30 days per year coincide with those regions with relative humidity of air less than 40%, which is the representation of the surface water content of the soil layer.
In Neimongo, RH was 30% less or more, as shown in weather map and in the vertical distribution of RH simulated by MM5 meteorological model (Figure 2 and 3). A narrow zone of isobaric contours lay from the southern part of Mongolia (NW)

toward Zheongzhou (SE) in China and produced strong northwesterly wind higher than 10 m/s and that area was in a good condition for the generation of the dust (Chung, et al., 2003). However at 500mb, positive relative vorticity advection is a maximum above the surface low, while negative relative vorticity advection is strongest above the surface high.

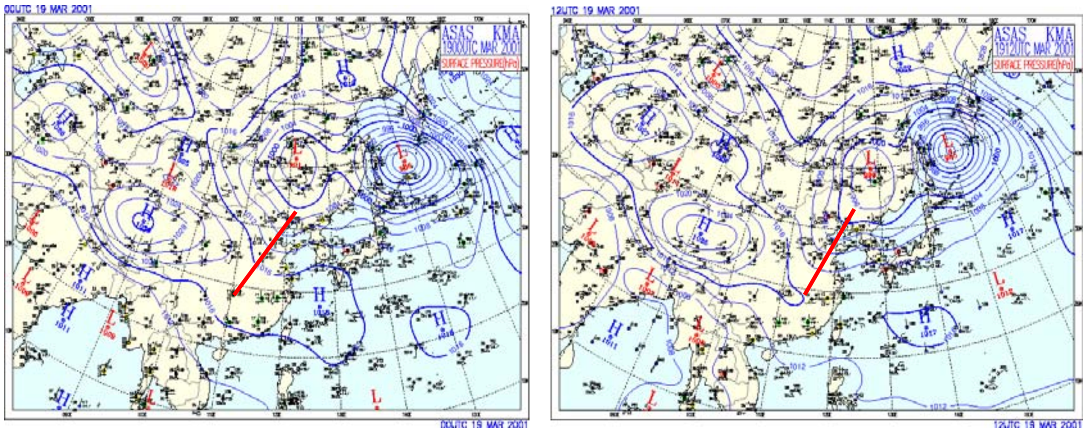

(a) (b)

Figure 2. Surface weather map (a) 00 UTC (09 LST) and (b) 12 UTC, March 19, 2001.

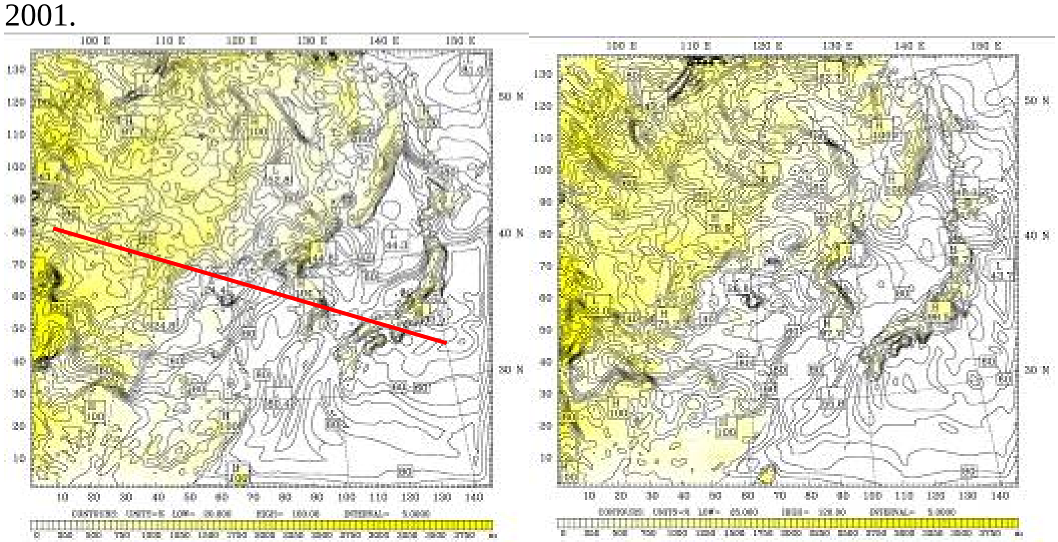

(a)

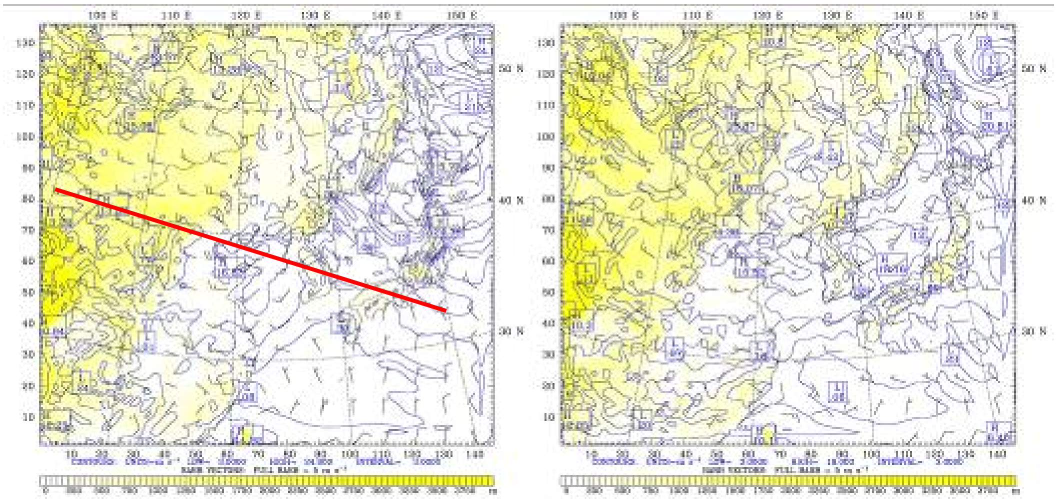

(b)

Figure 3. (a) Relative humidity (%) and (b) wind seed (m/s) at 00 UTC and 12UTC, March 19, 2001, from MM5 model simulations. Red line indicates a strait cutting line from the NW to the SE direction passing through Beijing, Seoul, Kyoto cities.

Next figures indicated that negative vorticity area (white color area) is found beside the maximum negative geopotential tendency, that is, in the left hand side of upper trough of cold low in Figure 4. Through the comparison of vorticity field with GMS (DCD-IRI-2) satellite picture provided by Japan Meteorological Agency, the area of negative vorticity, A and B (white color) at 0000 UTC, on March 19 directly coincide with the generation area of the duststorm and the transportation area of the dust follow the negative vorticity area stretched westward to Xinjiang province and eastward to Manchulia.

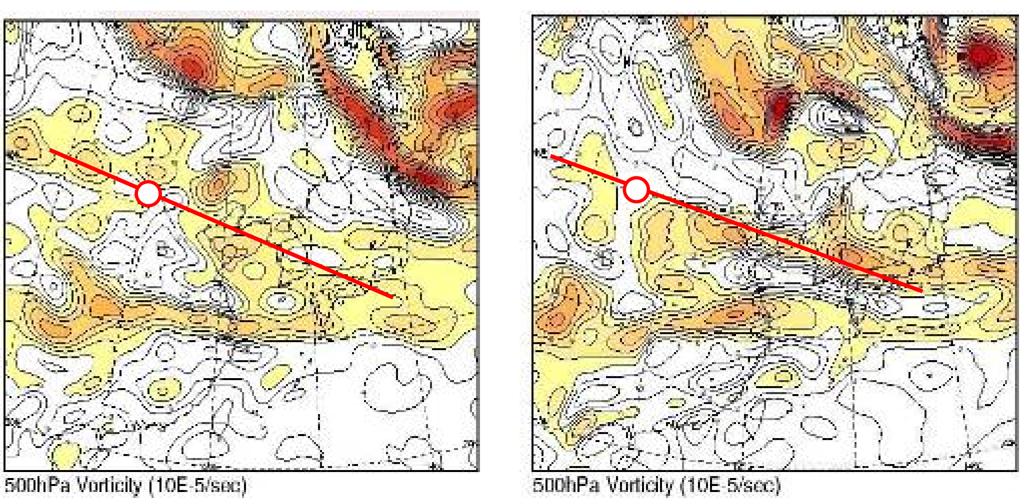


(a) (b)

Figure 4. (a) and (b) Vorticity ($10^{-5}$ $sec^{-1}$) at 500mb level at 1200 UTC on March 19, 2001. White area (negative relative vorticity area; red circle) on red line above B indicates the generation area of duststrom. In Figure (b), the duststorm area was

more extended on a line of west (Gansu province) and the dust was transported toward further west (C), south (D) and east (E) area.

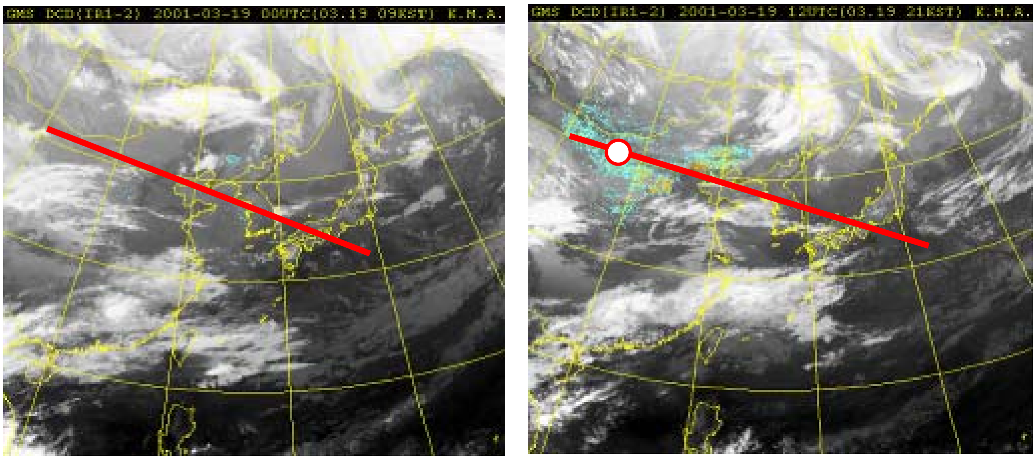


Figure 5. GMS (DCD-IRI-2) satellite pictures at 0300 UTC and 1200 UTC on March 19, 2001. Duststorm area coincides negative relative vorticity area. Even 0000 UTC picture was in bad resolution with cloud, it is possible to detect dust area, comparing with 1200 UTC one.

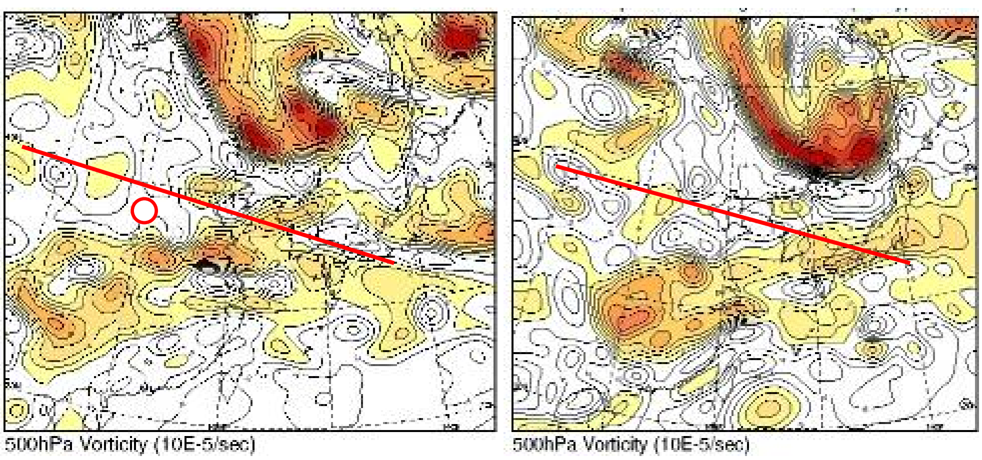


(a) (b)

Figure 6. (a) Vorticity at 500 mb level 0000 UTC and (b) 1200 UTC on March 20, 2001.

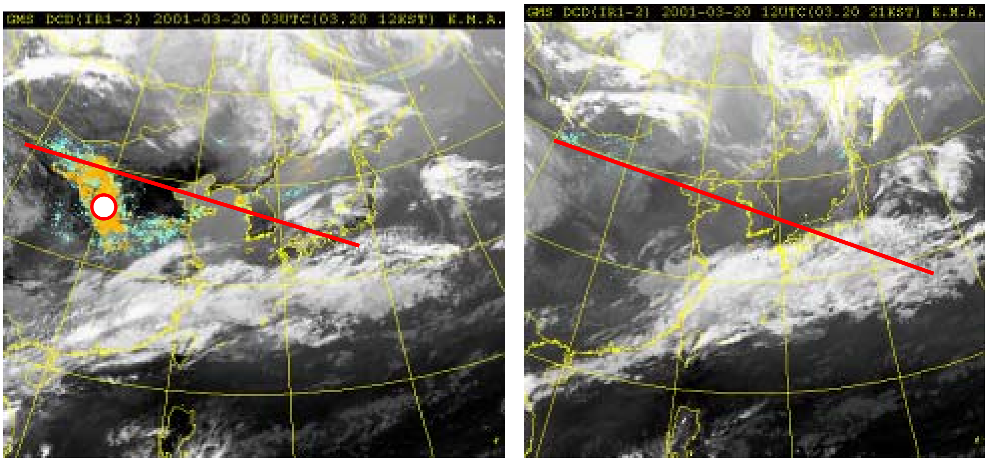


(a) (b)

Figure 7. GMS (DCD-IRI-2) satellite picture at 0300 UTC and 1200 UTC on March 20, 2001. As the picture at 0000 UTC was in bad resolution, 0300 UTC picture is given by replacing 0000 UTC picture. Red circles indicate dust area.

At 0000 UTC (0900 LST), March 19, on the strait cutting line of our figures (Figure 8a) simulated by MM5 model, which is on the high plain in the left hand side of model figure near sothern Mongolia and Nei-Mongo in the west-northern China, the layer of negative potential vorticty (here, less than zero in the unit) in its vertical distribution is found over the highest mountain region in the horizontal distance of about 1000 km away from the western boundary of the model domain (Figure 8 and 9). This negative potential vorticity (less than zero; white color layer) indicates unstable layer (convective boundary layer; CBL) of about 200 m with a mixed layer of about 1 km depth above the CBL, while positive potential vorticity layer (more than 1.5 PVU; black color layer) is also found in the surface boundary layer and upper atmosphere near 400 mb level

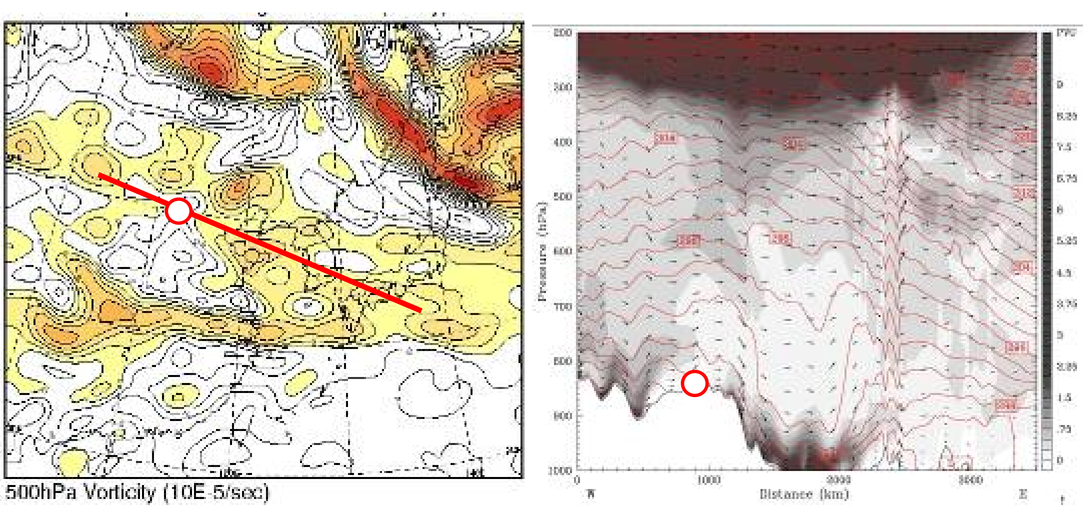


(a) (b)

Figure 8. (a) Relative vorticity and (b) potential vorticity fields at 0000 UTC (0900 LST), March 19, 2001 at the beginning stage of the duststorm. Red line is a straight

cutting line from southern Mongolia-Beijing, China-Seoul, Korea-Japan. White color, gray color and dark color area in (b) indicate convective boundary layer of about 200m with mixed layer of 1 km in Nei-Mongo and stable layer of 200 m ~ 700 m in the other area. Red circle denotes duststorm area, where unstable convective boundary layer occurred.

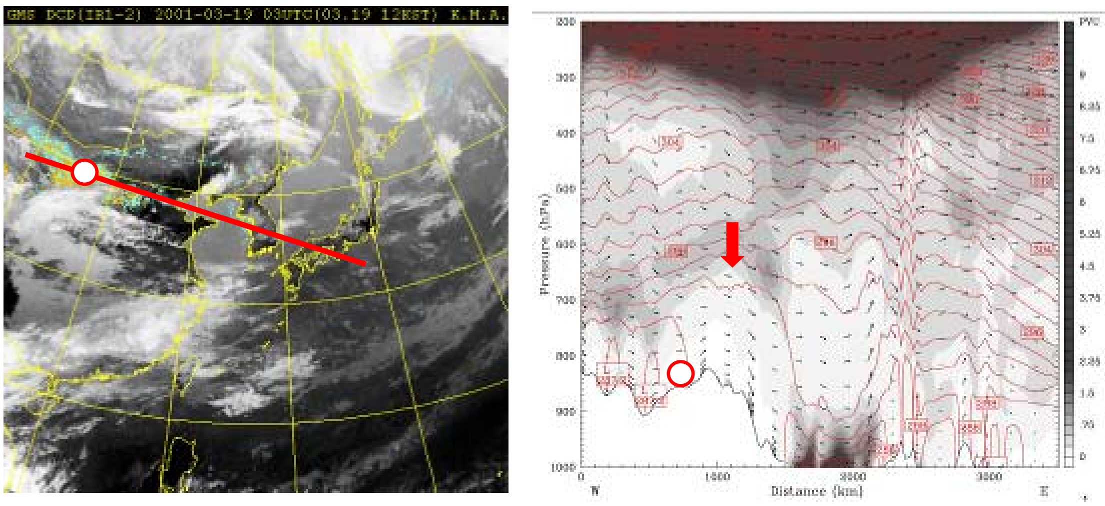


(a) (b)

Figure 9. (a) GMS satellite picture at 0300 UTC (1200 LST) and (b) potential vorticity. March 19, 2001. Red line in (b) is potential temperature. The 0300 UTC picture with partially cloud was used due to its bad resolution of 0000 UTC picture. Duststrom area in the satellite on the cutting line coincides the convective boundary layer-white color in the mountain sites in (b). Red arrow indicates the line (level) of $\partial\theta/\partial p = 0$, between dark and gray layers and the level limits the uplift of dust.particles.

In the upper atmosphere, positive potential vorticity indicates the air coming from the stratosphere into the middle troposphere. Our main concern is confined to the atmospheric boundary layer for the dust generation. Positive potential vorticity layer near the surface, which indicates stable atmospheric boundary layer during the day or nocturnal surface inversion layer at night reaches about 400 m in the southern Mongolia of upwind side and about 500 m in the downwind side. A shallow unstable layer (CBL) of about 200 m exists over the highest mountain in the inner Mongolia, but relatively big mixed layer of about 1 km (the height of $\partial\theta/\partial p = 0$) exists above the CBL (Figure 9b).

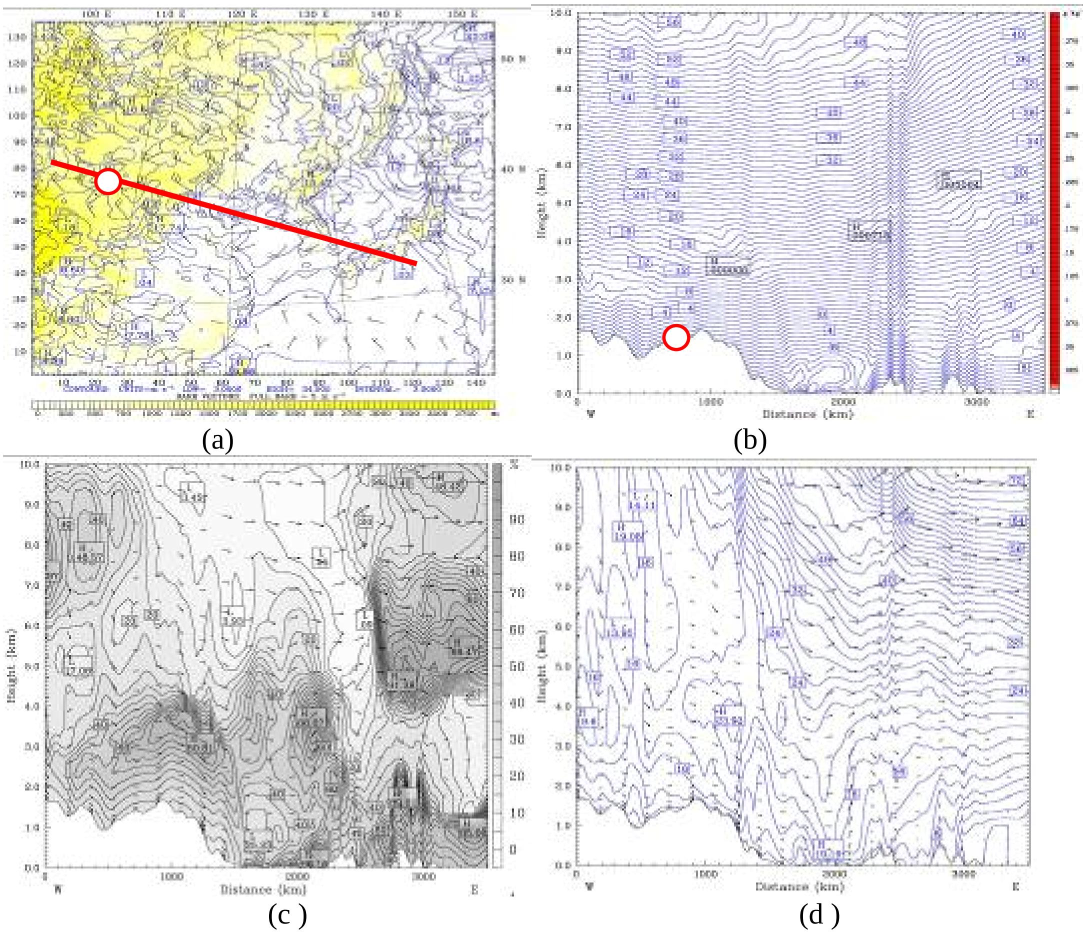


Figure 10. (a) Horizontal wind vector (m/s), (b) vertical distribution of air temperature, RH(%) wind speed(m/s) and horizontal wind speed(m/s) at 1200 LST, March 19, 2001

Above 700 mb level, there is stable upper atmosphere influenced by the stratosphere. Within 3km height, convective boundary layer (CBL; negative potential vorticity value-PVU < 0) exists with a depth of less or more than 1 km and initially dust particle in the CBL floats from the ground surface toward the atmosphere, reaching the mixed layer (ML) of about 1.5 km above the CBL, with its remaining inside the ML and then, westerly wind drive the particles to the downwind side. The reason why the mixed layer is much bigger than the CBL may be due to the daytime thermal induced vertical mixing process under less than 40% of RH (Figure 10c) and mechanical mixing process by strong wind (Figure 10a, 10d) below the 700 mb level. Since baroclinic potential vorticity equation contains both thermal and mechanical process with respect to time, one can easily catch up the evolution of potential vorticity such as the vertical and horizontal movement of air parcels. Especially, negative vorticity area at the 500 mb level, inducing upward motion of air parcel from the ground (duststorm generation area) is well matched with dust distributed area on GMS satellite (Figure 8 and 9).

### 3.2 Origin of air masses during duststorm

In order to investigate the root of dust transportation from its generation area in ther southern Mongolia and west-northern China (Gansu province) toward Beijing city, China, back trajectories of air masses at ever 6 hour were given for duststorm period from March 19 (its beginning stage) to 20, 2001 (Figure 11). Three levels through the surface to 10km height such as 500m ~ 1500m (showing roughly atmospheric boundary layer), 3km ~ 4500m (middle atmosphere) and 5000m ~ 6000m (high atmosphere including the effect of stratosphere) were considered.

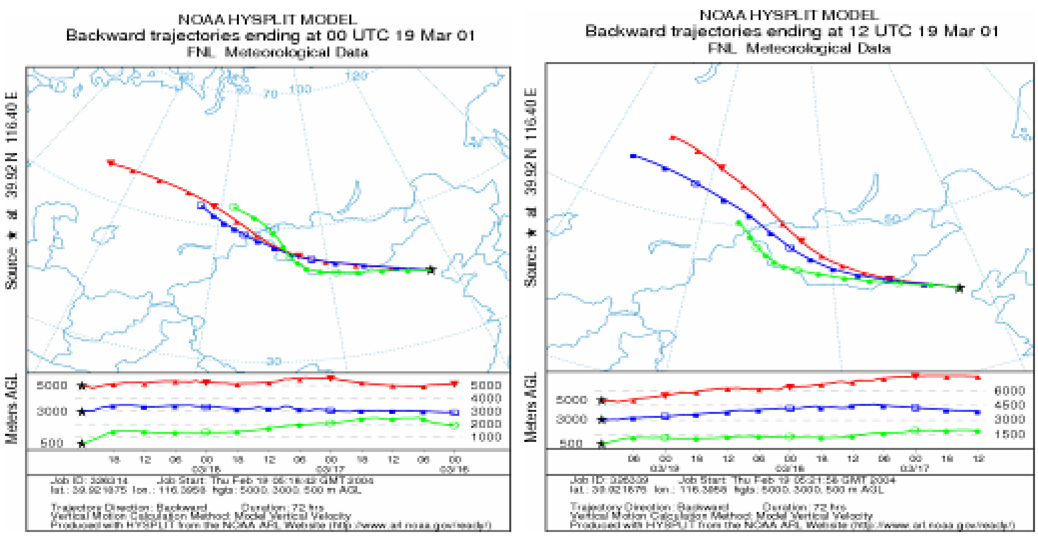


(a) (b)

Figure 11. Back trajectory at every 6 hour on 3 levels-5000m (high level; red), 3000m (middle
level; blue) and 500m (low level; green) over the ground at Beijing, at 0000 UTC, March 19 and 0000 UTC, March 20, 2001.

Air trajectories on the beginning stage of DS in China on from 0000 UTC and 1200 UTC, March 19 gave us that air masses in the upper and middle atmospheres of 5 km and 3km heights passed through southern part of Mongolia and partially, through its middle part, while the masses in the lower atmosphere (atmospheric boundary layer) always passesed through southern part of Mongolia. Since back trajectory does not directly reflect all directions of moving parcels and only their major direction, it is a good qualitative method for the transport of dust to the interested area and .

### 4. CONCLUSION

the area of maximum negative vorticity which induces the strong upward motion of air coincides the area of the duststorm generation in the inner Mongolia under the relative humidity less than 30% and wind speed more than 7 ~ 8 m/s and the dust transportation always follows the negative vorticty area in the downwind side. The source region of the duststorm (maximum negative vorticity area) is the same region of the unstable atmospheric layer (negative potential vorticity value), near the ground surface in the vertical distribution of baroclinic potential vorticity, which is a function of daibatic heating and frictional terms with respect to time.

From isentropic potential vorticity (IVP), during the day, the air parcels (dust) are uplifted to about 700 mb level (about 3 km height), where potential temperature gradient with pressure ($\partial\theta/\partial p$) is zero. Above 700 mb level, there is stable upper atmosphere influenced by the stratosphere. Within 3km height, convective boundary layer (CBL; negative potential vorticity value-PVU < 0) exists with a depth of less or more than 1 km and initially dust particle in the CBL floats from the ground surface toward the atmosphere, reaching the mixed layer (ML) of about 1.5 km above the CBL, with its remaining inside the ML and then, westerly wind drive the particles to the downwind side. The depth of the CBL decreases early in the morning and late afternoon, but the ML doses not much change all day long. At night, a shallow stable atmospheric boundary layer (or nocturnal surface inversion layer; big positive potential vorticity value) due to the cooling of the ground surface and the particle inside the stable layer merge to the ground surface and moves downwind side by the wind. The dust particles in the ML still move downwind side by wind and their dry deposition near the top of stable layer into the surface may occur.

## 5. ACKNOWLEDGEMENTS

Authors much thanks the College of Environmental Sciences, Peking University, China for using computer system and analysis from the period of 2003 ~ 2004.

## REFERENCES

Austin, J., Midgley, R., 1994. The climatology of the Jet Stream and straopspheric intrusions of ozone over Japan. Atmos. Env., 28, 39-52.

Bates, T. S., Quinn, P. K., Coffman, D. J., Covert, D. S., Miller, T. L., Johnson, J. E., Bates, T. S., P. K. Quinn, D. J. Coffman, D. S. Covert, T, L. Miller, J. E. Johnson, G. R. Carmichael, S. A. Guazotti, D. A. Soderman, K. A. Prather, M. Rivera, L. M. Russell and J. T. Merrill, 2003: Marine boundary layer dust and pollutant transport associated with the passage of frontal system over eastern Asia. J. Geophy. Res., in press.

Carmichael, G. R., Hong, M. S., Ueda, H., Chen, L. L., Murano, K., Park, J. K., Lee,H., Kim, Y., Kang, C., Shim, S., 1997. Aerosol composition at Cheju Island, Korea. J. Geophy. Res., 102(5), 6047-6061.

Chen, S. J., Kuo, Y. H., Zhang, P. Z., Bai, Q. F., 1991. Synoptic climatology of cyclogenesis over east Asia, 1958-1987. Mon. Wea. Rev., 119, 1407-1418.

Chung, Y. .S., Kim, H. S., Jugder, D., Natsagdorj, J., Chen, S. J., 2003. On sand and duststorms and associated significant dustfall observed in Chongju-Chongwon, Korea. Water, Air, and Soil Pollut: Focuss 3: 5-19.

Fuelberg, H. E., Kiley, C. M., Hannan, J. R., Westberg, D. J., Avery, M. A., Newell, R. E., 2003. Meteorological conditions and transport pathways during the transport and chemical evolution over the Pacific (TRACE-P) exeriment. J. Geophy. Res., 108 (D20), in press.

Haynes, P. H., McIntrye, M. E., 1987. On the evolution of vorticity and potential vorticity in the presence of diabatic heating and frictional or other s forces. J. Atmos. Sc., 44, 828-841.
Qian, Z, Hu, Y., 1997. Survey and analysis for “93.5.5.” strong dust storm, dust storm research in China. Meteorology press, Beijing, 37-43.
Reed, R. J., 1979. Cyclogensis in polar air stream. Mon. Wea. Rev., 107, 38-52.
Reed, R. J., Albright, M. D., 1986. A case study of explosive cyclogensis in the Eastern Pacific. Mon. Wea. Rev., 114, 2297-2319.
Reed, R. J. and F. Sanders, 1953: An investigation of the development of a mid-tropospheric frontal zone and its associated vorticity field. J. Meteor., 10, 338-349
Rossby, C. G., collaborators, 1937. Isentropic analysis. Bul. Amer. Meteor. Soc., 18, 201-209.
Rossby, C. G., 1940. Planetary flow patterns in the atmosphere. Quart. J. Roy. Meteor. Soc., 66, Suppl., 68-87.
Sanders, F., Gyakum, J. R., 1980. Synoptic-dynamic climatology of the “bomb”. Mon. Wea. Rev., 108, 1589-1606.
Tegen, I., Fung, I, 1994. Modeling of mineral dust in the atmosphere: Source transport and potical thickness. J. Geophy. Res., 99(D11), 22987-22914.
Xuan, J., Sokolik, I. N., 2002. Characteristization of sources and emission rates of mineral dust in Northern China. Atmos. Environ. 36, 4863-4876.
Zhang, Y. and Y. Zhong, 1985: The simulation and diagnosis for a strong wind associated with northeast low. Acta Meteor. Sinica, 43, 97-105.

*Proceedings of the Third International Symposium on Air Quality Management at Urban, Regional and Global Scales. 26-30 September 2005, Istanbul – Turkey*

# CONCENTRATIONS OF PM10, PM2.5 AND PM1 INFLUENCED BY SEA-LAND BREEZE CIRCULATION AND ATMOSPHERIC BOUNDARY LAYER IN THE KOREAN MOUNTAINOUS COAST DURING DUSTSTORM PERIOD

**Doo Dun Choi, Hyo Choi and Sang Kook Kim***

Kangnung National University, Department of Atmospheric Environmental Sciences, Kangnung, Kangwondo 210-702, Korea, du8392@hanmail.net
Gangwon Meteorological Administration, Department of Information and Analysis, Kangnung, Kangwondo 210-070, Korea

## ABSTRACT

The concentrations of 100 nano-particle size to 20ug/m$^3$ at the eastern coastal region of Korea have been measured by GRIMM aerosol samplers from March 7 through 17, 2004, at two aerosol sampling points in the high mountain (Mt. Taeguallyung; 896m) of upwind side in the west of which Kangnung Meteorological Administration (KMA, called C-point) of Kangnung coastal city adjacent to the East Sea in the east. PM10, PM2.5 and PM1 near the ground surface at C-point until 1200 LST, March 8 before the passage of dust storm were very low with the magnitudes of about 40, 35 and 30ug/m$^3$, which showed not much different concentrations each other. The maximum concentration of PM10 from March 7 before dust storm occurred near the beginning time of on duty around 0800 LST and off duty around 1700 LST, due to the increase of fuel combustion of vehicles on the street. From the afternoon on March 10 through 16, when the great amount of dust passed through Kangnung coastal city under westerly wind, PM10 concentration reached 340ug/m$^3$ and PM2.5 and PM1 concentrations were 105ug/m$^3$ and 60ug/m$^3$, showing twice higher concentration of PM10 than PM2.5, respectively. The majority of dust transported from China consisted of larger particle size than PM2.5 and PM1. High concentration of particulates was detected at 0900 LST, beginning time of office hour and after the ending time of office hour to 2200 LST at night. Howevere,, the occurrence of low concentration of particulates was found near noon. The transported dust from the upwind side in the west (mountain area) under the westerly wind toward to the downwind side (Kangnung city) were combined with the particulates generated by easterly sea-valley breeze, vehicles, boilers from resident area in the city after sunrise and resulted in the high concentration of particulates at the beginning time of office hour, 0900 LST. For daytime, the upslope wind combined with easterly sea breeze and valley wind drove the dust particles or particulates in the city to be dissipated into the mountain side in the west, resulting in the decrease of particulates at C-point in the coast near noon. The high concentration of particulates occurred again due to the increase of fuel combustion of vehicles at the ending time of office hour and boilers. Under westerly land-mountain breeze toward Kangnung city, returning of particulates floated for daytime near the mountain to the city and emmitted particulates from the city at night increased high concentrations of particulates before midnight with a maximum at 2200 LST and a

shrunken depth of nocturnal surface inversion layer in the city further result in the increase of particulate concentration..

**Key Words :** PM10, PM2.5, PM1, Duststorm, Sea-Valley Breeze, Land-Mountain Breeze

## 1. INTRODUCTION

Asian duststorm or called , Yellow Sand and KOSA is quite different from that in other regions of the world such as Sahara and Australian deserts (Reiff et al., 1986; Middleton, 1986). Asian Dust have requently and periodically occurred under strong wind blowing soil in the dried area of the northern China and Gobi desert in Mongolia, and the storms have transported a great amount of dusts to eastern China, Korea, Japan, even north America (Chon, 1994; Chung et al., 2001; Chung and Yoon, 1996; Jigjidsuren and Oyuntsetseg, 1998; Middleton, 1986; Natsagdorj, and Jugder, 1992a). The dust is to make a great contribution to low visibility and air quality in spring in northern Asian countries and even U.S.A.(Carmichael, et al., 1997; Choi and Song, 1999; Chung, et al., 2003; David et al., 2001; Gao et al., Kim, et al., 2001; McKendy et al, 2001; Murayama, 1988). In the recent years, newspaper and TV news reported the diseases of livestock in China, Taiwan, Korea, Japan and Thailand were under the influence of duststorm, which may accompany various bacilli and germ in the countries along the path of the duststorm and caused uncountable thousands of livestock to be killed, due to bacterial disease (KBS TV, 2004; Joong-ang, 2004).

Kim and Kim (2003) and Kim et al. (2003) explained that particulate matters during Asian Dust event in 2001 and 2002 could be transported toward Seoul city in Korea under strong westerly wind of about 20 m/s. Zhang and Zhong (1985) insisted that about the half of the total quantity of particulate matter are deposited near the source area (30%) and re-distributed on a local scale (20%) and the other half of them are expected to be subject to long-range transport. The transported amount of dust can serve as one of the major particulate matter sources all across the Asia and Pacific regions. An investigate aerosol experiment was performed by many scientific groups in many locations of east Asia of Korea, China and Japan in 2004, but major measurement and researches in Korea have been done at Gosan Supersite of Jeju island in the southern Korea. Except for Gosan, some of scientists personally carried out the measurement of aerosol in the west part of Korea, but no measurement was done in the mountainous coastal region of Korean peninsula.

Thus, the objective of this study is to investigate diurnal aerosol concentration, especially PM10, PM2.5 and PM1, which greatly influenced upon local climate change and human health condition dary and to explain the high concentration time band, considering synoptic and meso-scale motions of atmosphere.

## 2. MEASUREMENT OF AEROSOL AND TOPOGRAPHY

### 2-1. Instrument

The concentrations of 100 nano-particle size to 20ug/$m^3$ at the eastern coastal region of Korea have been measured by GRIMM aerosol samplers from March 7 through 17, 2004, which included dust storm period of China in spring. Two aerosol sampling points were fixed at a measurement point in the high mountain, Mt. Taeguallyung (896m) (called M-point; ($37^0$ 41'N, $128^0$44'E)) upwind side in the west of which Kangnung Meteorological Administration (KMA; $37^0$45'N, $128^0$54'E) of Kangnung coastal city (called C-point) was adjacent to the East Sea in the east.
The GRIMM Model 1107 is an extremely small and portable particle analyzer. The Model 1107 is specifically designed for PM-10, PM-2.5 and PM-1 environmental ambient air analysis using the laser light scattering technology. This technology enables the Model 1107 to make very precise "cut points" for all three PM size classifications. This technique patented system allows the user to collect all three PM fractions simultaneously without changing sampling heads or weighing filters. However, the Model 1107 is the only PM monitor to offer dual technology consisting of both optical and gravimetrical analysis. The Model 1107 incorporates a removable 47 mm PTFE filter which allows the user to verify the optical analysis gravimetrically, as well as providing the option for other chemical analysis on the collected residue.
The 107 Environmental Particulate Monitoring Systems particulate measurements via 900 laser light scattering. Air with multiply particle sizes passes through a flat laser beam produced by an precisely focused laser and several collimator lenses. The scattered light are then detected by a 15-channel pulse height analyzer for size classification. The counts from each size classification are then converted to mass by a well established equation. The data are then presented in the P.S. EPA conventions for PM-10, PM-2.5 and PM-1. The complete 107 system is consisting of the 165 fiberglass housing, the drying temperature control system, the 107 PM dust monitor, sensors for humidity and temperature and the 170M sampling system. Dislays real time data of PM-1 and PM-2.5 and even PM-1 is detected as quickly as every as every six seconds. Sensitivity is from 0.1 microgram/m3 upwards. Stand-alone system is able to be operated directly all times out in the field. No sample pipe heating needed, therefore no loss of VOC's. Auto-zero, self-diagnostic and continuous performance recording are done after each starts.

### 2-2. Topography in study area

The study area is located in the eastern mountainous coastal region of Korean peninsula and two GRIMM aerosol samplers were equipped at the sampling points in the high mountain, Mt. Taeguallyung (896m) (called M-point) upwind side in the west of Kangnung coastal city and Kangnung Meteorological Administration (KMA) of (called C-point) adjacent to the East Sea in the east (Figure 1 and 2). $2.5^0$ degree interval terrain date was used for the largest domain and then 1km interval data was used for fine mesh domain, on a straight cutting line from the west toward east, which was major transportation root of dust from the dust storm generation area, China toward Korea like a straight cutting line of Mogolia-Beijing-Seoul-Kyoto-Pacific Ocean like; (10, 90), (130, 40), respectively.

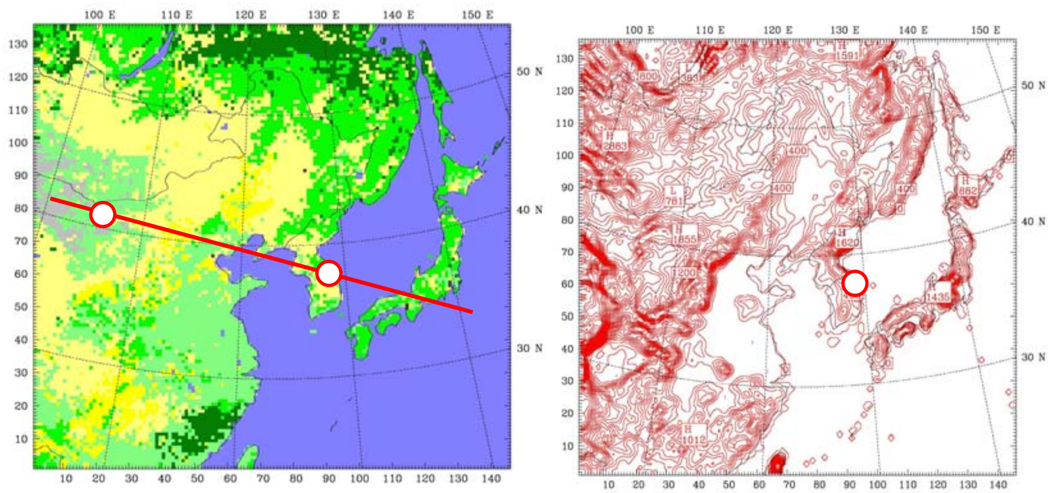


(a) (b)

Figure 1. (a) Land-use data and (b) topography for a coarse domain of a horizontal grid size 27 km. Circles denote duststorm area (China) and Kanunu city (Korea).

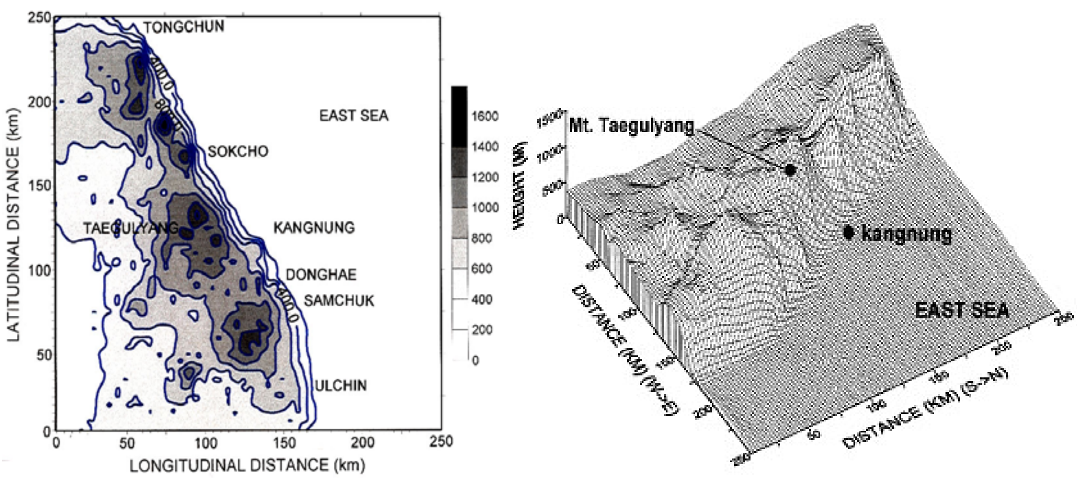


(a) (b)

Figure 2. 2D (left) and 3D (right) topographies (circle area shown in Figure 1b) with a horizontal grid size 5 km near Kangnung city (20m above mean sea level; 10 km width) and Mt. Taeguallyung (860 m), Korea.

## 3. RESULT AND DISCUSSION

### 3.1 Aerosol concentration in Kangnung city and Mt. Taeguallyung

PM10, PM2.5 and PM1 near the ground surface at C-point (KMA) of Kangnung coastal city until 1200 LST, March 8 before the passage of dust storm were very low with the magnitudes of about 40, 35 and 30ug/$m^3$, which showed not much different concentrations each other. The maximum concentration of PM10 from March 7 before dust storm occurred near the beginning time of on duty around 0800 LST and off duty around 1700 LST. Under the weak influence of dust transportation from China into Korean peninsula from March 8 until 1200 LST, March 10, the concentrations of PM10 and PM2.5 and PM1were twice increased over about 50ug/$m^3$ to 95ug/$m^3$. From the afternoon on March 10 through 16, when the great amount of dust passed through Kangnung coastal city, PM10 concentration reached 340ug/$m^3$ and PM2.5 and PM1 concentrations were 105ug/$m^3$ and 60ug/$m^3$, showing twice higher concentration of PM10 than PM2.5, respectively.

The majority of dust transported from China consisted of larger particle size than PM2.5. Except for the period from 1800 LST, March 10 through 0300 LST, March 11, when the maximum concentrations of PM10 and PM2.5, PM2.5 and PM1 concentrations still very low, similar to those before the period of dust transportation. It means that the dust transportation from China into Kangnung city could great influence upon the increase of PM 10 concentration in the local area, but not much influence upon PM2.5 and PM1 concentrations. An important thing is that the relatively high concentration of particulates is detected at 0900 LST, beginning time of office hour and after the ending time of office hour to 2200 LST at night. Another thing is the occurrence of low concentration of particulates near noon.

The transported dust from the upwind side in the west (the mountain area) under the westerly wind toward to Kangnung city combines with the particulates generated by easterly sea breeze and valley wind, vehicles, boilers from resident area in the city after sunrise and results in the high concentration of particulates at the beginning time of office hour, 0900 LST. As daytime goes on, the upslope wind combined with easterly sea breeze and valley wind drives the dust particles or particulates in the city to be dissipated into the mountain side in the west, resulting in the decrease of particulates at C-point in the coast near noon.

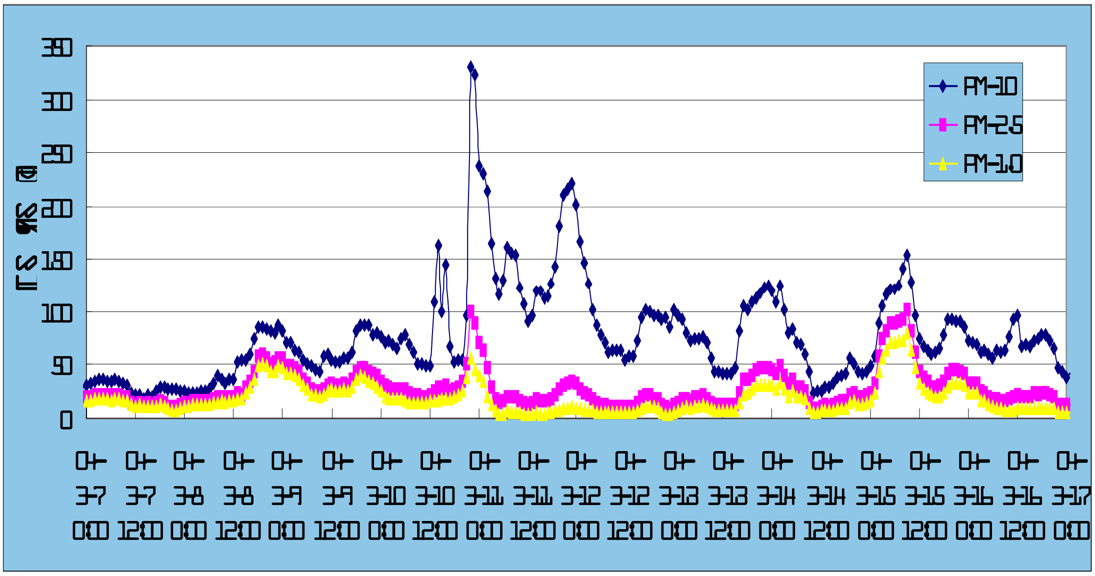


Figure 3. Hourly based concentration (ug/m$^3$) of PM10, PM2.5 and PM1 at an aerosol sampling point of Kangnung Meteorological Administration from March 7 through March 17, 2004.

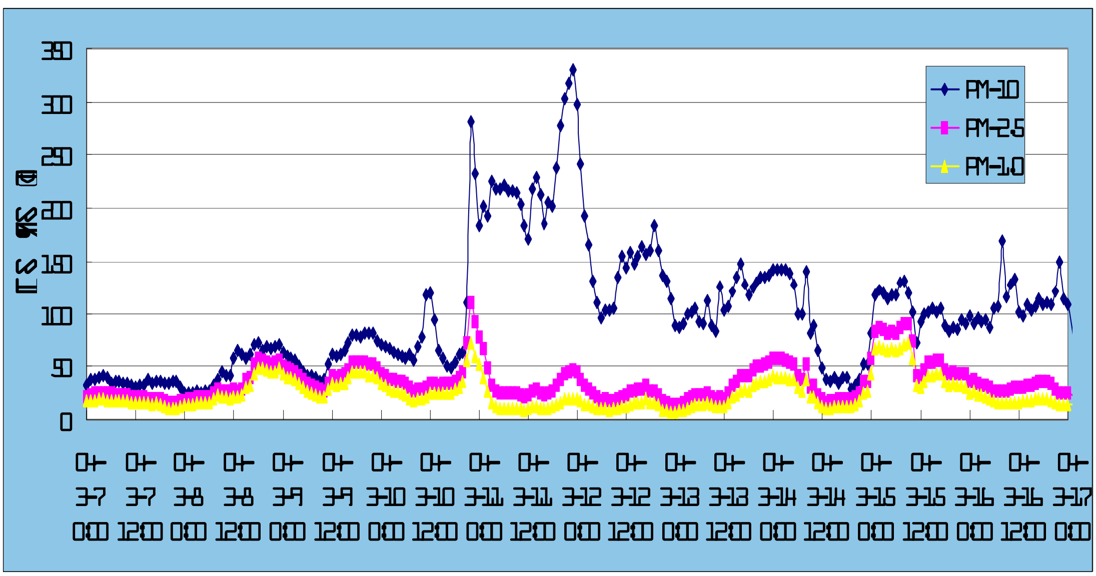


Figure 4. As shown in Figure 4, except for Mt.Taeguallyung (896m) from March 7 through March 17, 2004.

The high concentration of particulates occurred again due to the increase of fuel combustion of vehicles at the ending time of office hour and boilers. These high concentrations of particulates gradually increase before midnight with a maximum at 2200 LST, due to the shrunken depth of atmospheric boundary layer, when the reduction of surface heating of the ground induces the shrunken convective boundary layer and when nocturnal cooling of ground surface generates a shallow depth of nocturnal surface inversion in the city. After sunset, which nocturnal cooling of the ground surface induces the formation of nocturnal surface inversion layer and it showed much shrunken depth of atmospheric boundary layer, compare to the daytime convective boundary layer. Thus, the concentrations of particulates in the early night should much increase than in the daytime.

From 2300 LST, the high concentration of particulates gradually decreased before the beginning of office hour in the next day morning. The reason of the decrease concentration of particulate was due to westerly synoptic wind associated with mountain wind after sunset became relatively strong downslope surface wind toward the coastal city and this surface wind was also associated with land breeze toward the East Sea, resulting in driving the floating particulates to flow in the city into the sea and the decrease of the particulate concentration of 110ug/m$^3$at 0600 LST, March 11, Kangnung city.

Then, the transported dust from upwind side in the west toward to Kangnung city combined with the particulates generated by surface wind, vehicles, boilers from resident area in the city after sunrise and the high concentration of particulates at the beginning time of office hour, 0900 LST was detected and after that time intensified sea breeze and valley wind drove the particulates into the mountain side in the west again, resulting in the low concentration of particulate of 80ug/m$^3$at near noon.

## 4. CONCLUSION

For the dust stsorm period from the afternoon on March 10 through 16, when the great amount of dust passed through Kangnung coastal city under westerly wind, PM10 concentration reached 340ug/m$^3$ and PM2.5 and PM1 concentrations were 105ug/m$^3$ and 60ug/m$^3$, showing twice higher concentration of PM10 than PM2.5, respectively. The majority of dust transported from China consisted of larger particle size than PM2.5 and PM1. High concentration of particulates was detected at 0900 LST, beginning time of office hour and after the ending time of office hour to 2200 LST at night.

Howevere,, the occurrence of low concentration of particulates was found near noon. The transported dust from the upwind side in the west (mountain area) under the westerly wind toward to the downwind side (Kangnung city) were combined with the particulates generated by easterly sea-valley breeze, vehicles, boilers from resident area in the city after sunrise and resulted in the high concentration of particulates at the beginning time of office hour, 0900 LST. For daytime, the upslope wind combined with easterly sea breeze and valley wind drove the dust particles or particulates in the city to be dissipated into the mountain side in the west, resulting in the decrease of particulates at C-point in the coast near noon.

The high concentration of particulates occurred again due to the increase of fuel combustion of vehicles at the ending time of office hour and boilers. Under westerly land-mountain breeze toward Kangnung city, returning of particulates floated for daytime near the mountain to the city and emmitted particulates from the city at night increased high concentrations of particulates before midnight with a maximum at 2200 LST and a shrunken depth of nocturnal surface inversion layer in the city further result in the increase of particulate concentration..

## 5. ACKNOWLEDGEMENTS

Authors much thanks Gangwon Meteorological Administration located in Gangnung city and Taeguallyung Meteorological Office for the measement of aerosol from March through April, 2004 during Asian Dust period.

**REFERENCES**


Carmichael, G. R., Hong, M. S., Ueda, H., Chen, L. L., Murano, K., Park, J. K., Lee,H., Kim, Y., Kang, C., Shim, S., 1997. Aerosol composition at Cheju Island, Korea. J. Geophy. Res., 102(5), 6047-6061.

Choi, S. W., Song, H. D., 1999. Variation of concentration of heavy metal during Yellow sand period of winter season at Taegu area. Bulletin of Envron. Sci., 4(11), 1-13.

Chon, H., 1994. Historical records of yellow sand observations in China. Res. Environ. Sci., 7-6, 1-11.

Chung, Y. S., Yoon, M. B., 1996. On the occurrence of yellow sand and atmospheric loadings. Atmos. Environ., 30, 2387-2397.

Chung, Y.S., Kim, H. S., Natsagdorj, L., Jugder, D., Chen, J. S., 2001. On yellow sand occurred during 1997-2000. J. Korean Meteor. Soc., 37, 305-316.

Chung, Y. .S., Kim, H. S., Jugder, D., Natsagdorj, L., Chen, J. S., 2003. On sand and duststorms and associated significant dustfall observed in Chongju-Chongwon, Korea. Water, Air, and Soil Pollut: Focuss 3: 5-19.

David, M.T., Robert, J. F., Douglas, L. W., 2001. April 1998 Asian dust event: A southern California perspective. J. Geophy. Res., 106(D16), 18371-18379.

Gao, Y., Anderson, J. R., 2001. Characteristics of Chinese aerosols determined by individual particle analysis. J. Geophy. Res., 106 (D16), 18037-18045.

Jigjidsuren, S., Oyuntsetseg, S., 1998. Pastureland utilization problems and ecosystem. Ecological sustainable development. Ulaanbaatar, No.2, 206-212.

Joong-Ang, 2004, The influence of duststorm accompaning various bacilli and germ on Joong-Ang daily newspaper, March 10, 2004.

KBS TV, 2004, Korean Broadcasting Service, 9'oclock news, March 10, 2004.

Kim, H. K., Kim, M. Y., 2003. The effects of Asian dust on particulate matter fractionation in Seoul, Korea during spring 2001. Atmos. Environ., 51, 707-721.

Kim, K. W., Kim, Y. J., Oh, S. J., 2001: Visibility impairment during Yellow Sand periods in the urban atmosphere of Kwangju, Korea. Atmos. Environ., 35, 5157-5167.

McKendry, I. G., Hacker, J. P., Stull, R., Sakiyama, S., Mignacca, D, Reid, K., 2001: Long-range transport of Asian dust to the lower Fraser Valley, British Columbia, Canada. J. Geophy. Res., 106 (D16), 18361-18370.

Middleton, N. J., 1986. A geography of dust storms in southwest Asia. J. Climate., 6, 183-196.

Natsagdorj, L., Jugder, D., 1992a. Statistics method for prediction of dust storms over the Gobi and steppe area in Mongolia in spring. Scientific report, Ulaanbaaatar, pp83.

Murayama, N., 1988. Dust cloud "Kosa" from the east Asian dust storms in 1982-1988 as observed by the GMS satellite. Meteor. Sctell. Cent. Tech., Note, 17, 1-8.

Zhang, Y., Zhong, Y., 1985. The simulation and diagnosis for a strong wind associated with northeast low. Acta Meteor. Sinica, 43, 97-105.

# PHYSICOCHEMICAL CHARACTERIZATION AND ORIGIN OF THE 20 MARCH 2002 HEAVY DUST STORM IN BEIJING

**R.J. Zhang[1*] Z.F. Wang[2], J.J. Cao[3], S. Yabuki[4], Y. Kanai[5], and A. Ohta[5]**

[1]Key Laboratory of Regional Climate-Environment Research for Temperate East Asia(REC-TEA), START Regional Center for Temperate East Asia, [2]Nansen-Zhu International Research Centre, Institute of Atmospheric Physics, Chinese Academy of Science, Beijing 100029,China [3] State Key Laboratory of Loess & Quaternary Geology, Institute of Earth Environment, Chinese Academy of Sciences, Xi'an, China
[4] The Institute of Physical and Chemical Research, Wako, Saitama, 351-0198 Japan
[5]Geological Survey of Japan, National Institute of Advanced Industrial Science and Technology, [*]email: zrj@mail.iap.ac.cn

**ABSTRACT**

The dust storm event on 19-21 March 2002 in North China, which was very detrimental to the atmospheric environment quality over a wide area, was one of the heaviest events during the last decade. The total mass concentration, size distribution of mass concentration and number concentration of particles were observed during this heavy dust period in Beijing. The TSP concentrations in Beijing reached peak values of 12 mg $m^{-3}$ in dust period, which is the highest value that has ever been reported in Beijing and also is an infrequent value in dust source regions. During this dust storm, the distribution of mass concentration and number showed a characteristic increase especially in the size range of coarse particles. The mass concentration of coarse particles (>2.1μm) account for 91% of the total in the dust period and 61% in the non-dust period respectively. The number concentrations of fine particles (d < 2 μm) and coarse particles (d > 2 μm) increased sharply in dust storm period.. The dry deposition mass flux of in dust storm period reached 17.5 g $m^{-2}$ $d^{-1}$ in dust period on 20 March in Beijing. During the storm, the air mass was transported directly from southern of Mongolia, central Inner Mongolia, passing through Shanxi province, and then to Beijing, which was demonstrated by backward trajectory analysis. Concentrations of $Cl^-$, $NO_3^-$, and $SO_4^{2-}$ in TSP in dust storm period are about 10 times as that in non dust storm period, which implied that aerosols in dust period were influenced by anthropogenic sources during the transport process. Compared to the China Air Quality Standard, 20 March 2002 dust storm caused serious air pollution in Beijing.

**Key Words:** Dust storm, Size distribution, Number concentration, Backward trajectory analysis

## 1.INTRODUCTION

In North and Northwest China, East Russia, and Mongolia, there are a variety of environmental systems such as hyperarid, arid, and semi-arid areas where dust storms occur frequently. Dust storms, a kind of severe natural disaster in dust source regions (Fang et al., 1997; Ye et al., 2000), have a negative impact on air quality, human health, and industrial products and activities (Prospero, 1999; Chung et al., 2003a).

Great economic losses due to the dust storms are caused every year. A great amount of dust is produced by dust storms and is transported to the east and Pacific regions every year (Wang et al., 2000; Zhang et al., 2000). The dust particles, which are one of the main sources of atmospheric aerosols, have a great influence on ecosystems, environment, climate, and weather in the extended downstream areas (Iwasaka, et al., 1983, 2003; Tegen and Fung, 1994; Sokolik et al., 2001). Now dust storms are widely recognized as one of the issues in the intercontinental transport of pollutants (Zhang et al., 1997; Chun et al., 2001a; Gong et al., 2003; Zhang et al., 2003). In order to understand the effect of dust on the atmospheric environment and climate, it is important to investigate the concentrations and size distributions of dust particles when the dust storm occurs (Kanai et al., 2002).

During 2000-2002, sand-dust weather events occurred frequently in North China, which resulted in negative impacts on traffic, air quality, and people's daily life in local and downstream areas (Zou and Zhang, 2003; Zhang et al., 2002). During 19-21 March 2002, a rare heavy dust storm (with respect to the last decade) occurred in North China. It attacked Beijing on 20 March 2002, reducing the visibility to less than 200m. According to the classification of dust storms (Yoshino, 2000; Zhou, 2001), it can strictly be called a heavy dust storm. Here, the preliminary results of the physicochemical properties of this dust storm event by ground-base observation are presented, and the origin is sought in terms of the backward trajectory analysis method.

## 2. METHODOLOGY

The experimental site is located on the top of a two-storey building, 8 m above the ground, which between the North Third Ring Road and the North Fourth Ring Road in Beijing.

The high-volume air sampler HV-1000F manufactured by SIBATA Scientific Co., Ltd. is used to collect total suspended particles. The filters are the PF040 polyflon filter (25 cm × 20 cm) manufactured by Advantec Co., Ltd. The air flow rate is $1m^3\ min^{-1}$. The low-volume air sampler (Andersen) AN-200, manufactured by Shibata Scientific Co., Ltd., is employed. The flow rate is maintained at 28.3 L $min^{-1}$ to achieve ideal size separation. The Andersen sampler has eight stages and a backup filter. The particle size discrimination is as follows: >11, 11-7.0, 7.0-4.7, 4.7-3.3, 3.3-2.1, 2.1-1.1, 1.1-0.65, 0.65-0.43, and <0.43μm (backup filter). The filters used for the AN-200 are the PF050 polyflon filters with 80 mm diameter manufactured by Advantec Co., Ltd., for stage Nos. 0-6, and the 2500QAT-UP quartz filter manufactured by Tokyo Dylec Co., Ltd., for stage No. 7 and as the backup filter. Dry deposition flux is measured by an open box with the PF040 polyflon filter (25 cm × 20 cm), and the deposition area of the filter paper is 17.5 cm × 22.5 cm.

The filters before and after sampling were stored under a fixed temperature (25 □) and relative humidity (37%) condition for over 24 hours and then weighed by a balance LAC214 with resolution $10^{-4}$g. The balance LAC214 was manufactured by Changsu Balance Factory, China. The BCJ-1 optical particle counter(OPC) made in Suzhou, China is used to measure the size distributions of the aerosols. This counter measures six channels of aerodynamic diameters as follows: 0.3-0.5, 0.5-0.7, 0.7-1.0, 1.0-2.0, 2.0-5.0, and >5.0μm. The airflow rate is 2.83 L $min^{-1}$. The OPC instrument was calibrated before observation and detailed descriptions were presented in Zhang et al.(2001, 2003).

Four major ionic species ($Cl^-$, $NO_3^-$, $SO_4^{2-}$ and $NH_4^+$) of TSP samplers were measured by ion chromatography (Dionex, DX600). A CS12 column (150×4mm) was used for cation analysis and an AS14 column (150×4mm) was used for anion analysis. All the concentrations of ionic species were all corrected by using field blanks. The detection limits of $Cl^-$, $NO_3^-$, $SO_4^{2-}$and $NH_4^+$ were 0.5, 15, 20 and 15 μg $L^{-1}$ respectively. Before ion analysis, standard solution and blank test were conducted and standard curves were plotted for real sample analysis.

## 3 RESULTS AND DISCUSSION

### 3.1. TSP variations during the dust storm

The dust storm reached Beijing on 20 March 2002. At 0915 LST, the sky turned yellow and was permeated with a soil taste. Dust storm arrived in Beijing at 1000 LST with visibility less than 1000 m. At 1100 LST, the visibility was only 200 m and the sky became a red, soil-like color. After 1500 LST, the dust storm began to decay and visibility was restored to 800 m. The results by the high volume sampler indicated that the mass concentration of TSP reached 12 mg $m^{-3}$ from 1050 to 1530 LST during this heavy dust storm period (Figure 1), which was 40 times as much as the daily average value of the TSP second Air Quality Standards by the China Environment Protection Administration (China EPA). During a previous dust storm on 6 April 2000 in Beijing, the TSP mass concentration in the city reached about 6 mg $m^{-3}$ (Zhuang et al., 2001; Wang et al., 2002). Comparing the two events, we find that the 20 March 2002 event was much heavier, and was in fact the strongest one in Beijing over the last decade. This heavy dust storm was also observed with maximum values of 3006 μg $m^{-3}$ for $PM_{10}$ and 331 μg $m^{-3}$ for $PM_{2.5}$ in Chongwon, Korea on 21 March 2002(Chung et al., 2003b).

### 3.2. Size distribution of mass concentrations

Figure 2 presents the size distribution of particles in the non-dust (27 February – 4 March) and dust periods (19–21 March) during spring 2002 in Beijing. The size distribution of mass concentration differs slightly at different stages, ranging from 11.8 to 31.4 μg $m^{-3}$ in non dust period. The size distribution of mass concentration differs greatly at different stages, ranging from 11.0 to 304.3 μg $m^{-3}$ in dust period. The coarse particles (>2.1μm) account for 91% of the total in the dust period and 61% in the non-dust period. The mass concentrations of coarse particles and fine particles are 7.8 and 1.2 times those in the non-dust period, respectively. This shows that coarse particles dominated in mass concentration in the dust period. The mass concentrations increased greatly in the coarse stages and reached a peak of 304.3μg $m^{-3}$ in the range of 7–11 μm in the dust period. Kanai et al. (2002) reported that the mass concentration of particles in Japan usually reached peak values in the range of 4–5 μm. Because of gravity settling, not only will the concentration decrease but also the diameter range with peak values will be smaller the in downstream areas than in Beijing in the dust period.

### 3.3. Size distribution of number concentrations

Figure 3 shows the size distribution of the number concentration of particles with size range of 0.3~0.5, 0.5~0.7, 0.7~1.0, 1.0~2.0, 2.0~5.0, and >5.0 μm during 19-22 March 2002. During this time, the number concentrations of dust in six stage all increased obviously and reached a maximum at 1100 LST 20 March 2002. Here the number concentrations between 1100 LST 20 March 2002 in the heavy dust period and 1700 LST 19 March 2002 before the dust period are compared. The number concentrations of dust particles with diameters of 0.3~0.5, 0.5~0.7, 0.7~1.0, 1.0~2.0, 2.0~5.0, and >5.0 μm in the dust period were 3.8, 9.1, 15.9, 57.3, 59.7, and 89.1 times as much as those before the dust period, respectively. The number concentrations of fine particles (d < 2 μm), coarse particles (d > 2 μm), and total number of particles were 26.4, 63.8, and 30.5 times as much as those before the dust period, respectively. The stage of the number concentration of particles in the dust period are listed from high to low as follows:2.0~5.0, 1.0~2.0, 0.5~0.7, 0.7~1.0, >5.0, and >0.3~0.5 μm. This shows that the number concentrations of both fine and coarse particles increased considerably. Although the number concentrations of the fine and coarse particles were higher than in the non-dust period, the number concentration of coarse particles increased more than the fine particles.

Figures 1 and figure 3 show that both the TSP mass concentration and number concentration reach a peak at 1100–1600 LST 20 March 2002 in the heavy dust period. The observation results obtained with the high volume sampler are in good agreement with number concentration by the optical particle counter. Observations by the same optical particle counter indicated that the number concentrations of coarse particles (d > 2 μm) were about 20 times as much as those after the dust storm while the number concentrations of fine particles (d < 2 μm) were only 7 times as much as those after the dust storm (Zhang et al., 2000). So the 20 March 2002 dust storm event was much heavier than the 6 April 2000 dust event in Beijing.

### 3.4. Dry deposition flux over beijing

Dry deposition flux data of the aerosols were collected during the observation period from March 2002 to February 2002 over Beijing in Figure 4. The dry deposition flux reach peak in spring (1.14 and 1.44 g $m^{-2}$ $d^{-1}$ in March and April respectively) and minimum of 0.12 g $m^{-2}$ $d^{-1}$ in August. The monthly average dry deposition flux is 0.42 g $m^{-2}$ $d^{-1}$ Beijing, which is 3 times as that in Seoul, Korea of 0.137 g $m^{-2}$ $d^{-1}$ (Yi et al., 2001).

The reason caused the dry deposition flux higher over Beijing than over Korea, may be that as compared to Beijing, (a) Korea is far off the dust source, resulting in additional dust deposited already to the ground surface, and (b) the soil over Korea was relatively wet, resulting in less dust injected from the wetter surface into the boundary layer. The dry deposition mass flux of in dust storm period reached 17.5 g $m^{-2}$ $d^{-1}$(0900-2100 LST 20 March) which is much higher than average level.

### 3.5. Origin of dust storm on 20 March 2002

A 48-hour calculation of three-dimensional backward trajectories was made using the NOAA Hybrid Single-Particle Lagrangian Integrated Trajectory (HYSPLIT) model with FNL meteorological database for 0400 UTC20 March 2002 (1400 LST in

Beijing). The FNL archive data is generated by the America National Center for Environmental Prediction (NCEP) Global Data Assimilation System (GDAS) wind field reanalysis. Further information on the FNL meteorological database can be found at http://www.arl.noaa.gov/ss/transport/archives.html. The backward trajectory analysis in Figure 5 shows that the air mass which caused heavy dust storm over Beijing on 20 March 2002 came from Kazakhstan and Xingjiang province of China, passing through southern Mongolia, central Inner Mongolia, Shanxi province, and then to Beijing. This result is consistent with recent research results by Wang et al.(2004) that this pathway is the most important one contributing to Beijing high aerosol concentration events in the spring.

Figure 5 also shows that when the air mass passed over southern of Mongolia and central Inner Mongolia where considerable desert and semi-desert areas exist, its altitude turned to be less than 1.5km, making it easier for dust particles on the ground level to be injected into the air. This could imply that the dust storm over Beijing on 20 March 2002 is originated from Southern Mongolia and central Inner Mongolia, which was further confirmed by dust model simulation by Sugimoto et al.(2003). When the air mass passed through shanxi province, an industrial area in China, its altitude turned to be below 500m. So dust particles could be mixed with anthropogenic aerosols on the ground level during their transport process over Shanxi province. Backward trajectory analysis above strongly indicates for the origin of dust storms over Beijing through long-range transport.

### 3.6. Water-soluble ions variations

Figure 6 presented the evolutions of the concentrations of $Cl^-$, $NO_3^-$, $SO_4^{2-}$, and $NH_4^+$ in March 2002. Concentrations of $Cl^-$, $NO_3^-$, $SO_4^{2-}$, and $NH_4^+$ had similar trends and the highest concentrations were observed on 20 March in dust storm period, which corresponds to high concentration of TSP. Concentrations of $Cl^-$, $NO_3^-$, and $SO_4^{2-}$ in heavy dust period are about 10 time as that in non dust period, while $NH_4^+$ concentration is about 6 time as that before dust period. Higher concentrations of nitrate and sulfate in dust period may suggest aerosols in dust period were influenced by anthropogenic sources during the transport process (Cao et al., 2003). Back trajectory analyses in Figure 5 indicate that the air containing the dust had passed over North-west of Beijing-Shanxi Province where many large coal mines are located. Therefore, the mixing of material emitted from the anthropogenic source such as coal mines with the desert dust is a possible explanation for why $Cl^-$, $NO_3^-$, $SO_4^{2-}$, and $NH_4^+$ showed a high concentration during the dust storm period over Beijing. This results agree to previous study of dust storm on 6 April 2000 in Beijing by Zhuang et al.(2001).

## 4.SUMMARY

The dust storm on 20 March 2002 in northern part of China was one the heaviest in the last decade. In this paper, the physicochemical characteristics of Beijing dust storm aerosols were well depicted during March 2002. Evidences for this strong dust storm are as follows: The TSP concentrations in Beijing reached peak values 12 mg $m^{-3}$ on 1050-1530 LST 20 March, which is the highest value that has ever been reported in Beijing and also is an infrequent value in dust source regions. During this dust storm, the size distribution of mass concentration and number showed a characteristic increase much especially in the size range of coarse particles. The mass concentration of coarse particles (>2.1μm) account for 91% of the total in the dust period and 61% in the non-dust period respectively. The number concentrations of fine particles (d < 2 μm), coarse particles (d > 2 μm), and total particles were 26.4, 63.8, and 30.5 times as much as those before the dust period, respectively. The dry deposition flux of particles reach peak in spring (1.14 and 1.44 g $m^{-2}$ $d^{-1}$ in March and April respectively) and minimum of 0.12 g $m^{-2}$ $d^{-1}$ in August with monthly average of 0.42 g $m^{-2}$ $d^{-1}$. The dry deposition mass flux of in dust storm period is 17.5 g $m^{-2}$ $d^{-1}$ (0900-2100 LST 20 March). During the storm, the air mass was transported directly from Mongolia, central Inner Mongolia and Shanxi province of China, then to Beijing, which was demonstrated by backward trajectory analysis. Concentrations of $Cl^{-}$, $NO_3^{-}$, and $SO_4^{2-}$ in TSP in heavy dust period are about 10 times as that in non dust period, which implied that anthropogenic materials together with dust particles were transported to Beijing.

Beijing is located in downstream areas of Asian dust storms and easily attacked by dust storm. In consequence, it is necessary to strengthen the ground-based observations for dust storm in Beijing in the future in order to gain better understandings on origin, transportation and deposition of Asian dust storm.

## 5. ACKNOWLEDGMENTS

This research is supported by National Basic Research Program of China (2006CB400501), the National Natural Science Foundation of China (No. 40205017) and the Hundred Talents Program (Modeling the Transportation of Dust Storms and Their Effect on Climate and Environment) by the Chinese Academy of Sciences.

## REFERENCES

Chun, Y.S., Boo, K.O., Kim, J., Park, S.U., and Lee, M.: 2001a, Synopsis, transport, and physical characteristics of Asian dust in Korea, J.Geophys.Res.,106(D16), 18461-18469.

Chun, Y.S., Kim, J., Choi, J.C., Boo K.O., Oh, S.N. and Lee, M.: 2001b, Characteristic number size distribution of aerosol during Asian dust period in Korea. Atmos.Environ., 35, 2715-2721.

Chung, Y. S., Kim, H. S., Park, K. H., Jhun, J. G. and Chen, S. J.: 2003a, Atmospheric loadings, concentrations and visibility associated with sandstorms: satellite and meteorological analysis, Water, Air and Soil Pollution, Focus 3(2): 21–40.

Chung, Y.S., Kim, H.K., Dulam, J., and Harris, J.: 2003b, On heavy dustfall observed with explosive sandstorms in Chongwon-Chongju, Korea in 2002.Atmos.Environ. 37,

3425–3433.
Cao, J.J., Lee, S.C., Zheng, X.D., Ho, K.F., Zhang, X.Y., Guo, H., Chow, J.C., and Wang, H.B.: 2003, Characterization of Dust Storms to Hong Kong in April 1998, Water, Air and Soil Pollution, Focus 3(2): 213–229.
Fan, K. and Wang, H.J.:2004. Antarctic oscillation and the dust weather frequency in North China, Geophys. Res. Lett., 31, L10201, doi:10.1029/2004GL019465.
Fang, Z.Y, Zhu, F.K., Jiang, J.X., and Qian, Z.A.: 1997, Studies on dust storm in China, Beijing: China Meteorological Press, 158p.
Gong, S.L., Zhang, X.Y., Zhao, T.L.,McKendry, I.G., Jaffe, D.A., and Lu, N.M.:2003, Characterization of soil dust aerosol in China and its transport and distribution during 2001 ACE-Asia:2. Model simulation and validation, J.Geophys.Res., 108(D9),4262, doi:10.1029/2002JD2633
Iwasaka, Y., Minoura, H. and Nagaya, K.: 1983, The transport and spatial scale of Asian dust-storm clouds: A case study of the dust-storm event of April 1979. Tellus, 35B, 189-196.
Iwasaka, Y., Shibata, T., Nagatani, T., Shi, G.Y., Kim, Y. S., Matsuki, A., Trochkine, D., Zhang, D., Yamada, M., Nagatani, M., Nakata, H., Shen, Z., Li, G., Chen, B., Kawahira, K.: 2003, Large depolarization ratio of free tropospheric aerosols over the Taklamakan Desert revealed by lidar measurements: Possible diffusion and transport of dust particles, J. Geophys. Res., 108( D23), 8652, doi:10.1029/2002JD003267
Kanai, Y., Ohta, A., Kamioka, H., Terashima, S., Matsuhisa, Y., Shimizu, H., Takahashi, Y., Kai, K., Xu, B., Hayashi, M., and Zhang R.J.: 2002, Preliminary study on the grain-size distribution and concentration of Aeolian dust collected in Japan, Journal of Arid Land Studies, 11(4),307-314.
Prospero, J.M.: 1999, Long-range transport of mineral dust in the global atmosphere: Impact of African dust on the environment of the southeastern United States, Proc. Natl. Acad. Sci. U.S.A., 96, 3396-3403.
Sokolik, I. N., Winker, D.M., Bergametti, G., Gillette, D. A., Carmichael, G., Kaufman, Y. J., Gomes, L., Schuetz, L., and Penner, J.E.: 2001, Introduction to special section: Outstanding problems in quantifying, the radiative impacts of mineral dust, J. Geophys. Res. 106 (D16) , 18,015-18027 (2000JD900498).
Sugimoto, N., Uno, I., Nishikawa, M., Shimizu, A., Matsui, I., Dong, X.H., Chen, Y. and Quan, H.:2003, Record heavy Asian dust in Beijing in 2002: Observations and model analysis of recent events, Geophys.Res.Lett., 30(12), 1640, doi:10.1029/2002GL016349.
Tegen, I., and Fung, I.: 1994, Modeling of mineral dust in the atmosphere: Sources, transport, and optical thickness. J. Geophys. Res., 99, 22897-22914.
Wang, W., Yue, X., Liu, H.J. Pan Z., Tang D.G., Wang Y., Du R.G., Su H.M., Qian F., and Sakamoto K.,: 2002, Study on pollution characteristics of aerosols during sand-dust storm weather in Beijing, ACTA Scientiae Circumstantiae, 22(4), 494-498.
Wang, Y.Q., Zhang, X.Y., Arimoto, R., Cao, J.J., and Shen, Z.X.: 2004, The transport pathways and sources of $PM_{10}$ pollution in Beijing during spring 2001, 2002 and 2003, Geophys.Res.Lett., 31, L14110, doi:10.1029/2004GL019732.
Wang, Z.F., Ueda, H., and Huang, M.Y.: 2000, A deflation module for use in modeling long-range transport of yellow sand over East Asia, J. Geophys. Res., 105(D22): 26947-26959.
Ye, D.Z., Chou J.F., Liu J.Y., Zhang Z.X., Wang Y.M., Zhou Z.J., Ju H.B., and Huang

H.Q.: 2000, Causes of sand-stormy weather in northern China and control measures, ACTA Geographica Sinica, 55(5), 513-521.
Yi, S.M., Lee, E.Y., and Holsen, T.M.: 2001, Dry deposition fluxes and size distributions of heavy metal in Seoul, Korea during yellow-sand events, Aerosol Science and Technology, 35, 569-576.
Yoshino, M.: 2000, Problems in climatology of dust storm and its relation to human activities in northern China, J. Arid Land Studies,10, 171-181.
Zhang, R.J., Wang, M.X., Pu, Y.F., Liu, Q., Fu, J.Z., and Zhang, W.: 2000, Chemical and physical properties of "2000.4.6" super dust storm in Beijing(In Chinese), Climate and Environmental Research, 5(3), 259-266.
Zhang, R.J, Wang, M.X., and Fu, J.Z.: 2001, Preliminary research on the size distribution of aerosols in Beijing, Adv. Atmos. Sci., 18(2), 225-230.
Zhang, R.J, Han Z.W., Wang, M.X., and Zhang X.Y.: 2002, Dust storm weather in China: New characteristics and origins(In Chinese), Quaternary Sciences, 22(4), 374-380.
Zhang, R.J., Wang, M.X., Zhang, X.Y., and Zhu, G.H.: 2003, Analysis on the chemical and physical properties of particles in a dust storm in spring in Beijing, Powder Technology, 137(1),77-82.
Zhang, X.Y., Arimoto R., and An Z.S.: 1997, Dust emission from Chinese deserts linked to variation in atmospheric circulation. J. Geophys. Res., 102, 28041-28047.
Zhou, Z.J.: 2001, Blowing-sand and sandstorm in China in recent 45 years (in Chinese), Quaternary Sciences, **21**(1): 9~17
Zhuang, G.S., Guo, J.H., Yuan, H., and Zhao, C.Y.: 2001, The compositions, sources, and size distribution of the dust storm from China in spring of 2000 and its impact on the global environment, Chinese Science Bulletin, **46**(3), 191-197.

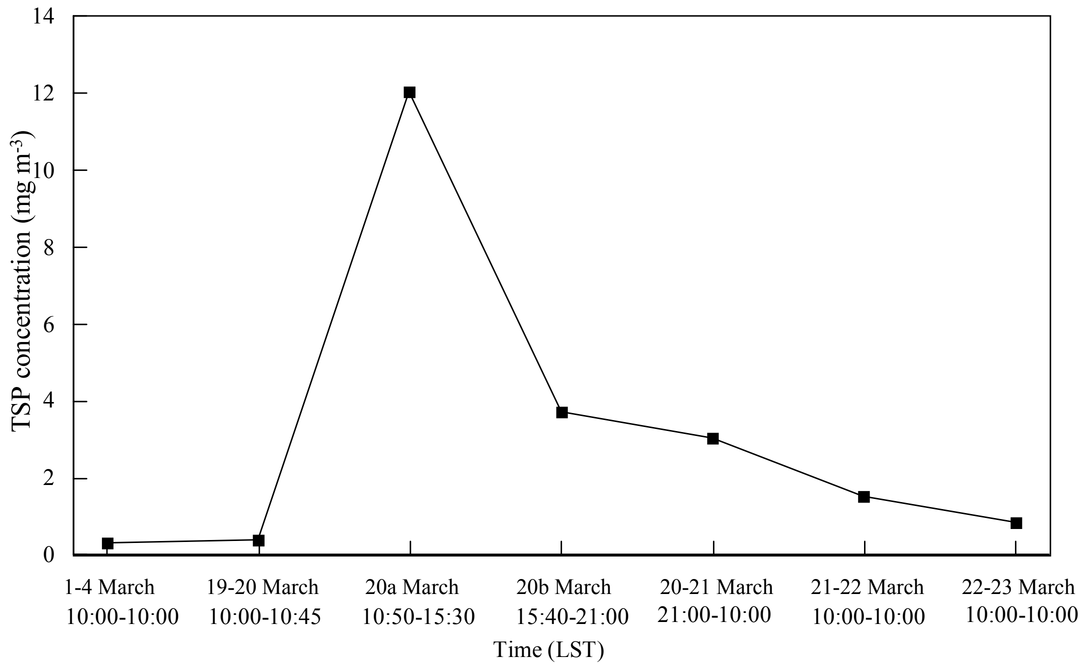


Figure 1. Mass concentration of total suspended particles (TSP) in Beijing in March 2002

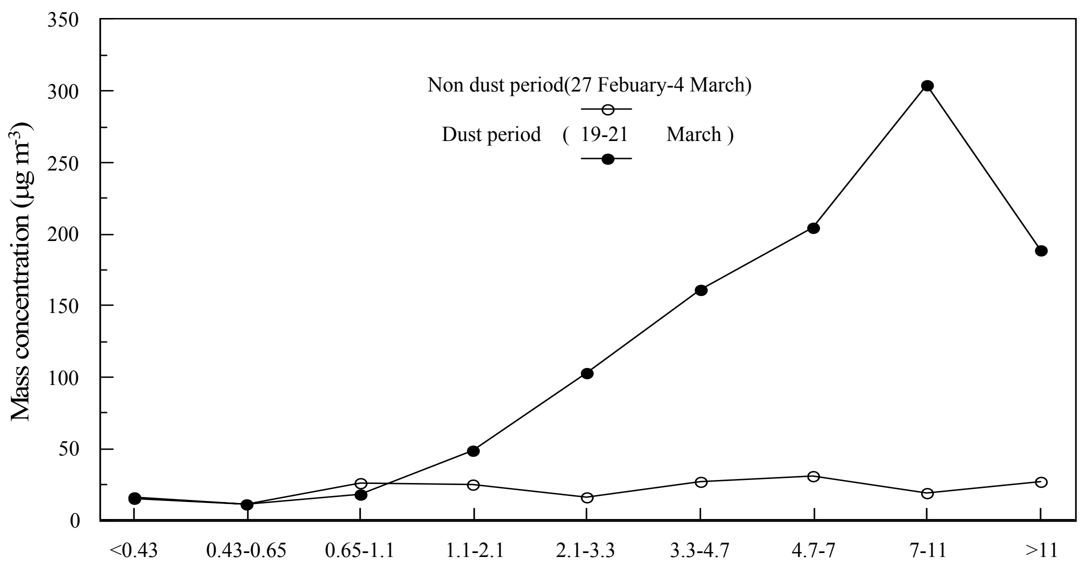


Figure 2. Size distribution of mass concentration of aerosols in the non-dust period (1000LST 27 February-1000LST 4 March 2002) and dust storm period (1000LST 19 March -1000LST 21 March 2002) in Beijing.

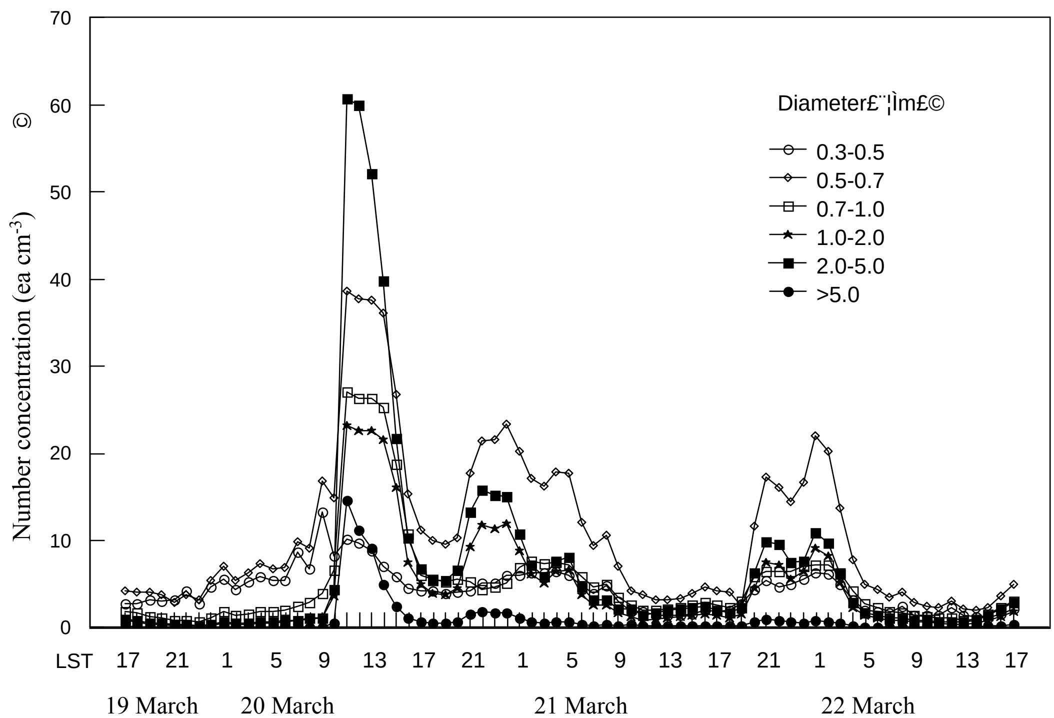


Figure 3. Size distributions of the number concentration of particles during 19–22 March 2002 in Beijing.

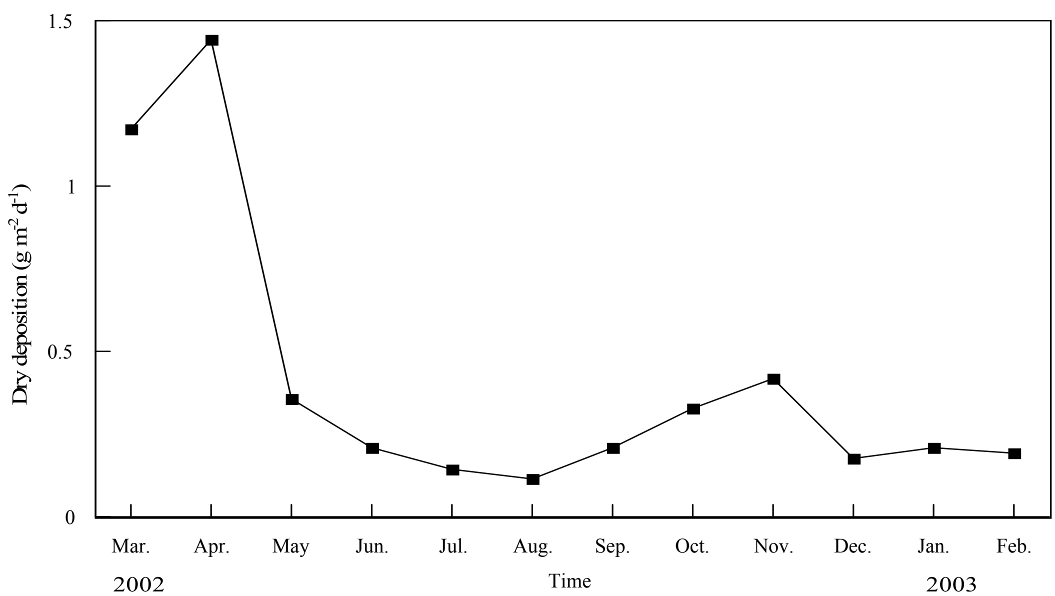


Figure 4. Seasonal variation of dry deposition of atmospheric aerosols in Beijing

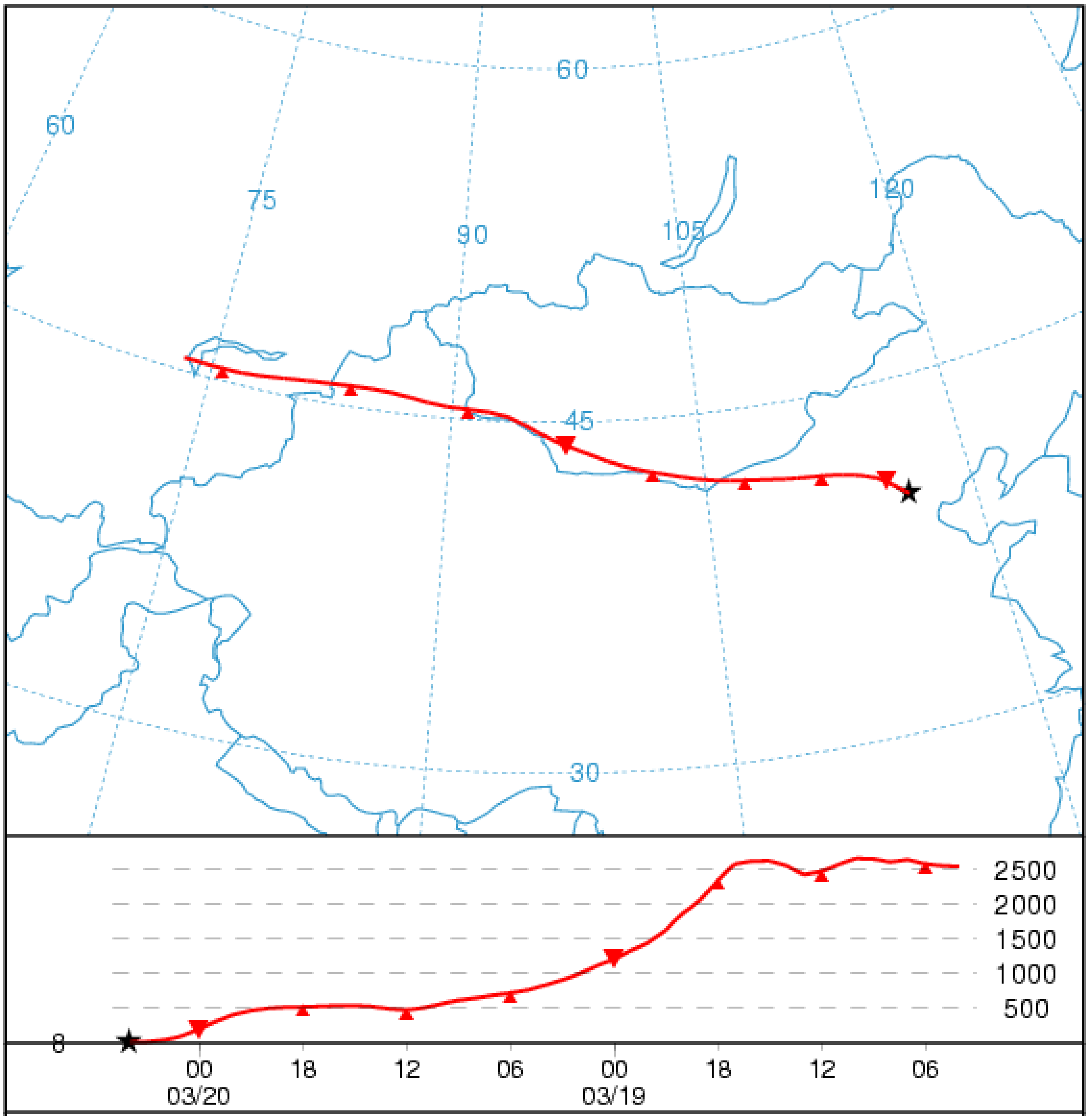


Figure 5. A 48-hour backward trajectory calculation for 0400 UTC 20 March 2002 for the observation site at Beijing. This shows the origin of the dust storm and its trajectory prior to reaching Beijing, China. The top and bottom panels display horizontal and vertical motion, respectively. Note that the time is in UTC not LST.

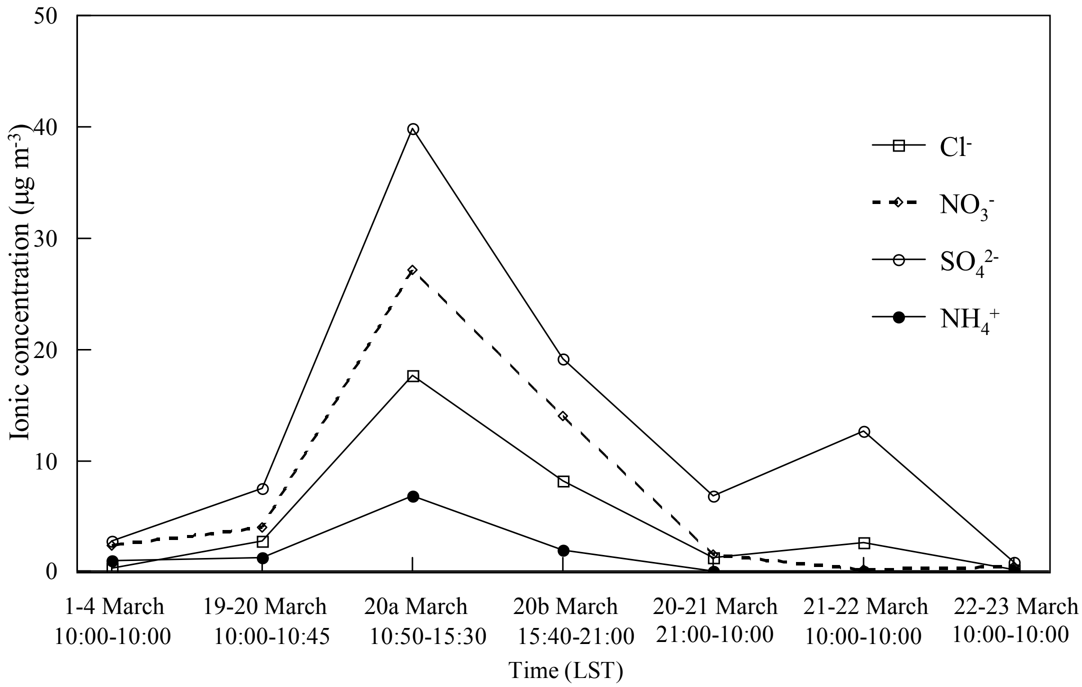


Figure 6. Concentrations of $Cl^{-}$, $NO_3^{-}$, $SO_4^{2-}$, and $NH_4^{+}$ in TSP in Beijing in March 2002

*Proceedings of the Third International Symposium on Air Quality Management at Urban, Regional and Global Scales. 26-30 September 2005, Istanbul – Turkey*

# SOURCE REGIONS OF DUST TRANSPORTED TO THE EASTERN MEDITERRANEAN

**Gülen GÜLLÜ, Güray DOĞAN* and Gürdal TUNCEL***

Hacettepe University, Dept. of Environmental Engineering, 06532, Ankara, Turkey, ggullu@hacettepe.edu.tr
*Middle East Technical University, Dept. of Environmental Engineering, 06531, Ankara, Turkey

## ABSTRACT

During the years of 1992, 1993 and 1998, a total of 46 strong dust episodes occurred in the Eastern Mediterranean Basin. During dust episodes, and at normal conditions in order to compare dust and non-dust period, daily PM-10 aerosol samples were collected at Antalya, an eastern Mediterranean location. Although similar absolute concentrations of anthropogenic elements were observed during dust and non-dust periods, for crustal elements like Al, Sc, Fe, and rare earth elements concentrations during strong dust periods up to a factor of four higher concentrations were measured. The potential source contribution function (PSCF) has been used to study the source-receptor relationship for dust episodes. Important source regions for dust observed in the eastern Mediterranean accumulate in three general areas; 1) in western parts of North Africa covering Morocco and Algeria where big sand dunes of Erg Iguidi, Grand Erg Oriental, 2) in Libyan deserts and 3) Arabian deserts.

**Key Words:** Saharan Dust, Eastern Mediterranean Atmosphere, Multilayer PSCF

## 1. INTRODUCTION

Annually, 300 to 700 million tons of dust originated from Saharan Deserts are transported over short to long distances to the Atlantic (Carlson and Prospero, 1971; Moulin et al., 1998), Mediterranean Sea (Kubilay et al., 2000; Özsoy et al., 2001; Molinaroli and Ibba, 1995; Ganor and Mamane, 1982), southern Europe (Mattsson and Nihlen, 1996) as reported and discussed in many publications. It has been estimated that yearly amount of Saharan dust leaving North Africa in a northeasterly direction towards eastern Mediterranean is some 100 million tons (Ganor and Foner, 1996). This large quantity of dust transport has a significant impact on climatic processes, nutrient cycles, soil formation and sediment cycles.

Geographic locations from where dust originates in North Africa and Middle East are important in reducing uncertainties in the modeling of past and future climate as they have significant consequences particularly in climate change. Although source regions of dust in the atmosphere had been studied by various researchers using remote sensing (Brooks and Legrand, 2000), surface dust observations (Herrmann et al., 1999), backtrajectory analysis (Chiapello et al., 1997) and total ozone mapping spectrometer (TOMS) (Hsu et al., 1999; Washington et al., 2003). The exact source locations of dust observed in the Mediterranean are not well known, but data from Total Ozone Mapping Spectrometer (TOMS) suggest two major source areas: the Bodélé depression and an area covering eastern Mauritania, western Mali and southern Algeria (Goudine and Middleton, 2001). The Horn of Africa and Nubian Desert in southern Egypt and northern Sudan are also suggested as important source regions (Brooks and Legrand, 2000).

In this study, episodic behavior of dust transport to the eastern Mediterranean has been studied by measuring elemental concentrations of aerosols collected at rural location for the years 1992, 1993 and 1998. The potential source areas of dust were defined with Potential Source Contribution Function (PSCF) analysis by using chemical concentrations and backward air trajectories.

## 2. MATERIALS AND METHODS

### 2.1 Sampling and Analysis

A total of 789 daily high aerosol samples were collected from Antalya Air Quality Monitoring Station in the south part of Turkey (30.34 °E, 36.47 °N), in the northeast Mediterranean Sea during the years 1992, 1993 and 1998, using Andersen Model HV-100 High Volume Air Sampler equipped with a PM-10 pre-impactor. Further details on sampling and analytical procedures have been reported elsewhere (Güllü et al., 1998).

Approximately 300 samples collected in 1993 were analyzed by INAA and 490 samples collected in 1992 and 1998 were analyzed by AAS for trace elements. Samples were analyzed for Al, K, Na, Mg, Fe, Zn and Ca by flame and Pb, Cu, Cd, Ni, V and Cr by graphite furnace atomic absorption spectrometry using a Perkin Elmer, model 1100B atomic absorption spectrophotometer coupled to a Perkin Elmer HGA 700 electrothermal atomization system. Different parts of the same filters were also analyzed for an additional 30 – 40 elements by INAA, at the Massachusetts Institute of Technology (MIT), Nuclear Reactor Laboratory (thermal neutron flux: $1x10^{13}$ n $cm^{-2}$ $sec^{-1}$), using the procedure developed by Olmez (1989).

### 2.2 Trajectory Data

Five days-long, three dimensional isentropic back trajectories, arriving to the sampling point at the midtime of each sample, were computed by the publicly available operational model on the CRAY C90/UNICOS computer at the European Center for Medium Range Weather Forecast (ECMWF) Center. This model is similar to the method developed by Martin et al. (1987). The model uses analyzed zonal (*u*) and meridianal (*v*) wind field components; plus the vertical velocities available in the archives of the center (MARS) in the form of a special online database gridded every 12 hours (00:00, 12:00) for standard pressure levels. In order to run this model from a remote site, a request file which contains the place and date information were sent to the center. After that, a data matrix containing the information of the position of the air parcel in latitude and longitude at each hourly time step is sent back to the user. The data arriving for trajectories at three different barometric levels; 900, 850 and 700 hPa were obtained, and the end altitude of all three barometric level trajectories was used in the statistical analysis**.**

### 2.3 Multi-layer potential source contribution function

The geographic locations of the source regions of dust observed in the eastern Mediterranean are determined by an approach called the potential source contribution function (PSCF) which is originally developed by Ashbaugh et al. (1984). It has been applied in a series of studies over a variety of scales (Zeng and Hopke, 1989; Gao et al., 1993, 1994, 1996; Cheng et al., 1993). In this model, it is assumed that a species emitted within a grid cell is swept into the air parcel and transported to the receptor site without loss through diffusion, chemical transformation or atmospheric scavenging.

The PSCF of an element $\underline{x}$ in subregion $\underline{ij}$ is defined as a conditional probability:

$$PSCF_{x,ij} = \Sigma m_{ij} / \Sigma n_{ij}$$

Where $\underline{\Sigma n_{ij}}$ is the total number of trajectory segments in the $\underline{ij}$-th subregion from three different levels (700, 850 and 900 mb) during the whole study period, and $\underline{\Sigma m_{ij}}$ is the total number of “dust loaded” trajectory segments in the same $\underline{ij}$-th subregion during the same study period. Hence, high values of $PSCF_{x,ij}$ will pinpoint geographical regions that are likely to produce high concentration values of an element $x$ at the receptor site if crossed by a trajectory. In this study, for the selection of “dust loaded” trajectory segments, we have used the predefined dust event sub data set.

In the PSCF analysis, a 120-h long 700, 850 and 900 mb arrival level back trajectories, corresponding to every sample collected in 1992, 1993 and 1998, were divided into 1-hr segments and these segments were counted in each subregion. Subregions are predefined as 1°x1° grids in the study area, which lies between 75°N latitude at north (north of Scandinavia), 15°N latitude at south (south of Algeria), 20°W longitude at west (west of UK) and 59°E longitude at east (east of Arabic Peninsula).

## 3. RESULTS AND DISCUSSION

### 3.1. General characteristics of data

In order to asses the impact of mineral dust on the composition of Eastern Mediterranean aerosols, the data set has been divided into 2 subsets; one corresponding to dust events and the other one corresponding to non dust samples. Samples that correspond to dust event were determined by using Al concentrations, TOMS data and backtrajectory information. Aluminum is widely used as a tracer for mineral dust in the Mediterranean region as it does not have any source other than crustal material in rural areas (Güllü et al., 1998; Kubilay and Saydam, 1995; Guerzoni et al., 1999). It is well documented that during Saharan Dust incursions to the Eastern Mediterranean region, crustal elemental concentrations like Al and Fe increase up to two-orders of magnitude. The baseline concentration of Al is approximately 100 ng m-3. However, during dust incursions this concentration varies between 300 and 6500 ng m-3. Consequently Al concentrations in dust-impacted samples should be high and this was set as the first criteria in selecting dust influenced samples. All the samples that had Al concentrations higher than twice the baseline concentrations were selected as samples potentially impacted by the mineral dust. As Al and Fe are markers for crustal material, they are not specific to Saharan Dust, to differentiate the dust episodes that originate from North Africa and Middle East, 5 days backward trajectory information were used. If either 850 and/or 700 MB level back trajectories originate or pass through North Africa and Arabian Peninsula and the sample Al concentration higher than twice the baseline concentration, that sample has identified as dust episode.

For the dust episodes of year 1992, 1993 (till May 1993) and 1998, the selected sample dates were visually inspected with TOMS aerosol data. And for the year 1998, SeaWiFS (Sea-viewing Wide Field-of-view Sensor) satellite produce pictures of the Eastern Mediterranean region were also used to check the episodes if there were no cloud. Although comparison of the dust events with satellite pictures and TOMS data are not available for the whole period, as a general comparison proved useful.

By applying these criteria's, a total of 46 dust episodes covering 157 days out of 789 days were identified within the study period. This data set is used as dust set in all subsequent statistical treatment of data.

The backtrajectory, TOMS and SeaWIFS data for one of the dust episode is given as an example in Figure 1. This example is for the dust episode during 10 to 17 April 1998. This was one of the longest and strongest episodes observed during the study period. Aluminum concentrations varied between 560 to 1500 ng m-3. A strong dust pulse entering the Mediterranean from the Libyan coast is clearly visible in the satellite pictures.

### 3.2 Elemental characteristics of mineral dust

Table 1 summarizes the major element concentrations of mineral dust as sampled in the eastern Mediterranean, for comparison the average concentrations in the region during the rest of the period (non-dust), and the dust to non-dust ratio of the elements are also given.

Although major element compositions of soil material do not show substantial differences worldwide, minor and trace element content of different soil types could be useful in differentiating between different types of crustal material in atmosphere. When concentrations of elements in samples corresponding to dust episodes are compared with concentrations in non-dust samples, it has been observed that the overall mean of lithophilic elements are factors of 2.0 to 4.5 higher in episodic samples. As the episode samples were selected based on their litophile concentrations, the results are not surprising. However, all litophilic elements do not have the same ratio, while dust-to-nondust ratio of the elements e.g. Al, La, Ce, Sm, Lu, Sc, Yb, Gd, Th, Eu and Hf are around 4, the ratio is around 2 for the elements Rb, Fe, Tb, Cs, Nd, Dy, Co and Ti.

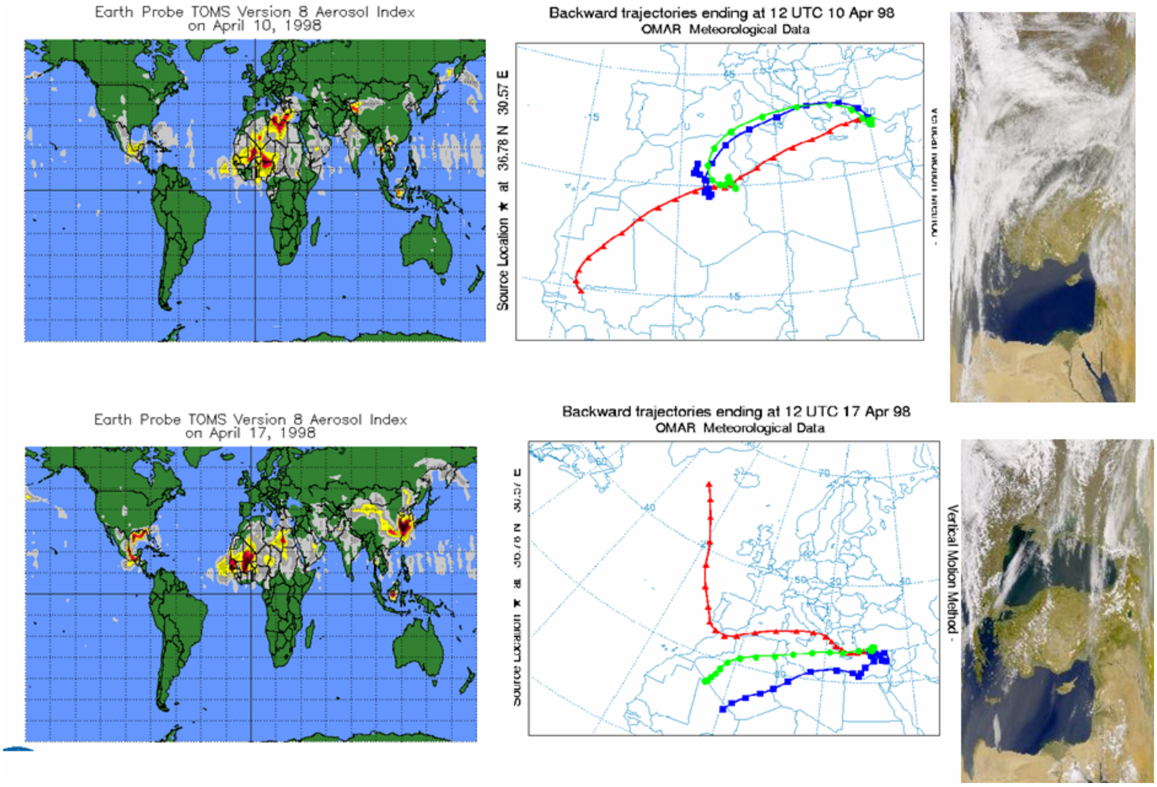


Figure 1. The TOMS Aerosol Index, backtrajectory and SeaWIFS data are given for the episode observed during 10-17 April 1998.

### 3.3. Source regions of dust in the eastern Mediterranean region

The geographic locations of the source regions of dust observed in the Eastern Mediterranean are determined by multilayer potential source contribution function. The dust data set are assumed to be “polluted”. The 900, 850 and 700 MB level PSCF values for Al are depicted in Figure 2. Important source regions for dust observed in the eastern Mediterranean appears to accumulate in three general areas. One of these regions is located in western part of North Africa covering Morocco and Algeria. In these areas there are big sand dunes of Erg Iguidi, Grand Erg Oriental which is called as sand sea and Dra desert in Morocco. These regions are frequently cited in the dust studies performed in the western Mediterranean. Also TOMS studies indicated that Aerosol Index in the central Algeria and eastern Mauritania varies between 6 – 20, suggesting high dust re-suspension in this region. High PSCF values calculated in these areas indicate that some of the dust observed in the eastern Mediterranean is transported from Western Sahara.

Table 1. Median concentrations of elements in dust and non-dust samples

| | Dust Samples (n=157) | $EF_{dust}$ | Background Concentrations (n=632 ) | $EF_{nondust}$ | Dust/Non Dust Ratio |
|---|---|---|---|---|---|
| **Na** | 1232 | 36,37 | 922 | 249,44 | 1,34 |
| **Mg** | 557 | 1,99 | 267 | 9,47 | 2,09 |
| **Al** | 995 | 1,00 | 237 | 1,00 | 4,20 |
| **Cl** | 1283 | 160,59 | 1042 | 1575,91 | 1,23 |
| **K** | 507 | 1,98 | 223 | 4,88 | 2,27 |
| **Ca** | 3097 | 0,66 | 1711 | 2,23 | 1,81 |
| **Sc** | 0,20 | 0,60 | 0,043 | 0,63 | 4,64 |
| **Ti** | 62 | 0,16 | 22 | 0,23 | 2,84 |
| **V** | 4,37 | 0,45 | 1,82 | 1,20 | 2,41 |
| **Cr** | 4,39 | 0,87 | 3,05 | 3,38 | 1,44 |
| **Mn** | 15,99 | 0,65 | 6,53 | 1,25 | 2,45 |
| **Fe** | 753 | 0,33 | 221 | 0,40 | 3,40 |
| **Co** | 0,34 | 0,69 | 0,11 | 2,81 | 2,98 |
| **Ni** | 3,59 | 1,71 | 2,00 | 4,91 | 1,79 |
| **Zn** | 16,23 | 8,67 | 9,52 | 14,46 | 1,70 |
| **As** | 1,27 | 8,06 | 1,24 | 89,47 | 1,02 |
| **Se** | 0,36 | 6,33 | 0,22 | 27,43 | 1,66 |
| **Br** | 15,44 | 83,39 | 13,47 | 749,18 | 1,15 |
| **Rb** | 1,59 | 2,34 | 0,50 | 4,30 | 3,20 |
| **Mo** | 0,25 | 5,72 | 0,21 | 79,77 | 1,18 |
| **Sb** | 0,35 | 21,26 | 0,30 | 133,54 | 1,18 |
| **Cs** | 0,13 | 2,78 | 0,06 | 7,74 | 2,22 |
| **La** | 0,65 | 1,17 | 0,15 | 1,29 | 4,25 |
| **Ce** | 1,27 | 1,35 | 0,29 | 1,56 | 4,35 |
| **Nd** | 0,70 | 2,18 | 0,30 | 8,79 | 2,34 |
| **Sm** | 0,096 | 1,14 | 0,021 | 1,12 | 4,42 |
| **Eu** | 0,020 | 1,26 | 0,005 | 1,38 | 4,05 |
| **Tb** | 0,010 | 1,15 | 0,002 | 1,37 | 3,70 |
| **Dy** | 0,083 | 0,18 | 0,030 | 0,48 | 2,68 |
| **Yb** | 0,038 | 1,17 | 0,008 | 1,14 | 4,71 |
| **Lu** | 0,006 | 0,90 | 0,001 | 0,89 | 4,43 |
| **Hf** | 0,049 | 1,41 | 0,012 | 1,30 | 4,02 |
| **Hg** | 0,021 | 79,10 | 0,037 | 889,87 | 0,58 |
| **Pb** | 22 | 22,90 | 18 | 149,98 | 1,25 |
| Th | 0,17 | 1,25 | 0,04 | 1,47 | 4,17 |

The second source region appears in the southeastern part of Libya and Negec desert in Egypt. This region is also found to have Aerosol Index values between 9 and 15 and suggested to be an important dust source in the previous studies (Goudie and Middleton, 2001). This source region identified by the PSCF also agrees with satellite pictures of 1998. Most of the dust episodes in 1998 were transported to eastern Mediterranean off the Libyan coast, which is in agreement with this second region found in PSCF calculations.

The third source region of mineral dust for the eastern Mediterranean region appears in the Middle East region. Idso (1976) recognized Arabia as one of five world regions where dust storm generation is especially intense. The TOMS data indicate that the Middle East especially Ad Dahna erg region of eastern and central Saudi Arabia is an important area of dust-storm activity (Washington et al., 2003).

Although the identified source regions in this study agrees fairly well with the source regions reported in the literature with different methodology. However, PSCF analysis did not indicate the Bodele Depression, which is the known dust source area (with aerosol index values of 30). The reason for this inconsistency between literature and our assessment is probably due to the lenght of trajectories used in this study. The trajectories were 5 days long in this study, and most of the backtrajectories didnot extend beyond southern borders of Algeria into Chad, where Bodele Depression is located.

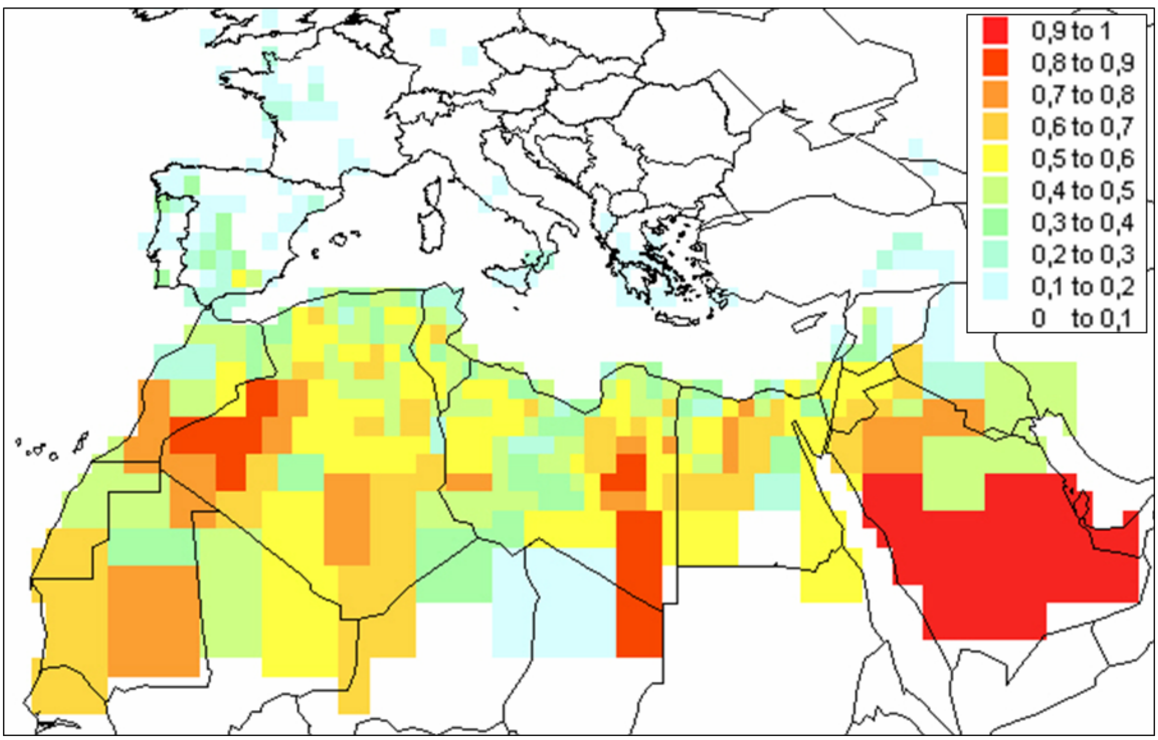


Figure 2. PSCF for eastern Mediterranean during 1992, 1993 and 1998

**4. CONCLUSIONS**

A source-receptor model has been used to identify potential source areas of mineral dust reaching eastern Mediterranean region. During the study period (the years 1992, 1993 and 1998) the strongest potential source areas are identified as western parts of north Africa covering Morocco and Algeria where big sand dunes of Erg

Iguidi, Grand Erg Oriental, Libyan deserts and Arabian deserts. Our findings are in excellent agreement with the recent independent analysis of Washington et al., (2003) etc.

## 5. ACKNOWLEDGMENTS

The work presented here is supported in part by the Turkish Ministry of the Environment, grant 92-03-11-01-07, International Atomic Energy agency grant 7263/RB and European Union grant AVI-CT92-0005.

## REFERENCES

Ashbaugh, L.L., Myrup, L.O., Flocchini, R.G., 1984. A principal component analysis of sulfur concentrations in the western United States. Atmospheric Environment, 18, 783-791

Brooks, N., Legrand, M., 2000. Dust variability over Northern Africa and Rainfall in the Sahel. In: McLaren, S.J., Kniverton, D. (Eds.), Linking Land Surface Change to Climate Change. Kluwer Academic Publishing, Dordrecht, 1-25.

Carlson, T.N., Prospero, J.M., 1971. Large-scale movement of Saharan air impulses over Western Trophical Atlantic. Bulletin of the American Meteorological Society, 52 (8), 779-792.

M.D. Cheng, Hopke, P.K., Zeng, Y., 1993. A receptor methodology for determining source regions of particle sulfate composition observed at Dorset, Ontario. Journal of Geophysical Research, 98,16839–16849

Chiapello, I., Bergametti, G., Chatenet, B.,1997. Origins of African dust transported over the northeastern trophical Atlantic. Journal of Geophysical Research, 102, 13701-13709.

Ganor, E., Foner, H.A., 1996. The mineralogical and chemical properties and the behaviour of the Aeolian Saharan dust over Israel. In: S. Guerzoni and R. Chester (Eds.), The Impact of Desert Dust Cross the Mediterranean (173-182). Kluwer Academic Publishers.

Ganor, E., Mamane, M., 1982. Transport of Saharan dust across the eastern Mediterranean. Atmospheric Environment, 16, 581-587.

Gao, N. Cheng, M.D, Hopke, P.K., 1993. Potential source contribution function analysis and source apportionment of sulfur species measured at Rubidoux, CA during the Southern California air quality study 1987. Analytica Chimica Acta, 277, 369–380.

Gao, N., Cheng, M.D., Hopke, P.K., 1994. Receptor modeling for airborne ionic species collected in SCAQS, 1987. Atmospheric Environment, 28, 1447–1470.

Gao, N., Hopke, P.K., Reid, N.W., 1996. Possible sources of some trace elements found in airborne particles and precipitation in Dorset, Ontario. Journal of the Air and Waste Management Association, 46, 1035–1047.

Goudie, A.S., Middleton, N.J., 2001. Saharan dust storms: Nature and consequences. Earth-Science Reviews, 56, 179-204.

Guerzoni, S., Chester, R., Dulac, F., Herut, B., Loye-Pilot, M., Measures, C., Migon, C., Molinaroli, e., Moulin, C., Rossini, P., Saydam, C., Soudine, A., Ziveri, P., 1999. The role of atmospheric deposition in the biogeochemistry of the Mediterranean Sea. Progress in Oceanography, 44, 147-190.
Güllü, G.H., Ölmez, I., Aygün, S., Tuncel, G., 1998. Atmospheric trace element concentrations over the eastern Mediterranean Sea: Factors affecting temporal variability, J. Geophysical Research, 103, 21943-21954.
Herrmann, L.A., Stahr, K., Jahn, R., 1999. The importance of source region identification and their propoerties for soil-derived dust: the case of Harmattan Dust Sources for eastern west Africa. Contributions to Atmospheric Physics, 72, 141-150.
Hsu, N.C., Herman, J.R., Torres, O., Holben, b.N., Tanre, D., Eck, T.F., Smirnou, A., Chatenet, B., Lavenu, F., 1999. Comparison of the TOMS Aerosol Index with Sun-Photometer Aerosol Optical Thickness: Results and Applications. Journal of Geophysical Research, 104/D6, 6269-6279.
Idso, S.B., 1976. Dust storms. Scientific American, 235 (4):108-11, 113-14.
Kubilay N., Saydam, C., 1995. Trace elements in atmospheric particulates over the Eastern Mediterranean; concentrations sources and temporal variability. Atmospheric Environment, 29, 2,289-2,300.
Kubilay, N., Nickovic, S., Moulinn, C., Dulac, F., 2000. An iluustration of the transport and deposition of mineral dust onto the eastern Mediterranean. Atmospheric Environment, 34, 1293-1303.
Kubilay, N., Cokacar, T., Oguz, T., 2003. Optical properties of mineral dust outbreaks over the northeastern Mediterranean, J. Geophys. Research, 108 (21), AAC 4-1, AAC 4-10.
Martin, D., Mithieux, C., Strauss, B., 1987. On the use of the synoptic vertical wind component in a transport trajectory model. Atmos. Environ. 21, 45-52.
Mattsson, J.O., Nihlen, T., 1996. The transport of Saharan dust to southern Europe: a scenario. Journal of Arid Environments, 32, 111-119.
Molinaroli, E., Ibba, A., 1995. Occurance of palygorskite in aerosol dust (dry and wet) of desert source in SE Sardinia, West Mediterranean, Giornale di Geologica, 57, 67-76.
Moulin, C., Lambert, C.E., Dayan, U., Masson, V., Ramonet, M., Bousquet, P., Legrand, M., Balkanski, Y.J., Guelle, W., Marticorena, B., Bergametti, G., and Bulac, F., 1998. Satellite climatology of African dust transport in the Mediterranean atmosphere. Journal of Geophysical Research, 102, 11225-11238.
Olmez, I., 1989. Instrumental neutron activation analysis of atmospheric particulate matter In: Lodge J.P, (ed.) Methods of Air Sampling and Analysis, 143-150.
Özsoy, E., Kubilay N., Nickovic, S., Moulin, C., 2001. A hemispheric dust storm affecting the Atlantic and Mediterranean (April 1994), analysis, modeling, ground-based measurements and satellite observations, J. Geophys. Res., 106, 18439-18460.
Washington, R., Todd, M., Middleton, N.J., Goudie, A.S., 2003. Dust-storm source areas determined by the Total Ozone Monitoring Spectrometer and Surface Observations, Annals of the Association of American Geographers, 93(2), 297-313.
Westphal, D.L., Toon, O.B., Carlson, T.N., 1988. A case study of mobilization and transport of Saharan dust. J. Atmospheric Science, 45 (15), 2145-2175.
Zeng, Y. and Hopke, P.K., 1989. A study of the sources of acid precipitation in Ontario, Canada. *Atmospheric Environment* 23, pp. 1499–1509.